UNIVERSIDADE D
COIMBRA

Beatriz Gaspar Teixeira

NOCICEPTION INFERENCE FROM VITAL SIGN MEASUREMENTS: THE INFLUENCE AND CORRECTION OF ECTOPIC INTERVALS IN THE ELECTROCARDIOGRAM

Dissertação no âmbito do Mestrado Integrado em Engenharia Biomédica orientada pelo Professor Doutor Paulo Fernando Pereira de Carvalho, pelo Professor Doutor Jorge Manuel Oliveira Henriques, pela Doutora Esther van der Heide e pelo Doutor Jens Muehlsteff apresentada à Faculdade de Ciências e Tecnologia da Universidade de Coimbra.

Outubro de 2021

FACULDADE DE CIÊNCIAS E TECNOLOGIA
UNIVERSIDADE D COIMBRA

Beatriz Gaspar Teixeira

Nociception inference from vital sign measurements: the influence and correction of ectopic intervals in the electrocardiogram

Thesis submitted to the Faculty of Science and Technology of the University of Coimbra for the degree of Master in Biomedical Engineering with specialization in Clinical Informatics and Bioinformatics

Supervisors:

Prof. Dr. Paulo de Carvalho (DEI)

Prof. Dr. Jorge Henriques (DEI)

Dr. Esther van der Heide (Philips)

Dr. Jens Muehlsteff (Philips)

Gabriele Papini, M.Sc. (Philips)

Coimbra, 2021

This work was developed in collaboration with:

Department of Patient Care and Measurements of Philips Research Eindhoven

Centre of Informatics and Systems of the University of Coimbra (CISUC)

ACKNOWLEDGMENTS

This dissertation marks the end of a five-year journey that has unfolded to be one of the most challenging and rewarding times. Although any possible acknowledgement of this comes up short, I would like to express my appreciation for each and every person who has embarked this adventure with me, who has joined along the way, and, foremost, to the ones celebrating today with me.

This dissertation could not have been possible without the professionals whom I had the opportunity to learn from over the past year. I would like to thank Professor Paulo de Carvalho, Professor Jorge Henriques, Doctor Jens Muehlsteff, Doctor Esther van der Heide, and Doctor Gabriele Papini for showing me the true essence of research, for sharing their knowledge with me, and for all the guidance to change directions while overcoming the difficulties that appeared along the way. A very special thank you to Professor Paulo, for all the valuable ideas and support throughout this dissertation, to Esther and Gabriele for all the patience, constant fruitful advice, and efforts to make my time in the Netherlands better, even with limited moments in person.

Obviously, my everlasting gratitude goes to whom I owe everything that I am, my family. My deepest appreciation to my parents, who have been my pillars in life, for always obligating me to fight and never letting me take anything for granted. Also, to my sisters (Matilde, Marta, and Eva) and my grandma for being my haven, having the friendliest words in every moment. On a very special note, I would like to express gratefulness to my grandad, who played the biggest prank on us. In loving memory of him, I hope he is proud of his dumb little girl and commemorating with us yet another victory.

I am forever grateful to my friends for their unwavering support in every moment, never letting me go down. A very special thanks to Mariana, my lifetime friend who has always been the most assertive person and has the dower of altruism. Andreia, the simple summer co-worker who has become a friend for every moment no matter how (physically) far apart we are; Paulete, for being the best friend I could ever ask for this journey and all the unforgettable adventures (especially those as roommates in Leuven and Copenhagen), camaraderie, and sincerity (GIGO). To all the friends that Coimbra brought me (*Jardim d'Impostores*, Marli, Maria João and my *academic goddaughters* Bia, Maria, and Marta), a heartfelt thanks for these incredibly years filled out of good memories. And to all the wonderful people that I got to meet in Eindhoven, thank you for making me feel completely at home in a city where I landed without knowing anyone and during such a peculiar time, you are the best luggage I brought with me.

Lastly, a big thank you to me for the courage to take all those big jumps into the unknown along these past 5 years and for filling them of opportunities to learn and grow. For all the resilience and, mostly, for not fearing failure.

"Ever tried. Ever failed. No matter.

Try again. Fail again. Fail better."

SAMUEL BECKETT

RESUMO

Sendo reconhecido que o processo de nocicepção está relacionado com o Sistema Nervoso Autónomo (ANS), os níveis de nocicepção podem ser indiretamente avaliados através da análise de parâmetros fisiológicos. Desta forma, a análise da variabilidade da frequência cardíaca (HRV) torna-se fulcral para o estudo das respostas autonómicas subjacentes aos estímulos nociceptivos. A importância da análise da HRV deve-se ao facto desta tornar possível a análise de alterações no equilíbrio do ANS. No entanto, torna-se bastante desafiador conseguir uma análise significativa e objetiva da HRV uma vez que este parâmetro é interdependente em sistemas regulatórios neuronais e cardíacos que se modelam a qualquer estímulo ambiental ou psicológico. Batimentos ectópicos representam um dos fatores que condicionam a análise significativa da HRV e, portanto, torna-se crucial que se limite o risco de conclusões erróneas aquando da interpretação de informações clínicas.

A Analgesia Nociception Index (ANI) é uma tecnologia atualmente comercializada com o intuito de possibilitar um melhor controlo do stress cirúrgico através de uma medida contínua e não invasiva do tónus do sistema nervoso parassimpático. Ao longo deste estudo, tirando vantagem da simulação controlada de dados, verificou-se a importância da correção de intervalos ectópicos antes da interpretação clínica dos valores de ANI, pois o algoritmo demonstrou ser sensível à identificação precisa da localização dos batimentos cardíacos.

Foram construídos conjuntos de dados editados através da introdução de intervalos ectópicos nos sinais HRV de controlo que foram previamente extraídos de dados reais de pacientes. Os dados clínicos incluídos neste estudo fazem parte da VitalDB, uma base de dados intraoperatória disponibilizada publicamente, tendo sido incluídos 105 pacientes sujeitos a cirurgias de conservação mamária. Diversos métodos foram explorados para a correção dos intervalos ectópicos que foram artificialmente inseridos nos sinais de HRV de controlo. Para diversos graus de ectopia artificialmente introduzidos, o desempenho dos métodos referidos foi avaliado através do erro absoluto médio (MAE) e da informação mútua normalizada (NMI).

Numa proporção de 10% de intervalos ectópicos e antes de aplicar algum método de correção ectópica, os valores de ANI calculados através dos sinais HRV editados eram significativamente diferentes dos valores ANI calculados através dos sinais HRV de controlo (MAE = 30.56 ± 10.18, NMI = 0.04 ± 0.07), limitando a monitorização adequada do tónus do sistema nervoso parassimpático. Depois de ser efetuada a validação estatística dos resultados, a técnica proposta neste trabalho para corrigir intervalos ectópicos consiste em substituir esses intervalos por intervalos R-R estimados com um modelo autorregressivo. As discrepâncias entre

as variáveis ANI calculadas através dos sinais de HRV de controlo foram significativamente reduzidas com a aplicação da técnica proposta (MAE = 1.66 ± 0.78, NMI = 0.41 ± 0.11). Assim, é plausível assumir que a técnica proposta para corrigir intervalos ectópicos tornará a interpretação clínica do algoritmo de ANI mais robusto à presença de batimentos ectópicos numa proporção de 10%.

Pode ser verificado que a previsão de amostras futuras dos sinais de HRV é um dos principais objetivos do processamento da sua informação, sendo benéfico para diversas aplicações clínicas, nomeadamente na monitorização de nocicepção em pacientes anestesiados. Apesar da dificuldade de treinar um modelo capaz de aprender o comportamento geral de sinais de HRV de diversos contextos clínicos e de ainda ser necessária uma futura validação dos resultados, a técnica proposta neste estudo poderá ser integrada no desenvolvimento de futuros algoritmos baseados na análise da HRV.

Palavras-chave: Nocicepção, Batimentos ectópicos, Simulação de electrocardiogramas, Analgesia Nociception Index, Variabilidade da frequência cardíaca

ABSTRACT

Nociception and the autonomous nervous system (ANS) are recognized to be remarkably related, and, consequently, nociception levels can be indirectly assessed through the analysis of physiological parameters. Accordingly, analysis of Heart Rate Variability (HRV) becomes of utmost importance while studying the underlying autonomic response to nociceptive stimuli since it attempts to tease out the shifts in the sympathovagal balance. However, meaningful HRV analysis is a major challenge, as it may be constraint by the fact that this parameter is interdependent on regulatory systems corresponding to the neurocardiac modulation to any environmental and psychological stimulus. Ectopic beats represent one of the factors conditioning the measurement of HRV, and, therefore, it is crucial to limit the risk of erroneous conclusions during the interpretation of clinical information.

The Analgesia Nociception Index (ANI) is a technology currently commercialized to allow better control of surgical stress by providing continuous and non-invasive measurement of the relative parasympathetic tonus. Throughout this study, taking advantage of controlled simulated data, the limits of the ANI were assessed, verifying the importance of correcting the ectopic intervals before attempting to clinically interpret the ANI values, as the algorithm would heavily rely on the precise identification of peak timing.

Edited datasets have been composed by artificially introducing ectopic intervals into control HRV signals (ectopy-free) extracted from real patient data. The clinical data included in this study is part of VitalDB, an open-source intraoperative database, and comprised 105 patients undergoing breast-conserving surgery. Several methods had been explored to correct the ectopic intervals artificially introduced to the control HRV signals. The performance of the referred methods was assessed in terms of mean absolute error (MAE) and normalized mutual information (NMI) at varying degrees of ectopy artificially introduced into the baseline HRV signals.

At a proportion of 10% of ectopy and prior to the correction of ectopic intervals, the ANI values calculated from the edited HRV signals were significantly different from the ANI values calculated from the control HRV signals (MAE = 30.56 ± 10.18, NMI = 0.04 ± 0.07), constraining the accurate monitoring of the parasympathetic tone. Posteriorly to statistical validation, the proposed technique to correct the ectopic intervals consists of replacing them with R-R intervals predicted with an autoregressive model. The discrepancies between the ANI variables calculated from the control HRV signals and the edited HRV signals were significantly reduced by the proposed strategy to correct ectopic intervals (MAE = 1.66 ± 0.78, NMI = 0.41 ± 0.11), being plausible to assume that the proposed technique for correction of ectopic intervals would robust the interpretation of the ANI algorithm in the presence of ectopic beats to an extent of 10%.

Therefore, it could be verified that the prediction of the HRV signals would be one of the main targets of information processing, being beneficial in several clinical applications, including the monitoring of nociception in anaesthetized patients. Notwithstanding the difficulty of training a model capable of learning the general behaviour of the HRV signal in a wide range of clinical settings and although further validation is required, the proposal of this study can be integrated into the development of oncoming HRV-based algorithms, thus allowing real-time correction of ectopic intervals present in HRV signals.

Keywords: Nociception, Ectopic Beat, Simulation of Electrocardiograms, Heart Rate Variability, Analgesia Nociception Index

CONTENTS

LIST OF ACRONYMS

AIC	Akaike Information Criterion
ANS	Autonomous Nervous System
ANI	Analgesia Nociception Index
ANI_i	Analgesia Nociception Index Instantaneous
ANI_{lb}	Analgesia Nociception Index calculated based on literature
ANI_m	ANI averaged on a 120-second window
AR	AutoRegressive model
ASA	American Society of Anesthesiologists physical status
AUC	Area Under Curve
BIS	Bispectral Index
BP	Blood Pressure
CARDEAN	CARdiovascular DEpth of ANalgesia
CISUC	Centre of Informatics and Systems of the University of Coimbra
CVI	Composite Variability Index
ECG	Electrocardiogram
EEG	Electroencephalography
EMG	Electromyography
FN	False Negative
FP	False Positive
GA	General Anaesthesia
GSR	Galvanic Skin Response
HBI	HeartBeat Interval
HR	Heart Rate
HRV	Heart Rate Variability
HF	Power of High Frequency band
IASP	International Association for the Study of Pain
ICU	Intensive Care Unit
LF	Power of Low Frequency band

MAE	Mean Absolute Error
MSE	Mean Squared Error
MDL	Rissanen's Minimum Description Length
NMI	Normalized Mutual Information
NN	Neural Network
Noc/ANoc	Nociception - Antinociception
NoL	Nociception Level Index
NSCF	Number of Skin Conductance Fluctuations
NSVT	Non-Sustained Ventricular Tachycardias
OR	Operation Room
PAC	Premature Atrial Contractions
PNS	Parasympathetic Nervous System
PPG	Pulse Oximetry
PPGA	Pulse Photoplethysmography Amplitude
PSD	Power Spectrum Density
PVC	Premature Ventricular Contractions
PVV	Precision
RBBB	Right Bundle Branch Block
RMSSD	Square Root of the Mean Squared Differences
RSA	Respiratory Sinus Arrhythmia
SA	Sinoatrial Node
SBP	Systolic Blood Pressure
SC	Skin Conductance
SD	Standard Deviation
SNS	Sympathetic Nervous System
SPI	Surgical Pleth Index
TP	True Positive
WTCRC	Wavelet Transform Cardiorespiratory Coherence

LIST OF FIGURES

LIST OF TABLES

1 INTRODUCTION

Global volume, complexity, and diversity of surgery has been increasing over the years [1], [2]. Consequently, challenges are created for the clinicians involved throughout the surgical care. Despite not being uniform worldwide, surgery is, undoubtedly, one of the components with the greatest impact for the global health development [1], [3].

Nowadays, it is hard to imagine what surgery would be like without anaesthesia. Seeking to improve health outcomes, anaesthesiology has been evolving alongside with the surgical procedures aiming to provide hemodynamic stability and a fast recovery for the patient [2]. Optimal adjustment of the anaesthetic state is beneficial to the patient's outcome but requires good insight in terms of physiological dynamics. This represents a major challenge for clinicians particularly during general anaesthesia, as the patient is unconscious and a direct assessment on the adequacy of anaesthetic management is not possible.

General anaesthesia (GA) is commonly described in literature as a triad of core components: hypnosis (level of unconsciousness), muscle paralysis (immobility), and analgesia (pain relief) [4], [5]. No single drug can lead the patient to an optimum combined state and, consequently, the anaesthesiologist relies on the combination of specific drugs to ensure the monitoring of each of the components of GA, aiming to provide homeostasis throughout the surgical procedure [5], [6]. Anaesthetic drugs combination and titration depend on the available information, including drugs pharmacokinetic properties, patient data, clinical background, and monitored physiological responses to treatment [6]. A more automated anaesthetic administration, which allows the control of the three main components of the GA, is desirable, as it can contribute to the maintenance of homeostasis during surgery and improve the patient's outcome [7]. Hypnosis and muscle paralysis have monitors widely accepted and commercialized, but there is no standardized solution capable of objectively translating the analgesic component [8]–[11].

Nowadays, the clinicians' decision-making process for the administration of analgesics mostly relies on the evolution of hemodynamic parameters controlled by the autonomous nervous system (ANS), such as heart rate (HR), sweating, pulse oximetry (PPG) and blood pressure (BP) [5], [11]. Nevertheless, it should be noted that these parameters lack specificity and sensitivity and, therefore, a state of homeostasis cannot be inferred from the absence of physiological response to stimulation.

Since the quantification of pain is extremely difficult due to the inherent subjective psychological aspects, research has been directed towards the development of technologies to assess the nociception-antinociception (Noc/ANoc) balance, i.e., the balance between noxious stimulation and antinociceptive effects of the induced analgesia

[11]. Hence, these technologies assume that an autonomic stress response is triggered with noxious stimuli and can be controlled by continuously monitoring the administration of analgesics, blocking the activity of the sensory neurons [2], [5]. However, clinicians find it difficult to differentiate sensory responses to noxious stimulation under different levels of administration of analgesics. And, therefore, judging the adequate state of analgesia becomes extremely challenging, with both under- and overdosing having adverse outcomes (see Figure 1.1).

In line with the above, it becomes of uttermost importance to develop an objective nociception index, allowing to personalize the analgesic component so that clinicians can make the best use of clinical information, validating predictions about the patient's homeostasis.

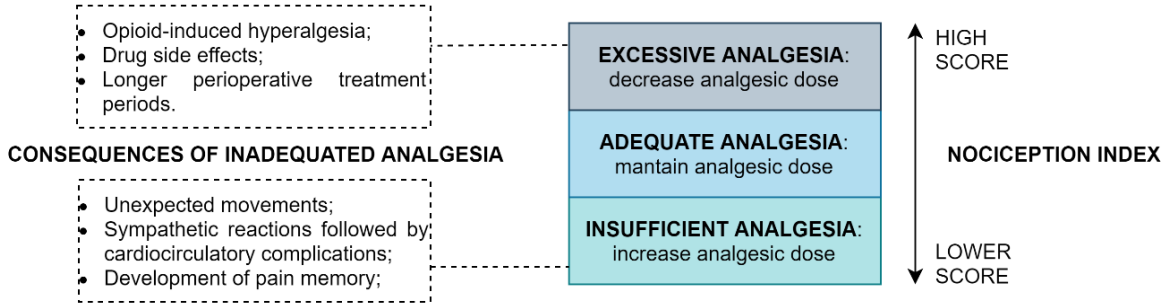

Figure 1.1: Consequences of improper analgesia monitoring [12], and possible structure of an index translating the Noc/ANoc balance.

1.1 MOTIVATION

Pain is a quality indicator for hospitals, as it can provide information about patient safety, improvements in the delivery of care, and better patient outcomes [13]. From an immobilized or uncommunicative patient, it does not follow that the perception of pain cannot be extremely prevalent. Thus, consideration must also be given to the fact that, beyond perioperative care, the development of solutions for pain measurement and management can greatly impact a wide range of patients with cognitive or verbal impairments, such as those in intensive care units (ICU), palliative care units, neonatal intensive care units, and paediatrics.

Not surprisingly, clinical monitoring of pain receives increasing interest among researchers. Despite enlarged scientific evidence in this area, the assurance of accurate levels of analgesia is still beyond some challenges to overcome, as perioperative complications related to improper analgesia monitoring are frequently reported, including postoperative delirium, awareness with recall after surgery and postoperative pain [14], [15]. Moreover, “more than a fifth of patients attending chronic pain clinics cite surgery as the cause for their chronic pain”[16] with perioperative pain control being

acknowledged as contributing to chronic pain after surgery and, subsequently, having a significant impact on the patient's quality of life [16], [17].

Thus, the major current goal of individually tailored anaesthesia is to develop a Noc/ANoc indicator to guide the maintenance of analgesia levels within a narrow therapeutic window. The reinforcement of best practices would lead to the administration of minimal efficient drug dose and, consequently, to the prevention of over- or underdosing avoiding adverse outcomes of improper monitoring of anaesthetics. So, moving towards a more dynamic monitoring of analgesia, it is not about suppressing everything (as much as it is not about not suppressing at all), but rather knowing what is being measured, combining the context and information obtained from the clinical monitors.

Nowadays, there is a growing number of commercialized solutions for monitoring nociception in sedated unconscious patients that appear to reflect intraoperative stimuli slightly better than the subjective use of vital signs by the anaesthesiologists [11], [18]. Yet, although there are promising results, there is also potential for improvement since all the technologies proposed so far lack reliability and validity by presenting limitations in defining the adequate state of Noc/ANoc balance [11].

In fact, predicting nociceptive responses by assessing the autonomic balance is a major challenge since the ANS is responsible for regulating many bodily functions and, so, its activity is susceptive to the modulation by different mechanisms [19]. Thus, it may be difficult to interpret changes in the physiological parameters driven by the ANS activity as they vary in a complex and non-linear way, whatever the cause that led to it. Furthermore, the impact that variability inter-patient has on the evolution of physiological parameters must also be considered [19], [20].

Consequently, the interpretation of information retrieved by the majority of the current technologies for nociception monitoring is contraindicated in the presence of confounding factors for the sympathovagal balance [21], [22]. Arrhythmias and any medication affecting the cardiovascular autonomic control are two of the factors identified as confounders [22], [23]. This may represent a significant hindrance to the routine use of these technologies, as it is estimated that patients with heart and cardiovascular comorbidities represent a substantial part of the population included in the daily anaesthesiology practice [24]. Moreover, in Europe, 42% of surgical complications during non-cardiac interventions are associated with cardiac complications [24]. The occurrence of ectopic beats represents one of the significant confounder factors assessing the autonomic activity [25] because ectopic beats are commonly seen in the perioperative period and are highly incident in apparently healthy individuals [26]–[29].

In this sense, a robust complementary quantitative solution is demanded to monitor nociceptive stress with sufficiently broad applicability. This measure would have to prove its clinical value by fulfilling numerous requirements, including be a real-time continuous

measurement of easy implementation and interpretability. While ensuring patient safety, it should allow predicting hemodynamic responses and reflecting the levels of responsiveness to noxious stimulation related to administration of analgesics in the various relevant clinical endpoints, taking into consideration the context and any confounding factors [30].

1.2 CONTEXTUALIZATION AND CONTRIBUTIONS

Moving towards a more automatic, personalized, and effective administration of analgesic drugs, the most ambitious goal would be to develop an objective measure of nociception that should be able to support clinical decisions in a wide range of applications and to lower the incidence of postoperative pain and side-effects related to improper monitoring of analgesia.

Given the broad scope of the pain measurement and management topic, this thesis is particularly focused on the exploration of the heart rate variability (HRV), because it is one of the most widely used parameters to assess changes in the autonomic activity and, over the past few years, research has been highlighting the potential of HRV for nociception measurement [22], [31]. Furthermore, HR is measured during all surgeries with anaesthesiologists primarily relying at variations in the HR as surrogate of the Noc/ANoc balance.

Notwithstanding, among the technical and biological artefacts that may distort the measurements of HRV, ectopic beats represent one of the significant confounder factors for the HRV analysis, which, consequently, conditions the assessment of the sympathovagal balance [31]. From a clinical point of view, it becomes of uttermost importance to limit the risk of erroneous clinical conclusions while assessing the measurements of HR dynamics.

In the light of the above, this thesis is not focused on the development of a new nociception monitoring tool, but rather on a new perspective to overcome the presence of ectopic beats or mis-detected heartbeats while analysing intraoperative HRV measurements. In this sense, since it provides both quantitative and qualitative information on the HRV, the Analgesia Nociception Index (ANI) was the main HRV measurement used throughout the assessment of the impact that ectopic beats could have on the HRV analysis [22]. To the best of knowledge, although studies have been concluding that the presence of ectopic beats distorts the ANI calculation [22], no study was found investigating to which extent the presence of non-sinus intervals would be acceptable.

Research grasping the topic of nociception measurement still lacks pilot studies balancing factors known to influence nociceptive response [11]. Addressing this gap, the acquisition of biomedical data combining different parameters to assess autonomic

reactivity to noxious stimulation was initially planned. However, the clinical trial has been delayed due to constraints related to the COVID-19 pandemic and, under the scope of the internship at Philips Electronics Nederland B.V. (Eindhoven), no publicly available database was found to meet the requirements of the General Data Protection Regulation. Therefore, this dissertation has been redirected to the simulation of electrocardiograms (ECG). Thus, the HR dynamics could be derived in a controlled manner, allowing the testing of different processing techniques and algorithms.

A comparative study was then carried out with the objective of exploring different methods of correction of ectopic intervals, attempting to diminish in some extent the sensibility of the ANI to the presence of ectopic beats. This part of the research was performed at CISUC and made use of both real intraoperative patient data and simulated data contaminated to various degrees of non-sinus beats. No data has been shared with Philips Research employees.

1.3 GOALS

From all that has been said, the main objective of this dissertation is to limit the impact that the occurrence of ectopic beats has on the analysis of HRV signals. In line with the main objective, specific goals have been defined as:

- Development and validation of a tool to simulate ECGs with known HR dynamics.
- Implementation of the ANI algorithm.
- Assessment and interpretation of the impact that the occurrence of ectopic beats has on the ANI calculation and on the information that is provided by this technology.
- Performance comparison between different methods applied for correction of ectopic intervals artificially generated.
- Reduction of the sensibility of the ANI to the presence of ectopic beats, making it sturdier and leading to a substantial improvement in its clinical interpretation.

1.4 STRUCTURE OF THE THESIS

In terms of structure, this dissertation is organized into 6 Chapters.

Chapter 2 describes the background concepts necessary for a better understanding of the work developed in this thesis. This chapter comprises the review of technologies currently proposed to augment the existing knowledge on the measurement of the

Noc/ANoc balance during GA. Moreover, the ANI index is revised in more detail so that the outlines of this study could be consolidated.

Chapters 3, 4, and 5 represent the three different phases of this dissertation, presenting the methodologies employed in each one and respective descriptions and interpretation of results. Specifically, Chapter 3 comprises the process of developing a tool to simulate ECG in controlled clinical contexts encompassing normal and ectopic beats. Chapter 4 focuses on the implementation and assessment of the limits of the ANI algorithm, namely with regard to its sensibility to the chosen beat detector and the occurrence of ectopic beats. Chapter 5 discusses the performance of different methods for correcting ectopic beats.

Finally, Chapter 6 presents the global conclusions of the work developed in this thesis and opens the door for further work to be done.

2 BACKGROUND CONCEPTS

The background concepts focus on the relevant clinical concepts addressed in this work.

The chapter starts with the understanding of the concepts of pain and nociception: the fundamental pathways, and the mechanisms inherent to a stress response, followed by an overview of the different biomedical signals that could be employed to translate the dynamic of the autonomic activity; a more comprehensive review on the HRV analysis, since this physiological parameter is extensively studied throughout this work. The chapter ends with the state-of-art of nociception monitoring technologies and a systematic review on the ANI.

2.1 PHYSIOLOGY OF PAIN

2.1.1 Pain and Nociception

It is noteworthy to mention that pain and nociception are distinct phenomena [32]. So, in order to proceed with the analysis, one needs to fully understand the difference between these two concepts.

By the definitions of the International Association for the Study of Pain (IASP), pain is "an unpleasant sensory and emotional experience associated with, or resembling that associated with, actual or potential tissue damage" [32], whereas nociception refers to "the neural process of encoding noxious stimuli" [32].

Contrary to pain, which is a multidimensional complex phenomenon influenced by biological, psychological, and social factors, nociception is not subjective and can be inferred from the activity in sensory neurons [32]. From nociception, it does not follow pain since pain involves the translation of the noxious stimulus in the cortex [32].

2.1.2 Mechanisms of pain perception

Pain is a complex neurophysiological phenomenon that can be seen as a defence mechanism in response to sources of noxious stimulation since it cannot be deducted that an unresponsive and uncommunicative patient cannot experience pain [32].

The encoding of sensory information is a highly plastic and non-linear process that involves the transduction of physicochemical stimuli, transmission across the neuroaxis and cortico-thalamic signal processing (see Figure 2.1) [33].

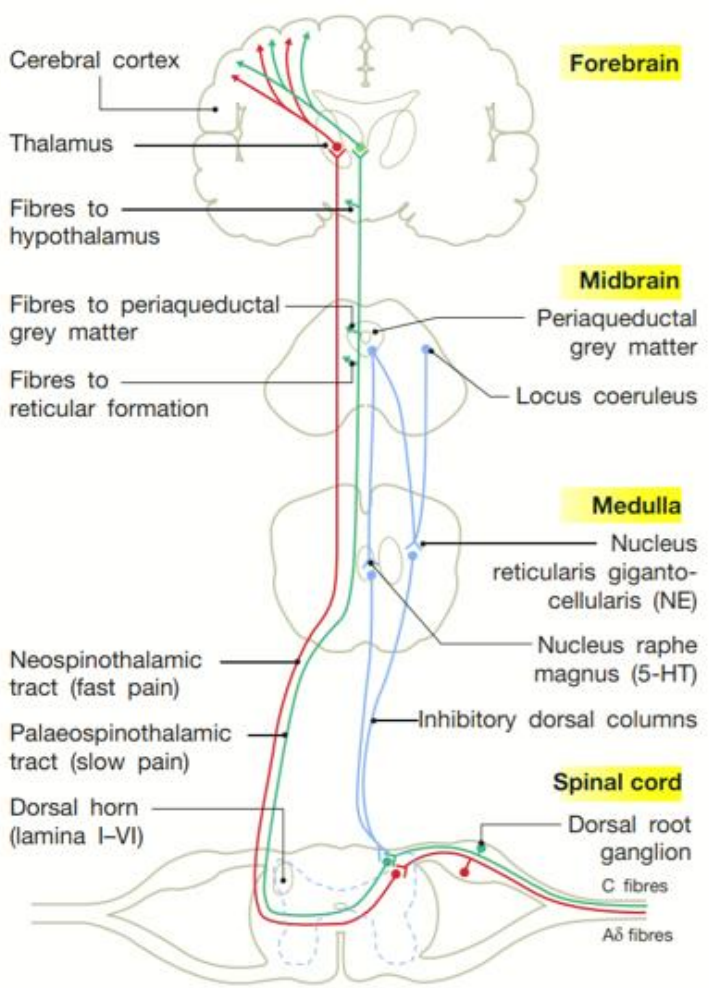

Figure 2.1: Spinal and supraspinal pathways of pain: ascending nociceptive fast (red) and slow (green) pathways; descending inhibitory tracts (blue). (Source: [33])

Ascending pain pathways comprise nociception through the detection of potentially harmful stimuli by the primary afferent nociceptors and subsequent arousal of extensive interactions involving neurochemical and neuroanatomic systems [5], [33], [34]. As from the nociceptive input discrimination, the descending pain modulatory system regulates pain signalling in the nervous system and initiates autonomic, endocrine, and motor outputs [17], [33]–[35].

Anatomically, the ANS is composed of two opposing branches: the sympathetic nervous system (SNS) and the parasympathetic nervous system (PNS). Known as the sympathovagal balance, the two branches of the ANS are tonically active and complementary: while the activation of the SNS is thought to promote "fight-or-flight" responses being quickly activated in processes of elevated activity (stress responses), the PNS stimulates the "rest-and-digest" mechanism in several aspects of function [2]. Functionally, many bodily functions depend on autonomic control, including breathing, cardiac activity and vasomotor activity [2].

Being part of an integrated central network, it is recognized that the nociceptive stimulus and the ANS systems are remarkably related [35]. Consequently, nociception levels can be indirectly assessed through the analysis of physiological parameters such as HR, respiration rate, stroke volume, BP, pupil diameter and galvanic skin conduction.

Furthermore, since the ascending and descending tracts of pain perception are within a loop, analgesic agents may be administrated to prevent stress responses by centrally inhibiting the pain pathways at the dorsal horn gate [5]. However, as previously mentioned, the administration of minimal efficient drug dose is still a major concern for clinicians because, despite being crucial to avoid adverse outcomes from improper monitoring of anaesthetic drugs, the precise mechanism by which these substances act is not fully understand and there is no quantitative standard technology to guide the administration of analgesic substances.

2.2 BIOMEDICAL SIGNALS RELATING THE ANS MISBALANCE

The understanding of how the experience of pain is processed in the brain has increased through clinical studies using neuroimaging techniques, such as Positron Emission Tomography and functional Magnetic Resonance Imaging [36]. While advances in neuroimaging have tackled the cortical structures related to the sensor neurons elicited by nociceptive stimuli, several biomedical signals have been studied to inspect autonomic activity through physiological parameters and augment the existing knowledge about manifestations of nociceptive stress [11], [36].

One of those biomedical signals is the ECG which allows detection of the electrical activity of the heart. The ECG is one of the most recognized and used biomedical signals since it is a non-invasive technique of easy acquisition that helps to diminish the patient's exposure to the risk of infection. Parameters derived from ECG measurements can provide clinicians a continuous assessment of ANS reactions to surgical stress [37], [38].

Providing a direct measurement on the electrical functioning of the brain, electroencephalography (EEG) has been extensively studied to inspect the autonomic activity regarding nociception. Namely, evoked potentials have been inspected through the EEG analysis in order to gain understanding on the cortical mechanisms inherent to nociceptive stimulation and perception of pain [39], [40].

Photoplethysmography is a non-invasive technique to detect local variations of blood volume [41], [42]. The standard PPG waveform comprises two components: direct current (DC) and alternating current (AC) components. While the DC component is mostly related with low-frequency variations (e.g., respiratory venous volume fluctuations, vasomotor activity, and thermoregulation), the AC component refers to beat-to-beat variations, high-frequency variations [41]. Several studies have addressed

the sympathetic vasoconstrictor reflex to measure nociception using techniques related to the AC component of the PPG waveform [21], [41].

Reflecting the cardiovascular status, non-invasive blood pressure measurements may also be used to reflect changes in the sympathetic tone, namely increases in blood pressure as a response to noxious stimuli [41].

Galvanic skin response (GSR) might be considered a vital sign representing the electrodermal activity in the palmar surface under sympathetic control [43].

Electromyography (EMG) measures somatic responses through the muscular electrical activity and can be employed to predict patient's movements in case of improper anaesthetic state [44].

Meanwhile, practical difficulties in biomedical signal acquisition (such as physiological artefacts, interference and/or patient discomfort and safety) might undermine the intraoperative use of some of the aforementioned measurements [37]. It should be also taken into consideration the accessibility of variables to measurement in the context of an operation room (OR).

Furthermore, as many factors can impact the interpretation of the different vital signs, it is required to inspect interrelationships and interactions among physiological systems. Hypothetically, a multivariate approach (comprising a combination of physiological parameters) might be required when attempting to strengthen nociception measures by diminishing sensitivity to confounding factors [11], [45]. Hence, a multi-parameter score would have to provide evidence of its advantageous usage by being capable of adding value to the anaesthesiology practice and provide a better (and more specific to surgical stress) insight into the ANS functioning.

2.3 HEART RATE VARIABILITY

The cardiac rhythm corresponds to the cycles co-ordinately controlled by an electrical conducting system composed of fibers that generate and conduct electrical potentials through the heart (see Figure 2.2) [37]. The sinoatrial node (SA), being considered the natural pacemaker of the heart, is controlled by autonomic processes and is crucial in determining cardiac electrical stability (see Figure 2.3) [19]. Because of autonomic regulation, triggering the SA leads to the release of neurotransmitters: acetylcholine for vagal stimulation; or epinephrine for sympathetic stimulation.

According to the American Heart Association and the European Heart Network, the HRV parameter is a non-invasive technique relatively easy to calculate which consists of the variation in time between consecutive cardiac cycles [25]. Hence, among the wide range of parameters employed to measure the sympathovagal balance, HRV analysis has proved

its clinical importance being currently acknowledged as one of the most promising available techniques to provide insight into the sinus rhythm modulated by the autonomic function [19].

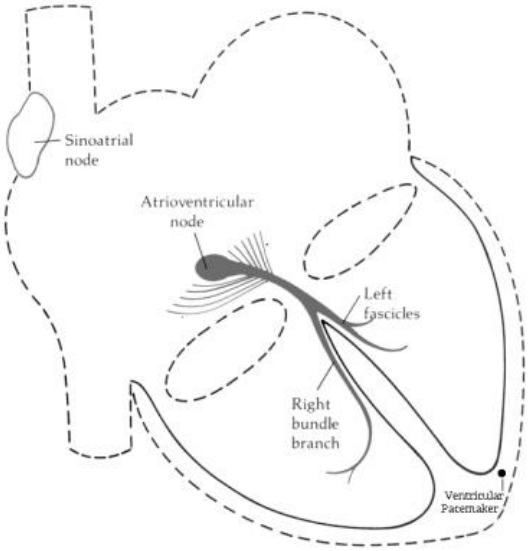

Figure 2.2: Representation of the heart (a hollow muscular organ composed of two atria and two ventricles) and the source nodes its electrical conducting system. (Source: [46])

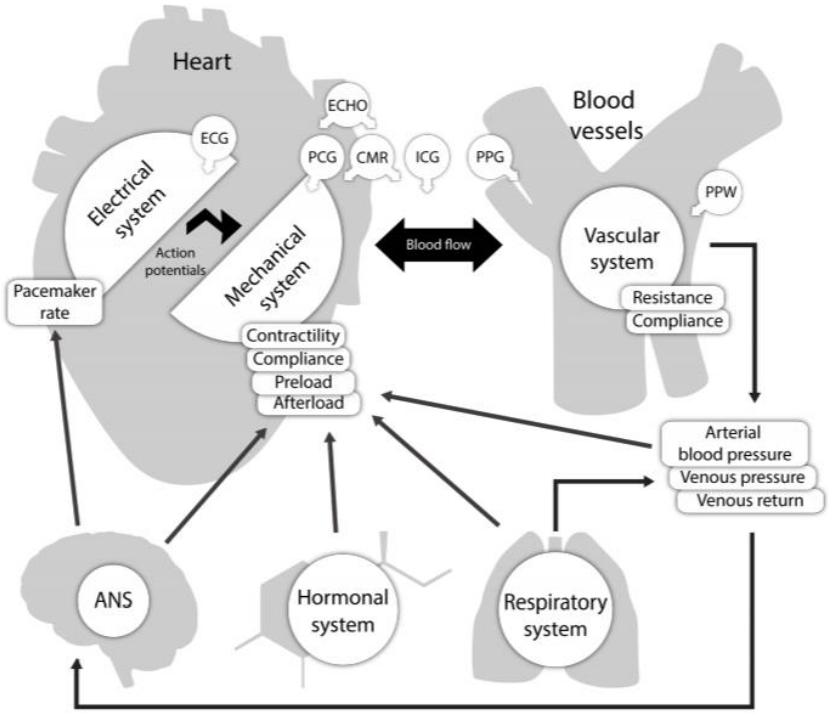

Figure 2.3: Schematic representation of the different monitoring solutions according to the interactions between the subsystems involved in cardiac activity. ECG (electrocardiography), PCG (phonocardiography), ECHO (echocardiography), CMR (cardiac magnetic resonance), ICG (impedance cardiography), PPG (photoplethysmography) and PPW (pulse pressure wave). (Source [47])

As a matter of fact, the spectral analysis of HRV has demonstrated its potential to add value on the understanding of the activity underlying ANS reactivity: while the power in the Low Frequency band (0.04-0.15)Hz is said to be linked to both the sympathetic and

parasympathetic tone, the power in the High Frequency band (0.15-0.4)Hz is mediated by the parasympathetic tone and respiration (through the Respiratory Sinus Arrhythmia (RSA)) [25].

As previously stated, the autonomic control is closely coupled with the systems modulating the perception of pain. Therefore, HRV analysis has been indicated as a surrogate measure to enhance the current knowledge on the measurement of the Noc/ANoc balance through the assessment of the ANS activity.

2.3.1 Measuring the HRV

The measurement of HRV involves calculating the time interval of consecutive cardiac cycles. As from Figure 2.3, the cardiac cycle may be described by studying different biomedical signals and their derived parameters. So, compared to other physiological parameters, the main clinical advantage of HRV is the fact of reflecting the autonomic activity and, simultaneously, being easily derivable from biomedical signals typically available in the OR. This thesis focus on the ECG waveform, as it is readily identifiable, aiding to identify fiducial points for further investigation of the cardiac cycle events [37].

The typical ECG waveform (Figure 2.4) is closely related with the manifestation of cardiac contractile activity throughout the cardiac cycle. The sequence of waves that characterize the events of the electrical activity of the cardiac muscle can be briefly summarized. The cardiac cycle begins with the SA triggering the depolarization of the atria which represents the P-wave on the ECG. Combined with atrial repolarization, the QRS complex is caused by the rapid depolarization of the ventricles. And the slow T-wave results from the repolarization of the ventricles [37], [48].

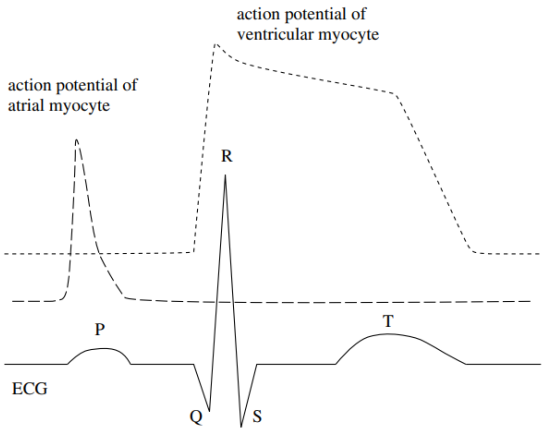

Figure 2.4: Typical ECG waveform for one heartbeat and the action potentials of atrial and ventricular myocytes. (Source [37])

Notwithstanding, it is noteworthy that the use of ECG signals to assess the autonomic activity through the HRV analysis becomes a challenge as ECG waveforms are measured as electrical potentials and may be seriously impacted by various types of artefacts [25],

[37]. For example, cardiovascular disturbances and abnormalities modify the ECG waveforms; therefore, the ability to locate the R wave (often used as a fiducial point for beat-to-beat analysis) rely on signal processing techniques being highly dependent on the patient, the ECG equipment, and the beat detection algorithm utilized [31].

2.3.2 Factors influencing HRV

Despite being an empirically and computationally tractable measure of the ANS processes, HRV lacks specificity as it is a complex and non-linear measure dynamically changing over time mediated by different factors [31], [49].

Inter-patient differences must be taken into account as multiple demographic factors contribute to differences in HRV baseline, including gender, age, genetics, and medical condition [20], [50]–[52]. Modifications of HRV may be introduced by several intervention strategies affecting the sinus node (the heart's natural pacemaker) to achieve a better circulatory stability, namely the usage of β-blockers, α-2 agonists, and atropine [23], [31].

On an intra-patient basis, as many bodily functions are dependent on a neurocardiac modulation, the HRV analysis might not be specific to stress or pain and it may account other factors such as RSA, changes in the stroke volume, the baroreflex and the vasovagal reaction, and circadian rhythms [31].

Moreover, artefacts may be electro-physically originated and temporarily disrupting the analysis of heart-brain interactions [31], [37]. Besides technical artefacts, ectopic beats may occur prematurely in the cycle due to blocking the propagation of electrical potentials from the SA to the ventricles [31]. The occurrence of these non-sinus beats may masquerade the HRV measurement on the assessment of autonomic function. Therefore, all the ectopic beats must be effectively corrected [31]. Otherwise, the HRV metrics may not be a representative measure of the SA activity.

VENTRICULAR PREMATURE BEATS

Since the cardiac electrical conducting system is composed of subsidiary pacemakers, the non-sinus beats can be generated from any region of the heart with varying frequency of impulse formation and morphologies [26], [29], [53]. The ectopic beats correspond to beat-to-beat intervals deviating from the normal heartbeat intervals and are usually classified as atrial, auriculoventricular junctional or ventricular. The focus of this work is the ventricular premature beats (PVC) [26], [53]. Figure 2.5 illustrates an example of a segment of ECG with a PVC in a set of sinus beats.

Instead of being initiated by the SA, PVCs are generated on the ventricles by the Purkinje fibers and are the most common arrhythmias detected in patients with no structural

heart disorder [54]. The mechanism underlying the occurrence of PVCs remains unclear, being hypothesized that it may result from more than one process [26], [53].

Although descriptions and morphology of PVCs may vary according to their origin, the ventricular ectopic beats are often characterized by a broaden QRS complex since the impulses are conducted through differing conduction systems comprising the excitation of the ventricular muscle fibers [37]. In addition, unless it occurs a retrograde conduction through the atrioventricular node, the PVC is typically followed by occurrence of a full compensatory pause prior to the next normal beat [37].

Precise detection and classification of PVC is of uttermost importance since, despite commonly occurring in healthy individuals, a high incidence of PVCs may lead to ventricular arrythmias associated with various cardiac conditions.

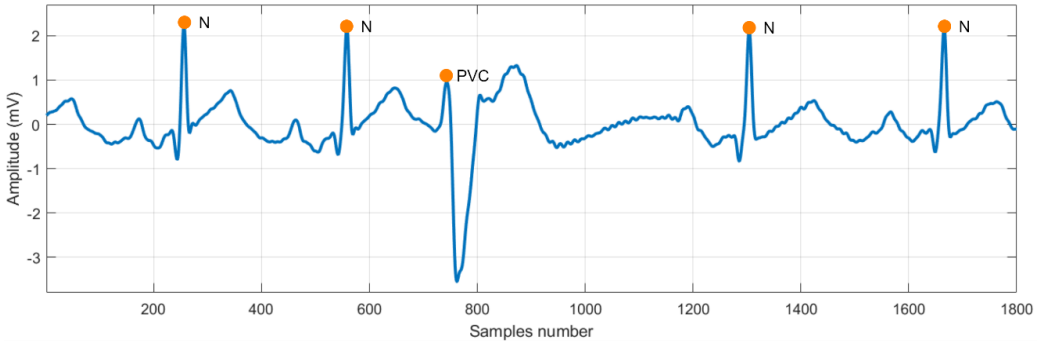

Figure 2.5: ECG signal with a ventricular ectopic complex (PVC) in a set of normal beats (N) for subject 228 of the MIT-BIH Arrythmia Database [55].

2.4 The state-of-art of nociception monitoring technologies

As already outlined, pain has been seen as the new quality indicator for hospitals with studies for the development of a nociception monitoring tool being a topic of great research interest. This section gives a comprehensive analysis on the most reported and tested nociception monitoring indexes in unconscious patients.

Nowadays, several methods are widely used to measure pain intensity or unpleasant sensations in conscious patients. These methods include numerical scales (e.g., Visual Analogue Scale, or Numerical Rating Scale) and multimodal questionnaires (e.g., McGill Pain Questionnaire) [56]. Although having proved to be valuable for pain management in conscious and communicative patients, these methods become obsolete when trying to assess pain in sedated patients.

Over the past few years, several approaches have been trying to provide insights into the management of pain perception in patients unable to communicate, as is the case of

patients undergoing surgery with GA. While some of the proposed approaches rely on dose-dependent responses ([57]) and others on the strength of the reaction to a given stimulation([58], [59]), the main trend focuses on the indirect assessment of the Noc/ANoc balance by evaluating the response to surgical stress, i.e., using physiological signals during GA to analyse ANS reactions (increase in sympathetic activity or corresponding decrease in parasympathetic tone). However, no golden standard is yet established for objectively monitoring nociception in sedated unconscious patients.

Only the technologies addressing the translation of the Noc/ANoc balance during surgery were investigated in this work. Table 2.1 presents an overview characterizing several indexes currently proposed to assist the anaesthesiologist in controlling analgesia during GA. More detailed review and comparison are available, e.g., in [11] and [60]. The aforementioned approaches differ mainly by the biomedical measurements explored for the translation of the Noc/ANoc balance, being generally based on algorithms that output an index score between a range of dimensionless values [11].

Even proving their ability to assess the surgical stress response, all the proposed technologies present significant limitations that hinder their clinical standardization. Clinicians can only rely on the purposed indexes under very specific conditions. Mathematical processing and interpretation are a major concern when developing a Noc/ANoc indicator because the baseline values of physiological parameters vary inter- and intra-patient [11]. In fact, a transversal limitation to the clinical use of any of these indexes is the definition of an adequate state of Noc/ANoc balance due to the sympathovagal balance being strongly influenced by confounding factors.

When attempting to implement and standardize a new analgesia assessment tool, one also needs to account for the economic feasibility demanded. The proposed approaches should warrant patient's safety (e.g., non-invasively measure) while striving to overcome the shortcomings eventually originated by implementation settings of the monitoring system (e.g., easy installation and interpretability) [30]. Additionally, the requirement for any additional sensors (e.g., CARDEAN, see Table 2.1) to those already clinically available in anaesthesia practice may also hamper the routine use of a purposed approach.

Several purposed technologies for nociception monitoring have been already commercialized (e.g., ANI and SPI). However, it should be emphasized that, beyond fully understanding the characteristics of the monitoring device, clinicians must still take into account the clinical context and the general purpose of monitoring in order to make proper use of the clinical information retrieved by the monitor and, eventually, adequate the administration of the analgesics.

From a clinical point of view, a standard index should represent a significant improvement for the anaesthetic practice, adding value to both the patient and the anaesthetic practice, efficiently controlling the administration of analgesics, postoperative outcomes, and hemodynamic maintenance.

INDEX	BIOMEDICAL SIGNAL	PHYSIOLOGICAL PARAMETERS	MEASUREMENT PRINCIPLE	LIMITATIONS	REFERENCES
ANI	ECG	HRV-HF	- Cardiac parasympathetic tone	- Physiological artefacts: arrhythmia, apnea, low respiratory rate, electric noise - Drugs or therapies affecting the sinus node - Irregular spontaneous ventilation due to speech, laugh or cough - Inconclusive studies revealed to validate ANI predictions of intraoperative hemodynamic changes	[22]
CARDEAN	Non-invasive continuous BP and ECG	HRV, SBP	- Sympathetic tone (cardiac baroreflex)	- Physiological artefacts: vasoconstriction, hypovolemia - Reports only an association between the inhibition of the cardiac baroreflex and nociceptive stimuli - Medication or therapy affecting the autonomic function - Designed to predict unexpected intraoperative movement in non-paralyzed patients - Requires additional sensors to those usually available in anaesthesia practice	[61], [62]
CVI	EEG and facial EMG	BIS, facial EMG	- Somatic activity	- Muscle relaxants may influence facial EMG activity - Physiological artefacts: hypoxia, hypotension, cerebral ischaemia or hypoperfusion, muscular activity - Unclear variability inter- and intra-patient due to the use of different types and concentrations of anaesthetics	[44], [63]

Table 2.1: List of some of the purposed nociception evaluating indexes; ANI (Analgesia Nociception Index), CARDEAN (CARdiovascular DEpth of ANalgesia), CVI (Composite Variability Index), NoL (Nociception Level Index), SC (Skin Conductance), SPI (Surgical Pleth Index), WTCRC (Wavelet Transform Cardiorespiratory Coherence)

INDEX	BIOMEDICAL SIGNAL	PHYSIOLOGICAL PARAMETERS	MEASUREMENT PRINCIPLE	LIMITATIONS	REFERENCES
NoL	PPG and SC	HR, HRV-HF, PPGA, SCL, NSCF, SC derivatives	- Sympathetic tone - Temperature - Accelerometery	- No proof of concept for clinical relevance on the use of NoL monitoring - No previous research on the applicability of this index on ICU or conscious patients.	[64]
NSCF	SC	Skin conductance	- Peripheral sympathetic tone	- Do not reflect antinociception reactions related to administration of analgesics - Many confounders and physiological artefacts - No proof of concept for clinical relevance on the use of SC monitoring	[43], [65]
SPI	PPG	PPGA, HBI	- Peripheral vascular sympathetic tone - Cardiac sympathetic tone	- Medication or therapy affecting the sympathetic nervous system act as confounders on the absolute SPI level - Patient's medical condition: intravascular blood volume and chronic history of hypertension - Variability interpatient - No correlation found between SPI values and stimulus intensities	[21]
WTCRC	ECG and capnometer	HR, Respiration Rate (%CO_2)	- Coupling between RSA and HR	- Physiological artefacts: arrhythmia, apnea - Medication, therapy, or disorders affecting autonomic function - The algorithm requires adaption for real-time analysis - Lacks sensitivity - Implementation settings of the monitoring system (capnometer usage)	[66]

Table 2.1 (continuation): List of some of the purposed nociception evaluating indexes; ANI (Analgesia Nociception Index), CARDEAN (CARdiovascular DEpth of ANalgesia), CVI (Composite Variability Index), NoL (Nociception Level Index), SC (Skin Conductance), SPI (Surgical Pleth Index), WTCRC (Wavelet Transform Cardiorespiratory Coherence)

2.4.1 Interpretation of the Analgesia Nociception Index

The ANI is claimed by the manufacturer as an innovative technology that provides a continuous and non-invasive measurement of the relative parasympathetic tonus (p∑ tone) allowing monitoring of comfort and better control of the surgical stress [22]. The ANI relies on the quantification of the RSA through the calculation of the area delimited by the lower and the upper envelopes of the R-R time series (more detail on the ANI calculation in Chapter 4), so the higher the computed area, the higher the parasympathetic activity, the higher the ANI value and possibly lower physiological stress, and less nociception [11], [22].

In terms of clinical interpretability, the ANI is a dimensionless score (0-100) that may have a probabilistic role in predicting hemodynamic reactivity following nociceptive stimulation [22]. Preliminary studies have settled that the analgesia level is adequate if the ANI value falls in the range between 50 and 70 with hemodynamic reactivity being unlikely to occur in the following 10 minutes; the analgesia level is inadequate if the ANI value is lower than 50 with hemodynamic reactivity being likely to occur in the following 10 minutes; there is possibly an excessive administration if the ANI value is above the level of 70 [11], [22].

Nowadays the MDoloris ANI monitor is the only commercialized one-parameter index based on HRV analysis. On the account of the goals of this thesis, a review was carried out to assess the importance and reliability of using the ANI monitor in different clinical contexts such as in surgeries under GA or in ICU.

2.4.2 Literature review of the performance and limitations of the Analgesia Nociception Index

Following the procedure described in Figure 2.6, the computerized databases PubMed and Scopus were searched in April 2021 without any restrictions to publication types or regions. To retrieve the possible relevant articles, the keywords “Analgesia Nociception Index”, “ANI”, “Mdoloris”, “pain monitoring”, “analgesia”, “nociception” and “pain” were used. An initial selection was performed only including studies (1) published between January 2018 and March 2021 in (2) English, and with (3) full text available. Then, after removing duplicates, manuscripts were assessed for eligibility if either title, abstract, and full text met the following criteria: (4) empirical investigation in (5) human, (6) adults (aged between 18 and 65).

Quantitatively assessing the overall results, it is possible to observe the increasing interest of the scientific community on this topic over the years. A total of 22 papers were included in the review and listed more detailed in Appendix A. When appropriate, studies prior to 2018 were also referenced for the robustness of the analysis performed.

Although the validation of the ANI monitor has been extensively studied under different conditions, reported results are controversially discussed, evidencing the clinical challenge of pain management.

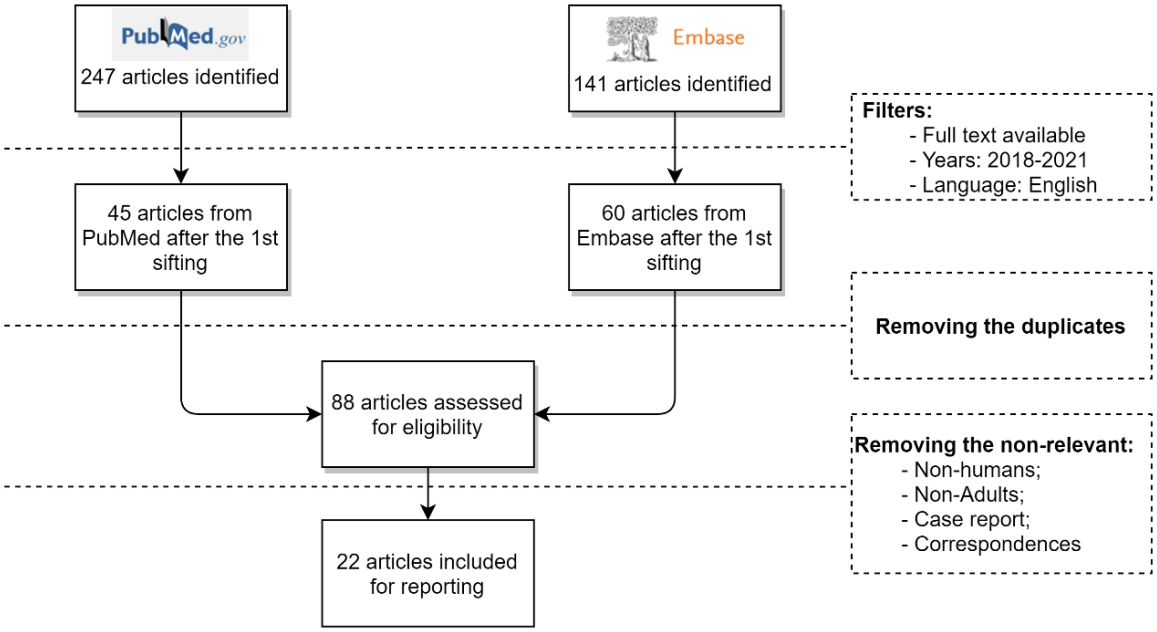

Figure 2.6: Flowchart of the studies search for systematic review.

Firstly, clinical effectiveness of ANI in monitoring nociception/pain is analysed, optimizing opioid consumption, and preventing opioid-related adverse events in adult surgical patients undergoing GA. In fact, the ANI monitor has been being evaluated through its potential to provide information equivalent to the actions of the clinicians regarding monitoring of analgesia during surgery. While several studies have been reporting that ANI may outperform traditional physiological parameters (such as HR and BP) at reflecting noxious stimulation [67]–[70], others were found inconclusive in proving that ANI objectively assesses the balance between pain and analgesia during GA [71].

The performance of the ANI on the assessment of different levels of responsiveness to noxious stimulus in terms of noxious stimulus intensity and different levels of analgesic drugs have not been extensively studied. In this respect, considering [72], the amplitude of the variation of the ANI variable in response to different intensities of induced noxious stimulus revealed to not be predictive of hemodynamic or somatic reactions; a previous study performed with awake patients also concluded that ANI was not able to differentiate between sham and noxious stimuli, but other factors such as stress and emotions were recognized to influence the results [73]. Moreover, only one study was found on the inspection of the performance of ANI-monitoring reflecting the stress response to tetanic stimulation for different concentrations of analgesic drugs [68]. The authors concluded that ANI significantly varied at lower, but not at higher, concentrations of remifentanil.

Overall, inconclusive results were found about the impact of ANI-guided analgesia decreasing intraoperative stress responses, including the occurrence of hemodynamic events. Some studies have observed that the ANI may be appropriate to anticipate the demand for a dose change so that intraoperative adverse events can be circumvented [67], [70], [74], [75]. Others concluded ANI monitoring not to be clinically relevant in predicting undesirable intraoperative hemodynamic changes [30], [71], [72], [76]. The main differences with respect to results on the predictive value of the ANI-monitoring may lie in the use of dynamic variations of ANI and in its evaluation in distinct predefined time points with different sedation levels such as induction of anaesthesia (including intubation period, if applicable), first skin incision, steady state, and at emergence from anaesthesia (including extubating period, if applicable).

Studies conducted over the past few years have been skimpy that ANI monitoring optimizes the opioid titration and may avoid under- or overdosing [77]–[81]. This finding is consensual among the studies, being transversal to the use of different opioids substances (remifentanil, sufentanil or fentanyl) and in different contexts (general anaesthesia, regional anaesthesia, or sedation in ICU) [77]–[81]. However, conflicting evidence is found regarding the postoperative opioid use and the capability of ANI-guided analgesia predicting opioid-related side effects, including acute postoperative pain. Visual Analog Scale, Verbal Rating Scales and Numerical Rating Scales are commonly employed to assess pain in conscious and cooperative patients during postoperative period. Previous studies have found a correlation between ANI-guided opioid administration and lower incidence of postoperative pain [82], [83], but, posteriorly, reports have concluded that ANI monitoring would not be clinically associated with reduced side effects or complication rates of improper analgesia [79], [84], being ineffective in predicting the occurrence of postoperative pain [69], [77]–[81], [85]. These differing findings may be attributable to the fact that these studies investigated patients undergoing surgeries with different incidence rates of postoperative pain and different protocolized anaesthesia techniques (for example, postoperative adverse events are specific to the type of analgesics administrated [6]). Yet concerning surgical outcomes, preliminary findings have been suggesting the potential of the ANI monitoring in predicting the risk of hypotension related to spinal anaesthesia [86]. Although a recent study suggested that maintaining ANI above 50 during, at least, 60% of the anaesthesia may be useful to reduce the length of stay in the postoperative recovery room [84], previous research found no statistical clinical benefit from ANI monitoring in terms of lengths of stay in the postoperative recovery room or hospital discharge [80], [81], [87], [88].

The results may seem to deviate since the findings on the usefulness of ANI monitoring in a perioperative context are overall inconclusive. In fact, to date, no proof-of-concept exists on clinical relevance of the use of ANI. Several reasons may be pointed out to partially explain the discrepancy observed between the findings from studies comprising patients under GA [19], [20]. These reasons may include the anaesthetic protocols [88],

[89] or severity of the painful stimulus during the type of surgery performed [69], [81], [84]. For example, hypnosis has been reported to cause an increase in the parasympathetic tone influencing the required administration of opioids and, so, although further validation is needed, ANI monitoring may be influenced by the type of hypnotic substances administrated and might be useful to measure the intensity of the hypnotic process [89].

Notwithstanding, none of the above-listed findings can be extrapolated to all patients under GA since studies eligible for analysis were commonly performed without a representative sample in terms of both type of surgical procedures and inter-individual variability factors known to influence hemodynamic and stress responses to noxious stimulation. Many of the studies considered eligible for reporting only included healthy volunteers (ASA I) and common exclusion criteria were patients prescribed with drugs affecting the sinus node (atropine, anticholinergic drugs, beta-receptor blockers, vasoactive drugs, etc.) or having any disorder affecting the autonomic activity or the respiratory patterns, such as arrhythmia, apnea, irregular spontaneous ventilation, implanted pacemakers, or heart transplant. Therefore, statistical artefacts may contribute to the controversial findings reported by researchers as no heterogeneous studies were yet published and a large proportion of patients who comprise the routine clinical practice was commonly withdrawn from conducted research.

The ANI was designed as a tool to monitor intraoperative pain in patients under GA, but its effectiveness has been investigated in (semi-) conscious patients, including sedated patients in ICU or under regional anaesthesia. To date, several studies in awake patients (with no effect of anaesthetic drugs) have concluded that the ANI may be employed to assess parasympathetic changes related to different emotional states, demonstrating that the higher levels of ANI are related to a more relaxed state [90]–[92]. Regarding conscious patients under the effect of analgesic drugs, contradicting results were published. Some authors reported significant differences in the ANI values between patients with and without pain [77], [78], [81], [93], [94], while others found no relationship between ANI and self-rated pain [76], [95]. This may be due to the fact that the interpretation of scores resulting from the application of the ANI to assess parasympathetic tone in conscious patients under the effect of analgesic medication must take into account the status of the patient. In fact, the ANI was designed to reflect the autonomic activity and, so, other than pain and anaesthetic protocols, a plethora of confounding factors experienced by the patient (such as emotions, stress, and anxiety) may cause an increased sympathetic tone. Consequently, the cut-off values for detecting pain in conscious state may be different from the suggested by the manufacturer for patients under GA and not proportional to the degree of analgesic dose [76], [77], [89], [96]. Moreover, a recent study with patients on ICU, diagnosed with COVID-19, and on mechanical ventilation revealed that the dynamic variations of ANI may reveal worse prognosis and higher mortality [93]. As for patients under GA, no evidence-based clinical benefit exists for ANI monitoring in

conscious patients in emergence units or ICU, demanding further research to validate the role of the ANI monitoring in the management of pain in conscious patients.

Furthermore, the ANI monitor has been being compared to other monitors in terms of effectiveness for the assessment of nociception. Yet, no evidence has been identified that either index outperforms the others. Constraint by the limitations hindering the clinical use of pupillometry, one study reported that the variation coefficient of pupillary diameter correlates more strongly with the self-rated pain (using the Visual Analog Scale) than ANI [85]. Several studies reported the SPI and ANI to perform comparably for detecting pain in conscious patients but not to outperform the intraoperative analgesia guided by the anaesthesiologist [80], [94], [96]. Additionally, one study showed that, under the administration of remifentanil, the SPI may reflect the degree of pain more effectively than the ANI [94].

Overall, within the noticeable limitations, the ANI monitoring already present promising results for being clinically relevant benefit under strict conditions. Nevertheless, nociception monitoring remains an unmet challenge, being required more studies to corroborate and optimize the ANI interpretation in numerous clinical conditions. Therefore, future research would only benefit of more heterogeneous studies performed in more controlled environments to accurately assess the clinical impact of ANI monitoring. Furthermore, most of the studies included in this analysis correspond to observational studies. The controversy of the results published so far may highlight the need to move from observation to experimentation.

3 SIMULATION OF ECG

HRV analysis and its clinical use have been recognized as of utmost importance for assessing the regulations of the autonomic and central nervous systems and obtaining the R-R intervals from ECG signal processing is one of the best-known methods for its calculation [31]. However, extracting useful clinical information from ECG requires reliable signal techniques to avoid erroneous conclusions.

Over the years, the promising results from the multiple applications of simulators have accelerated the pace of research. Therefore, simulated ECG signals may be preferable to compare performances of competing signal processing techniques since the underlying dynamics of the ECG signal is then known [37].

This chapter focus on the development of an ECG signal simulator that should be able to generate the heartbeat's morphology, while accurately reproducing the inputted beat-to-beat intervals according to the respective annotation vector on beats' classification. So, this tool would allow to infer the performance of algorithms in different clinical scenarios by allowing to include, for example, ectopic beats in a quantifiable and controlled manner.

3.1 METHODOLOGY

The strategy consisted of exploring the already available ECG simulators and focus on the one that could be the most promising by simultaneously reproducing the input R-R time series and generating realistic synthetic ECG [97]–[99]. As a result, the ECGSYN simulator was identified as the most promising [55].

3.1.1 ECGSYNmod: tool for ECG signal generation

The ECGSYN model is available at [55] and it is explained in full detail elsewhere [99]–[102]. Briefly, the software uses a model based on a three coupled ordinary differential equations to reproduce features of a typical human ECG signal with known characteristics [99]. The typical trajectory (Figure 3.1) is generated in a three-dimensional (3-D) state-space with coordinates (x, y, z) being obtained through a fourth order Runge-Kutta integration of dynamical equations of motion given by a set of three ordinary differential equations [102]. Accordingly,

$$\dot{x} = \alpha x - wy \tag{3.1}$$

$$\dot{y} = \alpha y - wx \tag{3.2}$$

$$\dot{z} = -\sum_{i \in \{P,Q,R,S,T\}} a_i \Delta\theta e^{\left(-\frac{\Delta\theta^2}{2b_i^2}\right)} - (z - z_0) \tag{3.3}$$

, where $\alpha = 1 - \sqrt{x^2 + y^2}$, $\Delta\theta_i = (\theta - \theta_i) mod\ 2\pi$, $\theta = atan2(y, x)$, w corresponds to the angular velocity [102]. The term z_0 refers to the baseline wander and it was specified according to [102], being defined as $z_0(t) = A\sin(2\pi f_2 t)$, with A = 0.15 mV and f_2 corresponding to the respiratory frequency. The average morphology is defined utilizing the motion of the trajectory in the z-direction and specifying the values of the parameters a_i, b_i and θ_i for the PQRST points [102]. The value of a_i represents the z-position of extrema, the value of b_i represents the Gaussian width of peaks and the value of θ_i represents the angles of extrema (in degrees).

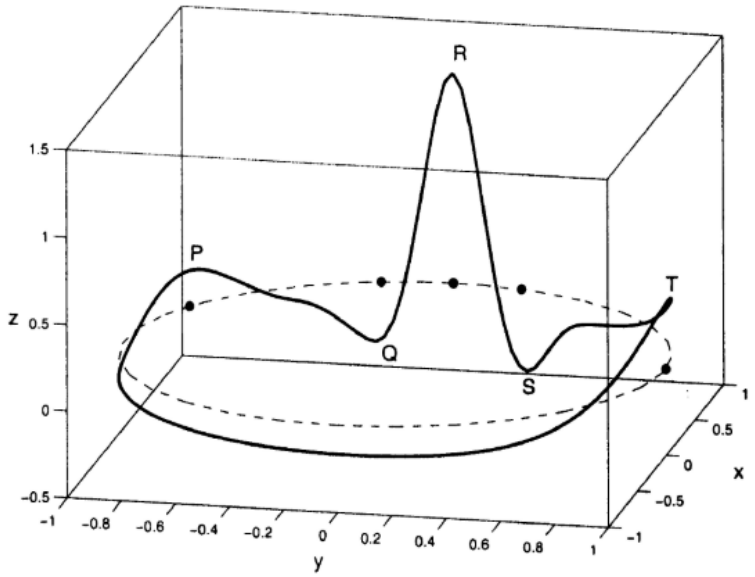

Figure 3.1: Typical trajectory generated by the proposed model. (Source [99])

In addition to the average morphology, the original software determines the heart rate dynamics by allowing the operator to specify the mean and standard deviation of the heart rate and some spectral properties [99]. So, the first modification to the original software consisted of modifying it so that the operator specifies the R-R series instead of the model parameters to calculate its dynamics.

From preliminary analysis performing the simulation of ECG with a normal sinus rhythm, it was noticed that the software had some limitations including timing discrepancies between the input and output R-R time series. Although these discrepancies were found not to be significant, they could lead to erroneous HRV analysis. So, the core of the software was inspected, and several potential causes were pointed, namely the use of different sampling frequencies, and different steps of integration. Both factors revealed to impact the generated ECG signal. To overcome these discrepancies and for further insertion of PVC, as suggested in [99], a beat-to-beat variation in the morphology was attempted by introducing a parameter to control the timing of the position of any of the

P, Q, R, S, and T events. The results still revealed differences on the R-R series. Since the priority was to obtain accurate reproduction of the location of the R peaks rather than detailed morphologies (e.g., useful to detect ST depression or elevation), a more pragmatic approach was therefore followed by introducing a post-processing step.

Figure 3.2 illustrates the functioning mode of the tool developed to generate ECGs with known dynamics, here called ECGSYNmod. This tool consists of using the ECGSYN software to, individually, simulate different types of beats ('Normal' or 'PVC'). Then, the simulated beats are concatenated with the previous segments to generate an ECG signal with known characteristics. Therefore, to operate the ECGSYNmod tool, one should define one vector with the positions of the R-peaks and another vector with the annotations for beat type. The annotation vector is binary, in which a value of 0 corresponds to a normal beat, and a value of 1 corresponds to a PVC beat.

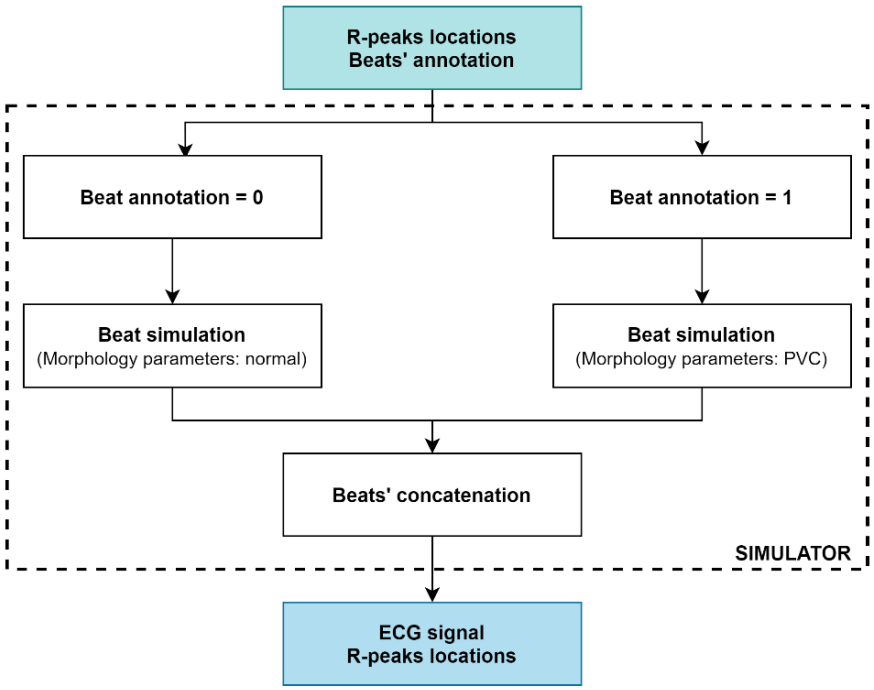

Figure 3.2: Flow chart describing the ECG signal simulator developed

The post-processing step differs between the beat types. Hence, it follows the description of the post-processing steps introduced when simulating normal or PVC beats.

3.1.1.1 Post-processing of normal beats

An annotation with value 0 corresponds to the so-called normal beats which represent the typical noise-free Lead II ECG waveform obtained from a signal with normal sinus rhythm. The generation of normal beats begins creating an interval time series within the range of 0.2 to 2 seconds and evenly spaced by $1/(sampling\ frequency)$. Then, an

ECGSYN engine with the morphological parameters a_i, b_i and θ_i defined in Table 3.1 is used to generate the PQRS and T waves for every interval.

As the exact location of the R-peaks is retrieved by the ECGSYN engine, the generated ECG signal is segmented through the R-peaks events and the beats are stored, forming a beat repository that also contains information on the location of the respective PQRST events.

Index (i)	P^{normal}	Q^{normal}	R^{normal}	S^{normal}	T^{normal}
θ_i	-70	-15	0	15	100
a_i	0.2	-2	15	-1	0.25
b_i	0.25	0.1	0.1	0.1	0.3

Table 3.1: Morphological parameters of the ECG model for the simulation of normal beats. θ_i represents the angles of extrema (in degrees); a_i represents the z-position of extrema; b_i represents the Gaussian width of peaks.

Generating a new normal beat, the ECGSYNmod tool performs a repository search for an existing beat with the specified R-R interval. If no result is found, the closest beat with a longer duration is selected, compressed, and concatenated into the new ECG signal.

3.1.1.2 Post-processing of PVC episodes

An annotation with value 1 corresponds to the simulation of a so-called 'PVC' beat, which represent a typical noiseless Lead II ECG waveform with a right bundle branch block (RBBB) morphology. PVC's morphology depends on the site of origin. Since this work aimed to keep the model simple in terms of morphological parameters and so, only RBBB morphology was focused [26], [103].

The following cases are considered for simulation: consecutive PVC (sequence of 0-N-0 in the annotation vector where N represents the sum of consecutive annotations with value one) and single PVC (sequence of 0-1-0 in the annotation vector, N = 1). According to the sequence of annotations, the locations of the previous beat with a null annotation, the N consecutive beats annotated with the value one, and the next beat with null annotation are considered to calculate the R-R time series of the PVC episode.

From the beat repository, the beat with the longest duration is selected and assumed as the normal beat template. Then, another ECGSYN engine (using the morphological parameters a_i, b_i and θ_i in Table 3.2) is seeded with the processed R-R time series outputting the PVC episode template.

Index (i)	P^{PVC}	Q^{PVC}	R^{PVC}	S^{PVC}	T^{PVC}
θ_i	-50	-50	0	15	100
a_i	0	0	30	-45.5	7.5
b_i	0	0	0.2	0.15	0.3

Table 3.2: Morphological parameters of the ECG model for the simulation of PVC. θ_i represents the angles of extrema (in degrees); a_i represents the z-position of extrema; b_i represents the Gaussian width of peaks.

As the ECGSYN engines provide the locations of the PQRS and T waveform peaks, the simulation of the respective PVC episode is completed by segmenting, time-adjusting, and matching the PVC template and a normal beat template according to the methodology depicted in Figure 3.3.

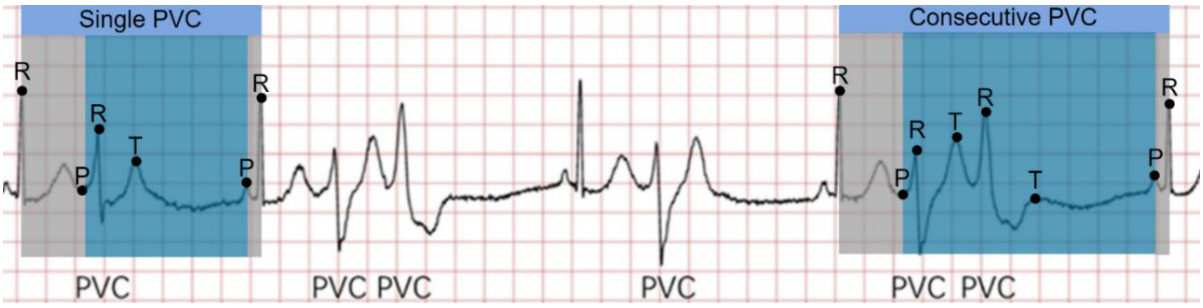

Figure 3.3: Reference points for the segmentation step on the simulation of a PVC episode. In grey the segments correspondent to the normal template and in blue the segments correspondent to the PVC template.

3.1.1.1 Estimation of artificial non-sinus R-R time series

Previous studies have revealed differing HRV analyses after the correction of ectopic beats [31], [104]. Comprehensively comparing techniques for ectopic correction, it would be preferable to have control data (the baseline data ectopy-free) and experimental data (data contaminated with ectopic beats) identically available, apart from the ectopic beats. However, as previously mentioned, the regulatory mechanisms of the HR are complex and constantly adapting to any stimulus and, therefore, it cannot be inferred HR dynamics to be stable over time [31].

In conformity with the above, one extension has been added to the ECGSYNmod tool so that ectopic beats would be artificially introduced in the tachogram, changing the positions of the R-peak. Reviewing the available methods in the literature, the model described in [104] seemed to be the more appropriate. The referred model has demonstrated quantitatively and qualitatively to reproduce reasonably ectopic beats [104] and, thus, it was embedded in the ECG generator tool described previously. Accordingly, the ectopic beats are artificially introduced modifying the intervals before (I_B) and after (I_A) the ectopic beat (equations (3.4) and (3.5), respectively) [104].

$$I_B = -0.0053 \cdot HR + b \quad (3.4)$$

$$I_A = -0.0125 \cdot HR + a \quad (3.5)$$

, where $b \in [0.9474, 1.1966]$ and $a \in [1.8956, 2.1024]$, chosen randomly. The I_B and I_A intervals are function of the average HR of the respective ECG.

The ectopic beats considered in this work are the PVC and consist of beats occurring instead of the sinus beat with an unusual timing (considerably earlier than expected and followed by a compensatory pause). This extension of the simulator can be executed by whether specifying the density of generated ectopic beats and randomly placing the resulting number of ectopic beats across the signal; or specifying the location of the ectopic beats, adapting the R-R time series accordingly. This study was based on the former alternative, while the latter is more useful when simulating specific medical conditions.

This feature of the ECGSYNmod is particularly useful for the comparative study later described in Chapter 5. Figure 3.4 illustrates the effects in the R-R tachogram of artificial addition of ectopic beats.

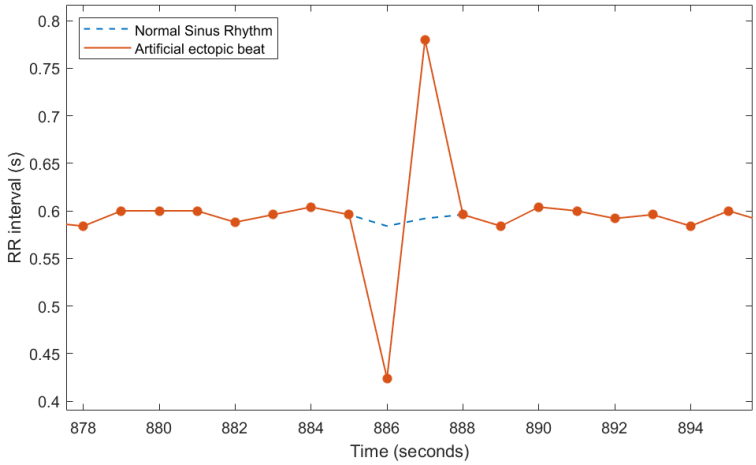

Figure 3.4: Control tachogram resulting from the baseline data ectopy-free (in blue) and superimposed artificially generated tachogram (in orange) resulting from the contamination of the baseline data with ectopic beats.

3.1.2 Simulation Quality Assessment

Across the development of the ECGSYNmod tool, it was necessary to evaluate the capability of the simulator to reproduce the inputted R-R time series. So, one training dataset was composed to analyse the simulator's performance. The training dataset comprises two subsets with ECG signals and their respective annotations of the R-peak location and classification: Subset A contains ECG signals with a normal signal rhythm;

Subset B includes ECG signals with ectopic beats [55]. A more detailed description of the training dataset is available in Appendix B. The ECG signals originally from the subsets are referenced as MIT signals and the respective ECG signals generated at a sampling rate of 250 Hz using the ECGSYN tool are referenced as SYN signals.

In order to assess the performance of the developed ECG generator tool, HRV metrics were computed for both the MIT signals and SYN signals. The computed metrics include the mean of the R-R intervals, the square root of the mean of the sum of the squares differences of successive R-R intervals (RMSSD), the absolute power of the low-frequency band (LF), the absolute power of the high-frequency band (HF), and the ANI variables. The measures in the frequency domain of HRV were computed by analysing the PSD, i.e., the distribution of power as function of the frequency. The PSD was estimated using a Welch's estimator with short-measurement window (300-second window) and 50% of overlap. The LF power is defined in the frequency range of (0.04-0.15)Hz and is said to be linked to both the sympathetic and parasympathetic tone; the HF power corresponds to the (0.15-0.4)Hz band and is mediated by the parasympathetic tone and RSA. The ANI variables considered in this chapter are the ANI instantaneous (ANI_i) and the ANI averaged on a 120-second window (ANI_{lb}). The calculation of these two variables is described in full detail in Chapter 4.

For statistical validation, as the variables were not normally distributed (evaluated with the Kolmogorov-Smirnov test), non-parametric tests were employed [105], [106]. In a first approach, the Spearman correlation coefficient (c) was employed in the statistical analysis to explore the relationships between the metrics extracted from the tachograms calculated from the reference R-peaks positions and that from the R-peaks outputted by the simulator. The interpretation of this coefficient is as follows: c is comprised between -1 and 1 with these limits meaning, respectively, that the variables are the reverse or identical [105]. The Wilcoxon signed-rank test was then employed whenever it was required to perform a comparison between the input and output tachograms from the ECGSYNmod tool [107].

3.2 Results and Discussion

Regarding morphologies, it can be visually inspected (Figure 3.5 for normal beats and Figure 3.6 for PVC episodes) that the adjustment of variables for the two distinct waveforms considered (Table 3.1 and Table 3.2) yield synthetic ECG with realistic morphologies (no normally distributed noise was added). Notwithstanding, further mathematical refinement is needed to overcome some still existing morphological differences.

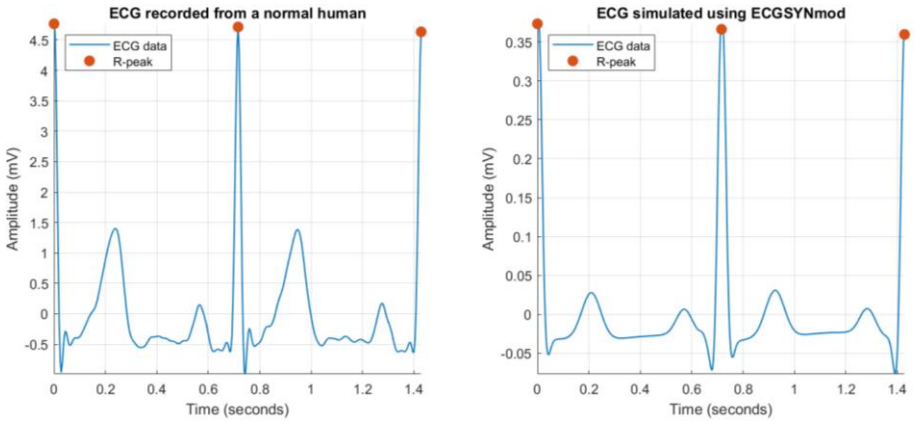

Figure 3.5: Comparison between a segment of ECG recorded from a normal human (on the left) and the respective synthetic segment generated with ECGSYNmod (on the right).

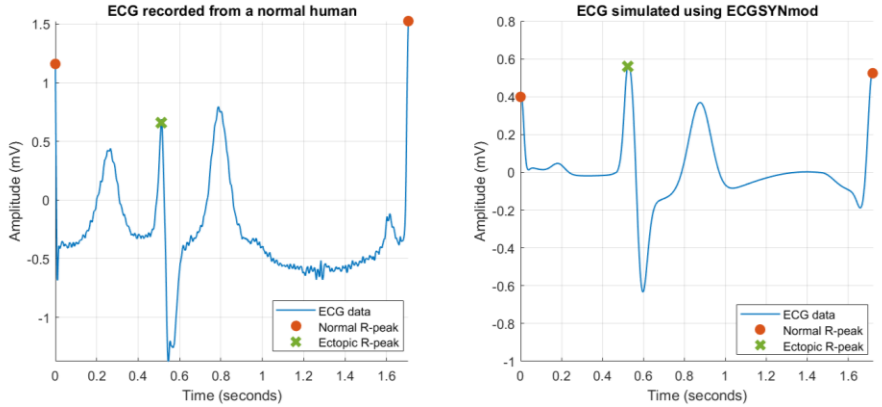

Figure 3.6: Comparison between a PVC segment of ECG recorded from human (on the left) and the respective synthetic segment generated with ECGSYNmod (on the right).

In terms of rhythmicity, exploring the performance of the ECGSYNmod tool in simulating signals with a normal sinus rhythm, the sum of the absolute values of the difference between the MIT R-R series and the SYN R-R series was found to be null in all simulations of subset A. Therefore, this tool was confidently validated for the simulation of ECG signals with a normal sinus rhythm.

Concerning the ECGSYNmod engine for reproducing the input R-R series comprising ectopic beats, the MIT R-R series and the SYN R-R series were found to be highly correlated ($c = 0.9997 \pm 0.0003$) with only slight differences observed when calculating the difference between the two series (see Table 3.3).

Although these are minor discrepancies, it was assessed if they could lead to erroneous analysis in the context of this work and, thus, HRV metrics were made available for both MIT signals and SYN signals.

MIT signal	SYN signal	| Δ R-R intervals (MIT, SYN) | (seconds)
MIT_B1	SYN_B1	0.0013 ± 0.0015
MIT_B2	SYN_B2	0.0018 ± 0.0013
MIT_B3	SYN_B3	0.0011 ± 0.0015
MIT_B4	SYN_B4	0.0018 ± 0.0013
MIT_B5	SYN_B5	0.0013 ± 0.0011

Table 3.3: Sum of the absolute values of the difference between the MIT R-R series extracted from the ECG signals of subset B and the respective SYN R-R series (Δ R-R intervals (MIT, SYN).

	R-R mean	RMSSD	HF	LF	ANI_i	ANI_{lb}
p-value	0.8934	0.9753	0.9753	0.7182	0.7886	0.8079

Table 3.4: P-values for the HRV metrics computed for MIT R-R series extracted from the ECG signals of subset B and the respective SYN R-R series

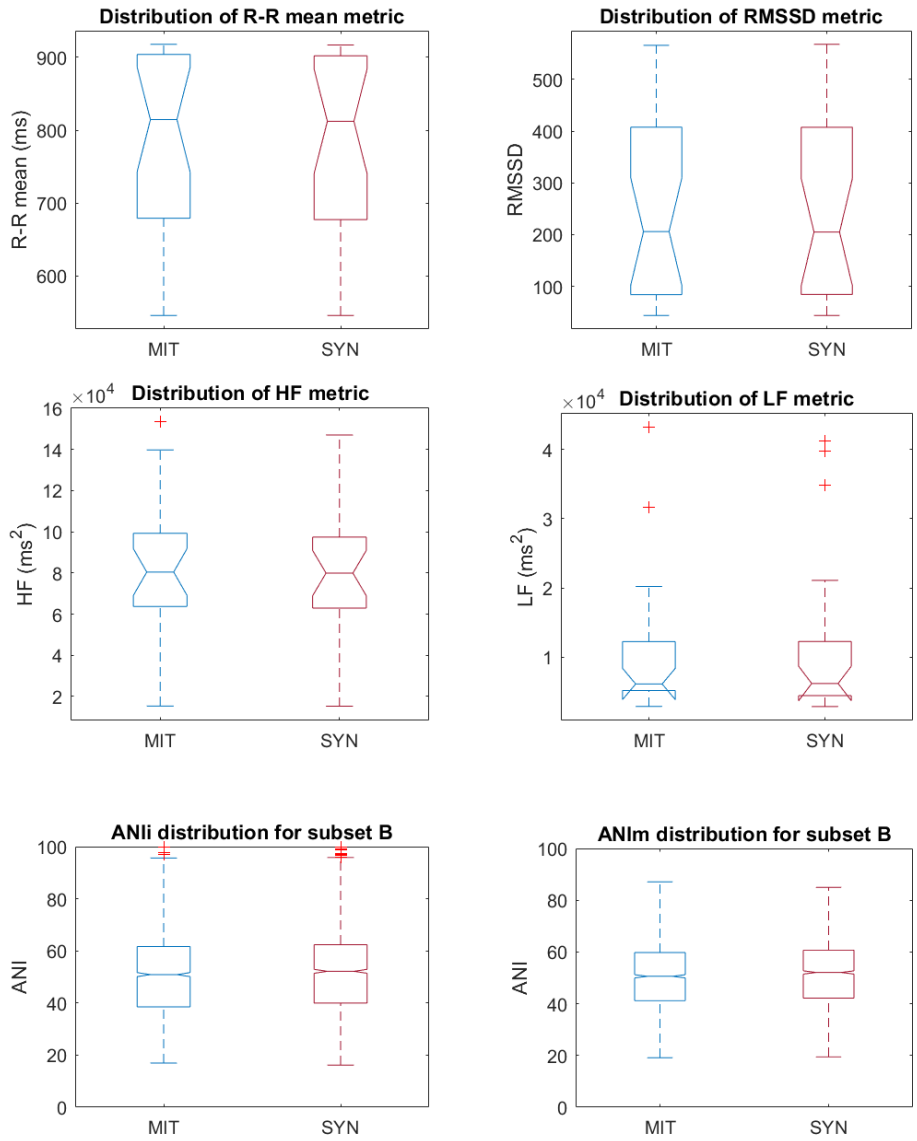

Figure 3.7: Boxplots showing the distributions of HRV metrics extracted for the MIT and SYN signals of Subset B.

From observation of Table 3.4, employing the Wilcoxon signed-rank test, the null hypothesis could be accepted for all comparisons performed and, so, there is no significant statistical difference between the R-R time series extracted from the MIT signals and the SYN signals. The more detailed distributions of the HRV metrics shown in Figure 3.7 corroborate these results.

Note that the discrepancies observed between the R-R intervals series of the MIT signals and the R-R intervals series of the SYN signals may be due to the usage of different sampling rates. The sampling frequency of the MIT signals of subset B is 360 Hz, whereas the sampling frequency of the respective simulated signals was settled at 250 Hz in order to comply with the ANI algorithm specifications (see Chapter 4). Lowering the sampling rate may introduce temporal jitter in the estimation of the R-R intervals. To evaluate if the source of discrepancies between the MIT R-R series and the SYN R-R series is the different sampling rates, the ECGs of subset B were simulated at 360 Hz, and the quality of the simulation was evaluated through the same methodology (except that the ANI variables were not included in the analysis). The results revealed to be similar to those found simulating ECG with normal sinus rhythm and, therefore, it is corroborated that the sampling rate must be carefully chosen, as this may account for some inaccuracies in the results of the simulation.

Overall, analysing the statistical properties of the simulated ECG signal, the ECGSYNmod tool could be validated within the context of this work as being performing according to the required for both normal sinus rhythm and PVC episodes. Figure 3.8 is representative of the generated output using the ECGSYNmod tool, including the ECG values, the R-peaks positions and respective classification (0 – normal beat; 1 – ectopic beat).

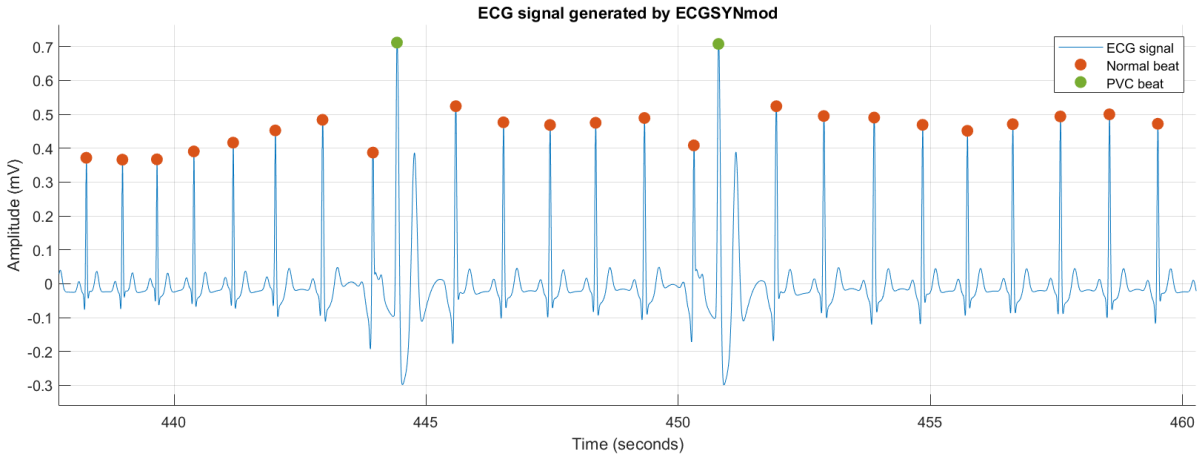

Figure 3.8: Segment of an ECG simulated with the ECGSYNmod tool.

3.3 CONCLUSIONS

The proposed modifications introduced to the ECGSYN software seem to suit the initial desired requirements, encompassing the realistic simulation of ECG signals in a controlled way and with characteristics known a priori. Notwithstanding the previously recognized limitations, the results revealed that the software is capable of simulating ECG signals (encompassing both normal and abnormal beats) statistically similar to the real signals taken from the training database.

Moreover, an extension has been added to the ECGSYNmod tool so that normal beats can be both selectively or randomly converted to ectopic beats (namely PVCs) by modifying the tachogram based on a normal sinus rhythm. This extension is particularly valuable for further assessment of the effectiveness of different processing techniques for computing clinical metrics from the ECG since the baseline would be identical to the contaminated data, except for the additional ectopic beats.

This tool can also be significantly beneficial for several other applications, allowing to identify possible sources of error and preventing their accumulation throughout the workflow. A more sophisticated approach to replace the post-processing step can be considered in the future in order to improve the performance of the ECGSYNmod tool.

4 LIMITS ASSESSMENT IN ANI

Studies comprising the effectiveness of the ANI in different clinical contexts were reviewed in Chapter 2. Although the ANI algorithm appears to be more sensitive to noxious stimulation than the subjective use of vital signs by the anaesthesiologists [67]–[70], the overall findings are inconclusive as the index reveals to be influenced by numerous confounders, including drugs or any other factor interfering with the parasympathetic tonus [22].

The occurrence of ectopic beats is recognized as one of the significant confounding factors for the meaningful HRV analysis [25]. Ectopic beats are commonly seen in the perioperative period and are highly incident in apparently healthy individuals, with increased incidence with age [26]–[29]. Specifically, making use of Holter ECG recording, ventricular premature beats (PVCs) have been detected in 40–75% of clinically normal individuals [28], [29]. Therefore, this chapter is intended to assess how PVCs can impact the interpretation of ANI, an HRV-based metric.

4.1 METHODOLOGY

The approach taken in this chapter started with the implementation of the ANI algorithm, followed by an evaluation of the impact that the performance of the beat detector and the occurrence of ectopic beats could have on the calculation of ANI values.

4.1.1 Implementation of the ANI algorithm

As described in 2.4.1, the ANI algorithm is intended to provide both a qualitative and quantitative measurement of HRV being a dimensionless score varying between 0 and 100 [11]. The implementation of this algorithm was based on both the publicly available descriptions in the literature and the MDoloris product brochure for the ANI Monitor V2 [22], [38], [60], [82], [83], [90], [92], [108]–[116]. Figure 4.1 depicts the schematization for the implementation of the ANI algorithm.

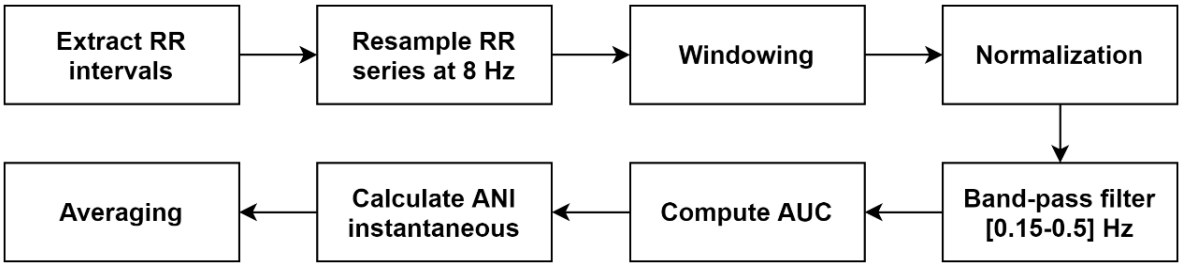

Figure 4.1: Steps described in the literature for the implementation of the ANI algorithm.

The ECG signal is digitized at 250 Hz and the R waves are detected using a R wave detection algorithm [110]. Inputting the R-peak positions, the computation method starts by measuring the evolution of R-R intervals over time.

Before the computation of the ANI values, a real-time filtering procedure is applied so that the unnatural R-R intervals are removed and corrected [116]. The filtered R-R series is resampled at 8 Hz using a linear interpolation algorithm and then, the R-R samples are isolated into a 64-second window sliding by steps of 4 seconds [110]. For inter-patient comparability, within each window, the resampled R-R series is mean-centered and normalized according to

$$RR'_i = \frac{RR_i - \frac{1}{N}\sum_{i=1}^{N}(RR_i)}{\sqrt{\sum_{i=1}^{N}(RR_i)^2}} \qquad (4.1)$$

, where RR_i represents the resampled R-R samples values and N is the number of samples in the window (N = 512) [113].

The method described in the literature is based on the analysis of changes in the HF band of the PSD, which is mainly modulated by the HRV in synchrony with respiration (RSA) [110], [112]. After normalization, the ANI algorithm proceeds to the usage of a numerical filter based on the 4 coefficients Daubechies wavelet to bandpass the respiration effect (0.15-0.5)Hz [115]. Given the sampling frequency of 8 Hz and the frequency bands listed in Table 4.1, levels 4 and 5 were kept and the frequency components between 0.125 and 0.5 Hz were extracted to obtain a signal representative of the RSA for further analysis [38], [92].

Wavelet component	Scale	Frequency band (Hz)
Detail level 1, d_1	2	2 – 4
Detail level 2, d_2	4	1 – 2
Detail level 3, d_3	8	0.5 – 1
Detail level 4, d_4	16	0.25 – 0.5
Detail level 5, d_5	32	0.125 – 0.25
Approximation level 6, a_6	32	0 – 0.125

Table 4.1: Frequency bands as function of wavelet decomposition levels, $f_s = 8\ Hz$

From the resulting series, the local minima and maxima are detected and connected, forming a lower and an upper envelope, respectively. Then, the 64-second window is divided into four sub-windows of 16-second and the area delimited by the envelopes is measured in the four sub-windows (AUC) (Figure 4.2) [113]. The AUC_{min}, defined as the

smallest of the four sub-areas, is retained and the instantaneous ANI value (ANI_i) is computed according to

$$ANI_i = \frac{5.1\, AUC_{min} + 1.2}{12.8} \tag{4.2}$$

Whereas the ANI_i is said to be related to the instantaneous response of the ANS to a particular stimulus, the ANI values averaged on a 120-second window are used to evaluate the imbalance between analgesia and nociception [113].

In terms of clinical interpretability, according to the manufacturer, this index might have a probabilistic role on the prediction of hemodynamic reactivity episodes (correspondent to 20% increase of heart rate or systolic blood pressure compared to a reference) during nociceptive stimulation. Preliminary studies suggest that, in the following 10 minutes, a hemodynamic reactivity episode is unlikely to happen if the averaged ANI is between 50 and 70, and very likely to happen if this measure is lower than 50 [22].

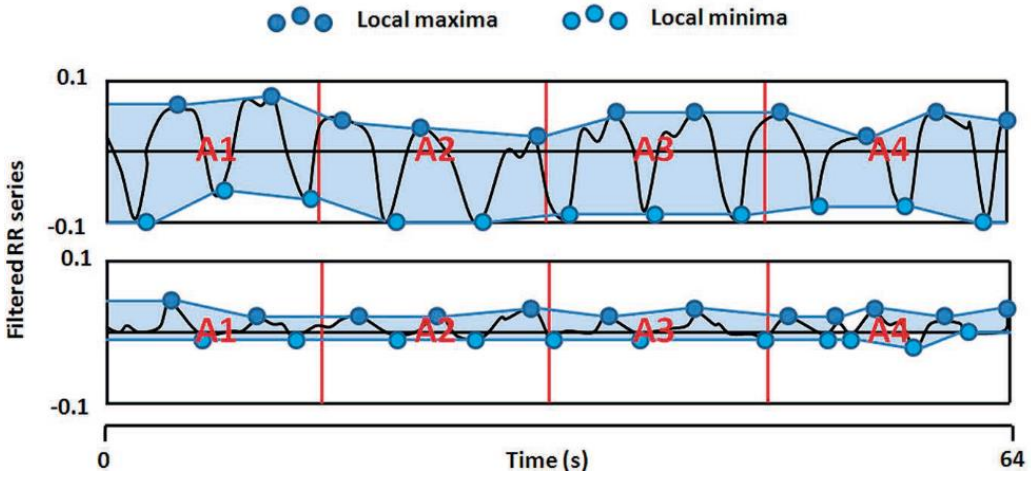

Figure 4.2: Mean centered, normalized and bandpass filtered RR series in a 64-second window during a surgical stimulus concerning an adequate NAN balance (upper panel) and in the case of inadequate anti-nociception (lower panel). (Source: [60])

4.1.2 Metrics and statistical validation for limits assessment in ANI

Results and analysis throughout this chapter were obtained with the training dataset used in the previous chapter to validate the ECGSYNmod tool and whose description is available in Appendix B. Thus, taking advantage of the ECGSYNmod tool, the SYN ECG signals were made available for subsets A and B according to the annotations of the MIT signals for the beat positions and respective classification.

Evaluated with the Kolmogorov-Smirnov test, the ANI variables were found not to be normally distributed and non-parametric tests were applied [106]. To inspect the relationship between the ANI variables computed throughout this chapter, the Spearman

correlation coefficient (c) was employed in the statistical analysis [105]. The Wilcoxon signed rank test was used to compare and infer on statistically significant differences between variables [107].

Regarding the performance assessment of different signal processing techniques, the parameters of sensitivity (equation (4.3)), precision (PVV, equation (4.4)), and F − measure (equation (4.5), metric weighting average of the recall and precision) were considered for analysis.

$$Sensitivity = \frac{TP}{TP + FN} \tag{4.3}$$

$$Precision = \frac{TP}{TP + FP} \tag{4.4}$$

$$F - measure = 2 \times \frac{Precision \times Sensitivity}{Precision + Sensitivity} \tag{4.5}$$

, where TP represents the true positives, FN represents the false negatives, and FP represents the false positives. Moreover, inspecting the performance of different peak detectors, the temporal jitter was also considered as a performance parameter. Temporal jitter corresponds to the standard deviation between the reference R-peak position and the detected R-peak position.

On the subject of the assessment of the impact of the occurrence of ectopic beats on the calculation of the ANI values through the implementation described, the mean absolute error (MAE) and the respective standard deviation (SD) were the evaluation metrics chosen in this chapter. Accordingly,

$$MAE = \frac{1}{n}\sum(|y - \hat{y}|) \tag{4.6}$$

$$SD = \sqrt{\frac{\sum((|y - \hat{y}|) - MAE)^2}{n}} \tag{4.7}$$

, where n represents the number of ANI values calculated, y represents the ANI values calculated for the reference R-peaks positions (ectopy-free), and $\hat{y}$ represents the respective ANI values calculated for the reference R-peaks positions with artificially generated ectopic beats.

4.2 RESULTS AND DISCUSSION

As described in chapter 2, the ANI is one of the currently commercialized technologies for nociception monitoring, being the only single parameter index based on HRV analysis. Therefore, throughout this thesis, the described literature-based implementation of the ANI algorithm (ANI_{lb}) was the metric considered in the analysis of HRV measurements. The detailed assessment of the literature-based implementation of the ANI algorithm is discussed in Appendix C.

4.2.1 Effect of beat detection in the computation of the ANI algorithm

Reliable techniques to identify a fiducial point on the ECG waveform are crucial so that a meaningful tachogram can be obtained [25]. This section intends to explore the impact of inaccurate beat detection in the computation of the ANI_{lb} variables.

The most striking feature of the typical ECG waveform (Figure 2.4) would be the R-peak and, therefore, only detection algorithms written to locate this feature were considered in this work. The following R-peak detectors were considered:

- Minimum detection: technique based on wavelet decomposition of the ECG signal in different frequency bands and employing a peak finding algorithm to detect the QRS complexes above the fixed threshold [117].

- Pan Tompkins: implementation of the Pan-Tompkins algorithm publicly available in [118]; This is a R-peak detector based on the peak energy-amplitude [37], [119].

- Ralph detector: R-peak detector provided by Philips Research, based on [120].

The three methods were then applied to the SYN signals of the two subsets and compared to the reference. Assessing the performance of different R-peak detectors, the detected peak was compared to the ground truth and considered a TP giving a detection tolerance of 72 ms. Otherwise, the detected beat is considered a FP. Within the range of the detection tolerance, the temporal jitter was calculated as the standard deviation between the reference R-peak position and the detected R-peak position. If no peak was detected within the range of ± 72 ms around the reference, it was accounted a FN. Since the objective was to assess whether the results would be dependent on precise timing detection by the R-peak detector, the temporal jitter was allowed to be large by arbitrarily establishing the detection tolerance at 72 ms. Table 4.2 and Table 4.3 list the performance for the R-peak detectors.

Detector	PVV (%)	Sensitivity (%)	F-measure (%)	Temporal jitter (ms)
Minimum detection	99.96 ± 0.06	99.97 ± 0.08	99.96 ± 0.04	3.35 ± 0.15
Pan Tompkins	100.00 ± 0.00	99.76 ± 0.02	99.88 ± 0.02	3.39 ± 0.25
Ralph detector	100.00 ± 0.00	99.88 ± 0.01	99.94 ± 0.01	0.00 ± 0.00

Table 4.2: Performance statistics for QRS detectors applied to the ECG signals of subset A.

Detector	PVV (%)	Sensitivity (%)	F-measure (%)	Temporal jitter (ms)
Minimum detection	99.25 ± 0.71	99.74 ± 0.38	99.49 ± 0.34	4.32 ± 7.04
Pan Tompkins	99.89 ± 0.19	99.63 ± 0.40	99.76 ± 0.24	2.47 ± 2.03
Ralph detector	100.00 ± 0.00	99.96 ± 0.01	99.98 ± 0.01	0.00 ± 0.00

Table 4.3: Performance statistics for QRS detectors applied to the ECG signals of subset B.

The Minimum Detection algorithm automatically identified the peak locations, but the performance of this algorithm depends on the prior adjustment of the threshold for R-peak isolation according to the patient and hardware configuration. Hence, the performance of this method was biased by the manual selection of different thresholds for the subsets A and B.

The evaluation of the results across the two subsets (Table 4.2 and Table 4.3) revealed that all the beat detectors perform comparably. However, it should be noted that for subset B, except in the Ralph detector, the performance of R-peak detectors dropped and diverged, demonstrating that the results from these methods are susceptible to artefact corruption. These discrepancies are even more noticeable for the Minimum Detection method.

The temporal jitter can greatly impact the HRV analysis since it reflects the time variations in the detected R-peak positions from their reference. From Table 4.2 and Table 4.3, analysing the performance of employed detectors, temporal jitter was not observed only when applying the Ralph detector. The minimum detection method, although not being the method with the largest average jitter for both subsets, is the one presenting the largest dispersion of temporal jitter, which may also account for a worse performance of this method on the training dataset.

More than identifying a beat detector outperforming the others, this section aims to inspect whether the use of beat detectors with different performance significantly impacts the calculation of the implemented ANI algorithm. So, the performance of the methods applied to the SYN signals of the two subsets was taken into consideration and the ANI_{lb} variables were made available for the reference R-peak positions and for the three different methods.

Figure 4.3 depicts the results of ANI computation from the different R-peak positions (reference, Ralph detector, and Pan Tompkins) for the different cases of subset A. Testing the hypothesis of this implementation of the ANI algorithm being highly sensitive to erroneous peak detections, the Wilcoxon signed-rank test was employed to perform three different comparisons between:

- ANI_{lb} values from the reference R-peaks vs ANI_{lb} values from the R-peaks by the Minimum Detection method

- ANI_{lb} values from the reference R-peaks vs ANI_{lb} values from the R-peaks by the Pan Tompkins algorithm

- ANI_{lb} values from the reference R-peaks vs ANI_{lb} values from the R-peaks by the Ralph detector

	Minimum detection	**Pan Tompkins**	**Ralph detector**
p-value	0.2015	0.2406	0.9978

Table 4.4: P-values for three different comparisons testing for significant differences between ANI_{lb} values from the reference R-peaks vs ANI_{lb} values from the R-peaks by another R-peak detector.

From the p-values in Table 4.4, with a significance level of 5%, there is no significant difference between an ANI_{lb} variable computed with the reference R-peaks and that from another R-peak detector.

Although the p-values above confirm that ANI_{lb} variables are not significantly different, qualitatively analysing Figure 4.3, one can observe that whereas the ANI_{lb} values from the R-peaks by the Ralph detector are superimposed with the ANI_{lb} values from the reference R-peaks, the ANI_{lb} values from the R-peaks by the Pan Tompkins and Minimum Detection methods are slightly different from that. It was expected to occur differences in ANI_{lb} variables, but not to this extent, as the different methods performed comparably in detecting the R-peak positions. The Ralph detector was not able to detect the last R-peak position in each signal from subset A so only the last ANI_{lb} value would change, as verified. The implementation of the Pan Tompkins algorithm was not able to detect the first and the last R-peaks positions in each signal of the subset A and, therefore, only the first and last ANI_{lb} values should be impacted, which was not verified.

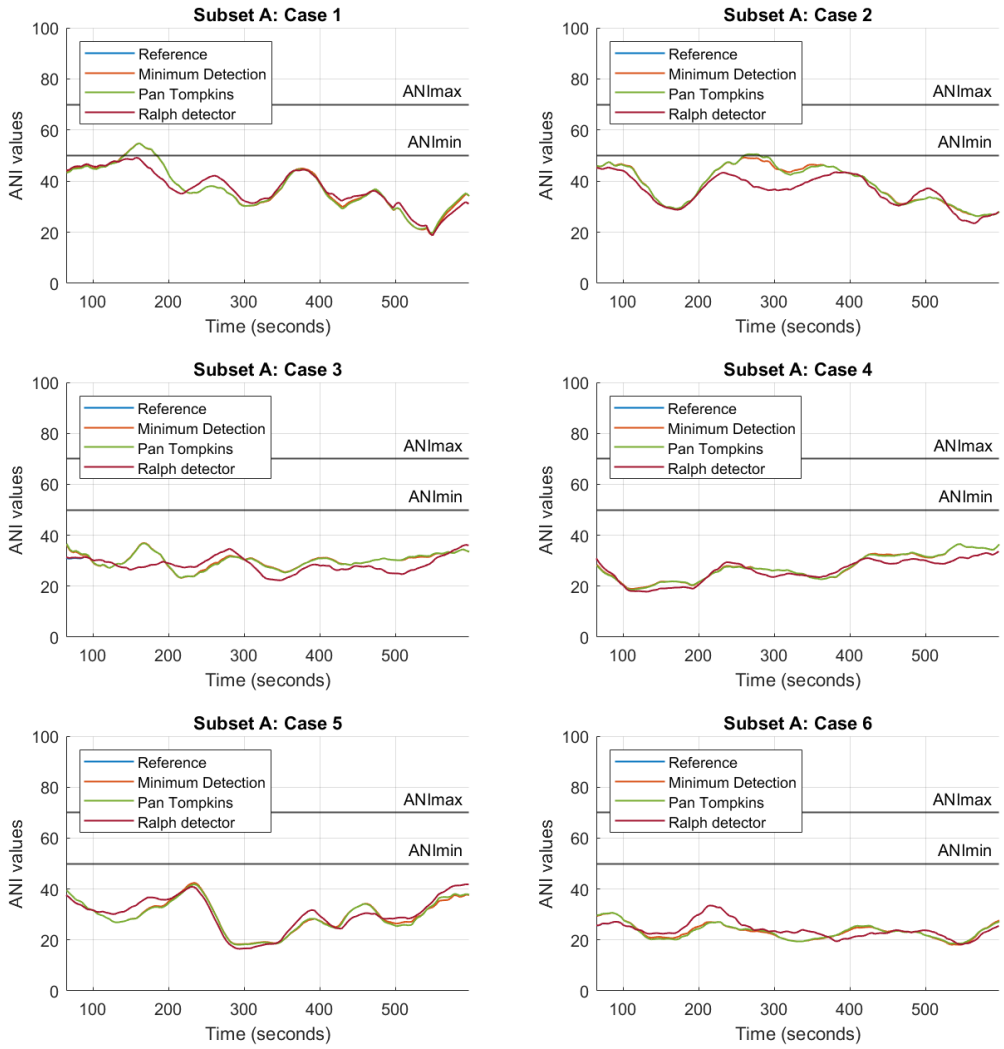

Figure 4.3: ANI_{lb} values from the R-peaks by the Ralph detector (in red) superimposed to the ANI_{lb} from the reference (in blue). Slightly differing from the previous, the ANI_{lb} variables from the R-peaks by the Pan Tompkins (in green) and that from the Minimum Detection method (in orange).

Inspecting the ANI computation, one can verify that the algorithm analyses the values within a 64-second window sliding in 4-second steps. This means that the non-detection of the first R-peak position introduces a border effect, lagging the R-R time series (see Figure 4.4). I.e., the windows of normalized and filtered R-R series resulting from the R-peaks detected by the Pan Tompkins algorithm will not match those resulting from the reference R-peaks positions. Consequently, the ANI_{lb} values computed are, inevitably, different (see Figure 4.5).

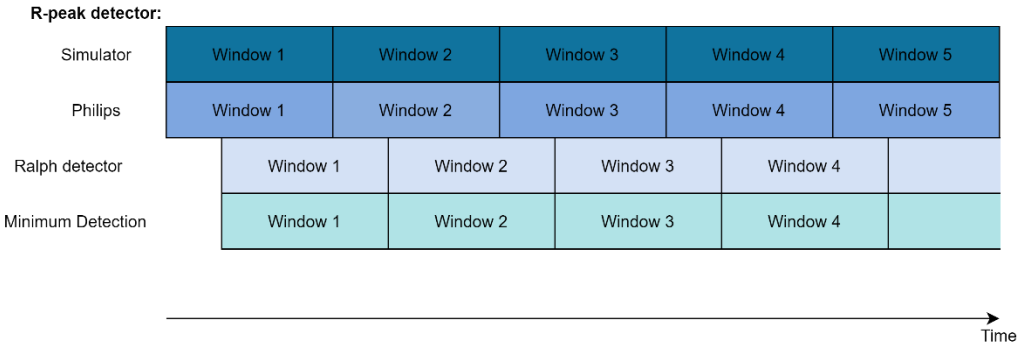

Figure 4.4: Representation of the border effect introduced in the ANI computation. As the implementation of the ANI algorithm performs in a sliding window, the values considered for AUC calculation are different between the methods. (Representation of the problematic, not scaled)

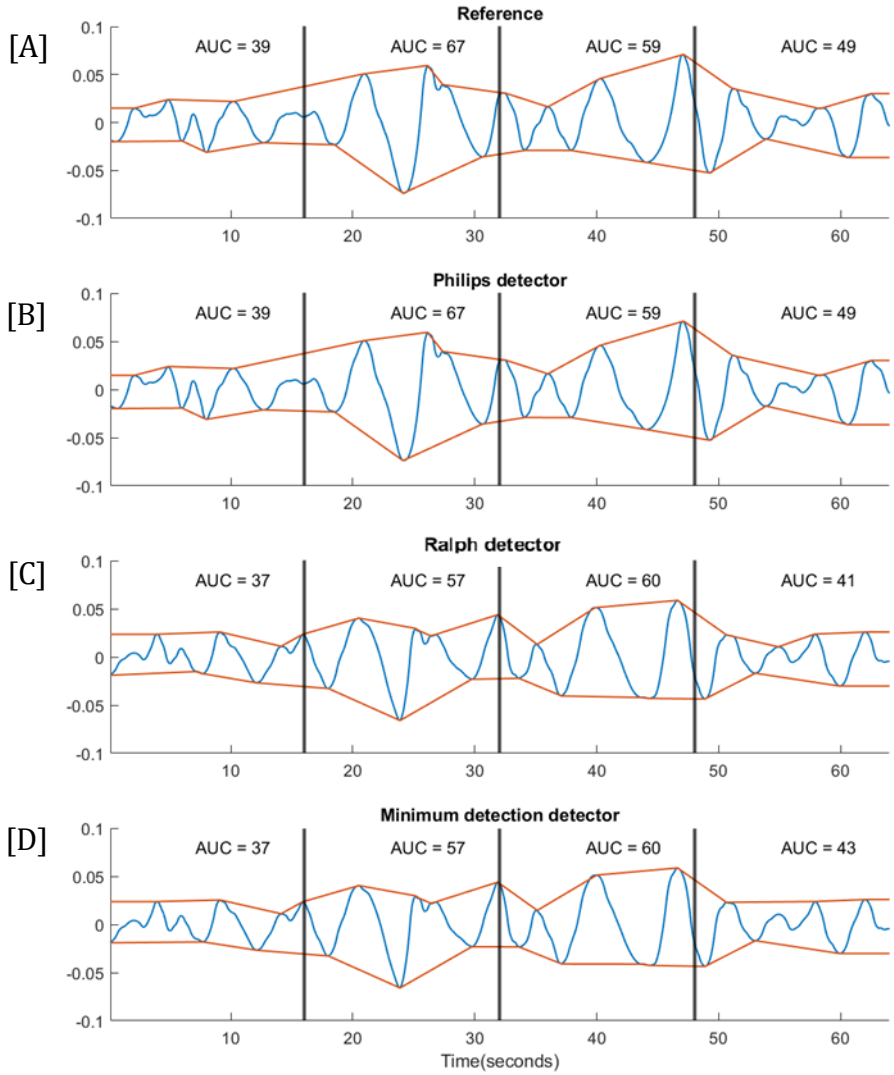

Figure 4.5: The first window of the normalized and filtered R-R series (in blue) resulting from the reference ([A]) and each peak detector ([B], [C], [D]). The ANI computation results from the minimum AUC delimited by the envelopes (in orange). As can be seen, by not detecting the R-peak of the first position, the resulting normalized and filtered R-R series on [C] and [D] differ from those on [A] and [B], which influences the AUC calculation and, posteriorly, on ANI computation.

These discrepancies can become problematic in practical situations, raising, for example, the question of when would be the ideal timing to start the recording. As this is an offline evaluation, it can be attempted to correct the discrepancies by synchronizing the vectors of detected R-peaks. Figure 4.6 summarizes the ANI_{lb} variables derived from the reference R-peak positions and the three different methods after synchronization. Then, as the variables are non-normally distributed, the Wilcoxon signed-rank test was again employed to perform the different comparisons.

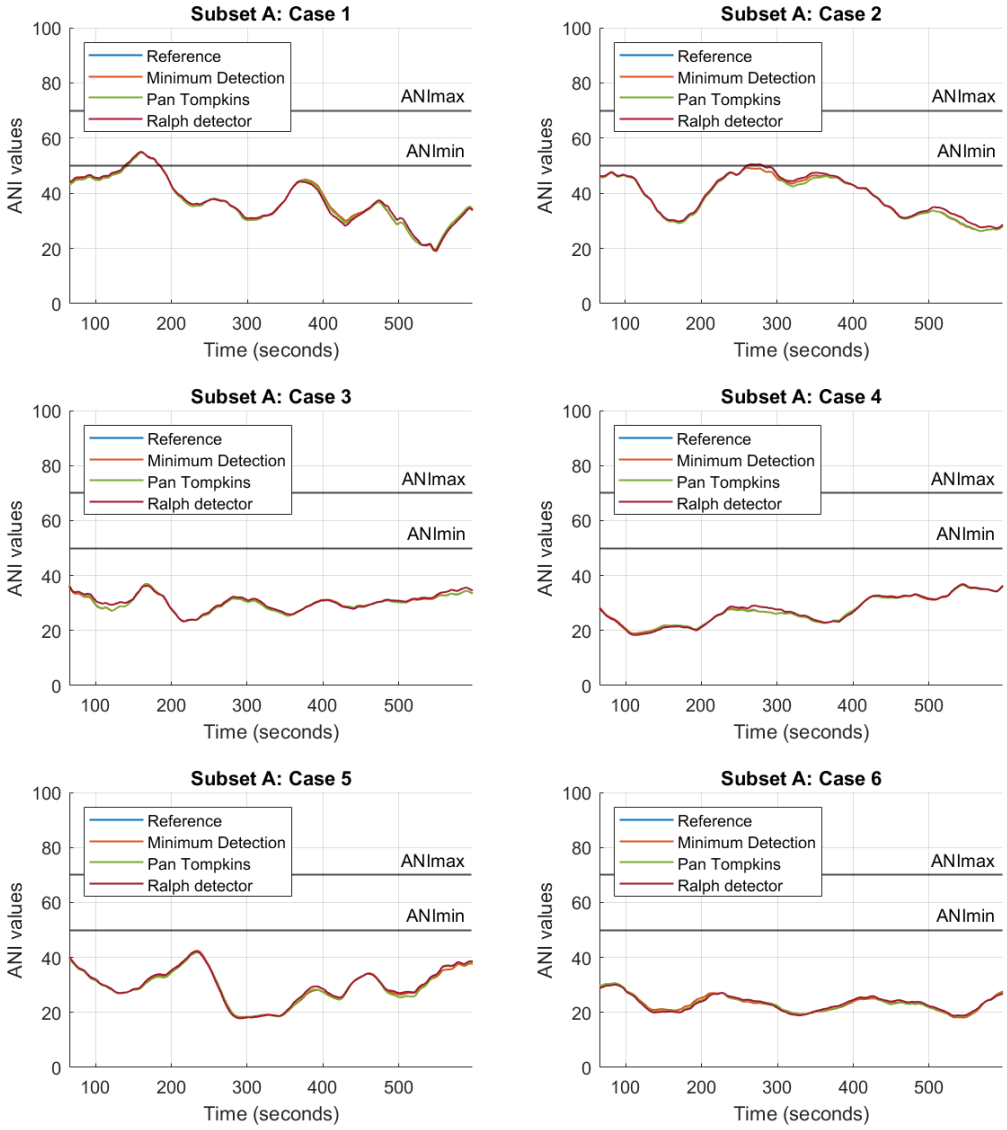

Figure 4.6: ANI_{lb} variables derived from the reference R-peak positions and the three different methods after synchronization.

	Minimum detection	Pan Tompkins	Ralph detector
p-value	0.4331	0.3738	0.9955

Table 4.5: P-values for three different comparisons testing for significant differences after synchronization between ANI_{lb} values from the reference R-peaks vs ANI_{lb} values from the R-peaks by another R-peak detector.

Overall, there is no significant difference between the ANI_{lb} variable computed from the reference R-peaks and that from the other R-peak detectors (Table 4.5). However, as qualitatively observed in Figure 4.6, there are still slight discrepancies between the ANI_{lb} variable computed from the reference R-peaks and that from the Pan Tompkins detector or the Minimum Detection method. After synchronization, there is no difference between the recall and precision parameters of any of the R-peak detectors and the reference R-peak positions, but the temporal jitter differs. The temporal jitter may represent an important indicator of performance in HRV analysis since it reflects the time variations in the detected R-peak positions from their reference. Thus, as the ANI algorithm is a measure of HRV analysis, the perceived discrepancies between the ANI_{lb} variables evidence the impact of the temporal jitter on ANI computation. From Table 4.2, one can conclude that the implementation of the Pan Tompkins algorithm is the method with the highest average jitter and the largest dispersion of this parameter. In fact, the observed divergences are more noticeable for ANI_{lb} values made available by the Pan Tompkins algorithm than for the Minimum Detection method.

To objectively assess the impact of the sensitivity of the R-peaks detector on the calculation of ANI variables, the reference R-peak at the 350^{th} position was intentionally deleted, forming the $R\text{-peaks}_{modified}$. Figure 4.7 summarizes the ANI_{lb} variables derived from the reference R-peak positions and the $R\text{-peaks}_{modified}$ for each ECG of subset A. Besides the deletion of the R-peak at the 350^{th} position, there is no other difference between the ANI calculation processes.

Testing whether this implementation of the ANI algorithm would be susceptible to detector sensitivity when failing to detect an R-peak, the differences between the ANI_{lb} variable by the reference R peak positions vs the ANI_{lb} variable by the modified vector were not considered significant (p-value = 0.0654). However, from Figure 4.7 the non-detection of one R-peak can already impact the ANI output in up to one minute. The observed prolonged discrepancies might be due to the usage of a 4-second moving window to calculate the instantaneous value of ANI and, posteriorly, the application of a moving average to compute the ANI_{lb} value.

It can also be noted that the effect on ANI calculation of not detecting one R-peak is neither linear nor constant and is dependent on the use of the respective R-R interval for the construction of the envelopes. I.e., missing a beat depends on the context: if, after normalization and bandpass filtering, the respective R-R interval is above half of the mean of the detected local minima and below half of the average of the detected local maxima, no influence on the ANI_{lb} calculation is introduced. Otherwise, different ANI values are possibly outputted.

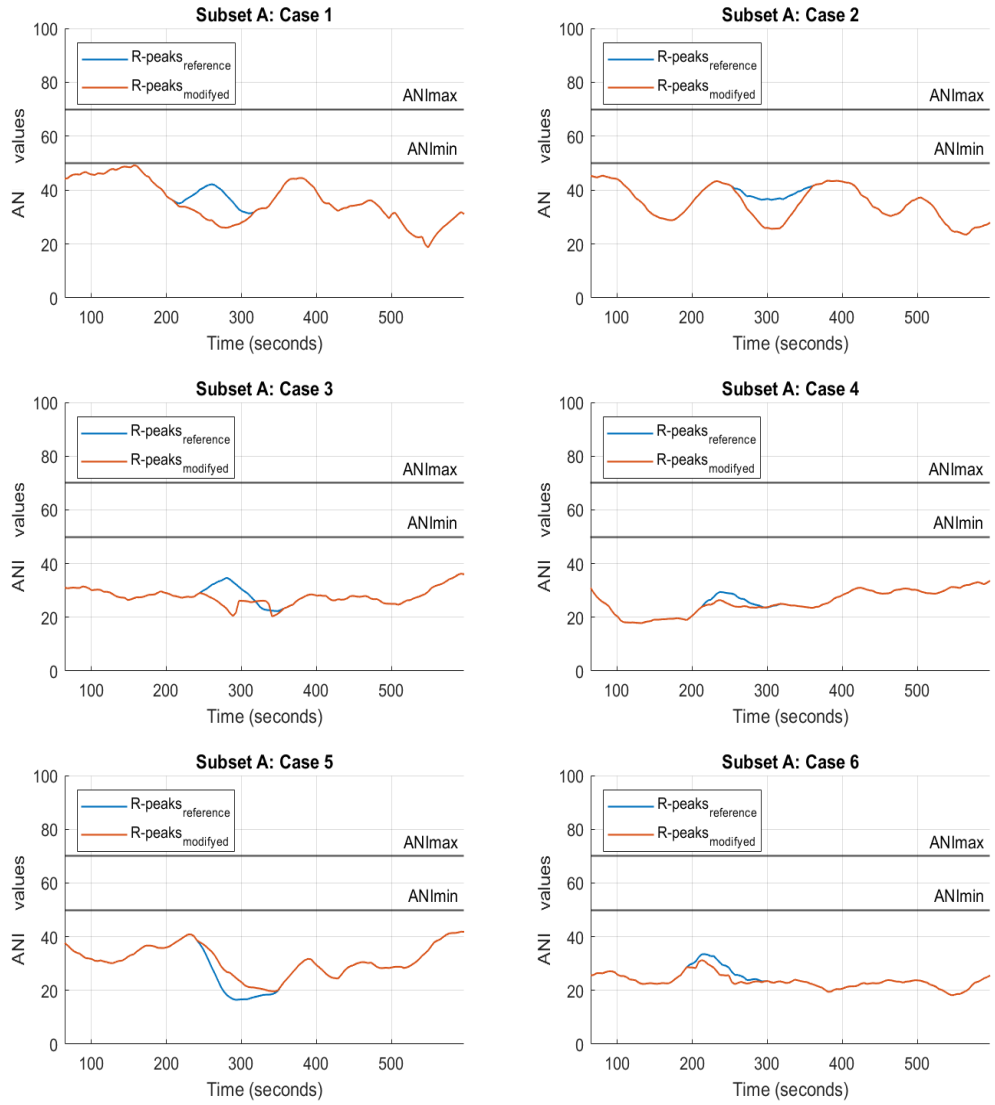

Figure 4.7: ANI_{lb} obtained with the reference R-peak positions and that removing the 350th R-peak.

As firstly hypothesized, whether resulting from misdetection or non-detection, inaccuracies of the R-peak detector can greatly impact the R-R tachogram and derived metrics, as is the case of this implementation of the ANI algorithm.

4.2.2 Effect of ectopic beats on ANI

As mentioned in Chapter 2, ectopic beats are thought to occur either through other physiological mechanisms rather than those responsible for the variability in the R-R intervals or false QRS detection. It is investigated in detail how the occurrence of non-sinus beats affects the calculation of ANI variables, allowing to verify if there is a need for correction of ectopic intervals before the analysis of this HRV metric.

Making use of the ECG generator tool described in Chapter 3, ectopic beats were added to the R-R time series with a normal sinus rhythm (extracted from ECG signals of subset

A) so that the underlying oscillations introduced to the R-R tachogram were known. The reference and the modified R-R series are similar, except for the ectopic beats introduced. Then, the ANI computation is performed as before.

Results obtained from varying the percentages of normal beats converted into ectopic beats (x) are illustrated in Figure 4.8 with the R-R tachogram extracted from the ECG signal of Case 5 of subset A as reference. It can be observed that this implementation of the ANI algorithm can be extremely sensitive to ectopic beats. Even in case of single ectopic beat addition ($x = 0.01\%$), slight discrepancies are noticed between the ANI_{lb} variables around the time of ectopic occurrence.

Averaging the results obtained for different random distributions and dealing with differing percentages of normal beats converted into ectopic beats, Figure 4.9 depicts the MAE and respective SD calculated between the ANI_{lb} variable computed from the reference R-R tachogram and that from the R-R tachograms artificially generated by converting normal beats into ectopic beats. Note that, starting with the tachograms in the no ectopic case, the MAE between the ANI_{lb} variables grows with increasing percentage of normal beats converted into ectopic beats. The results support the need for ectopic correction before the calculation of the ANI values.

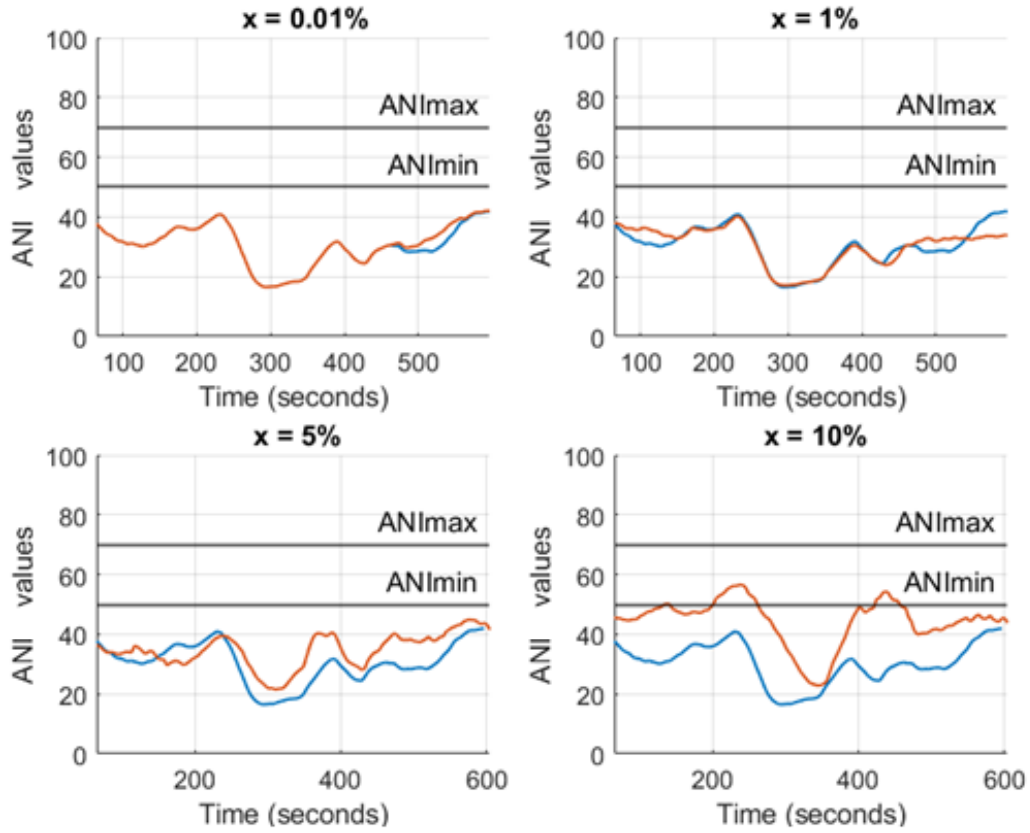

Figure 4.8: Using case 5 of subset A as an example, ANI_{lb} values computed from the reference tachogram (in blue) and that dealing with varying the percentage of normal beats converted into ectopic beats (in orange)

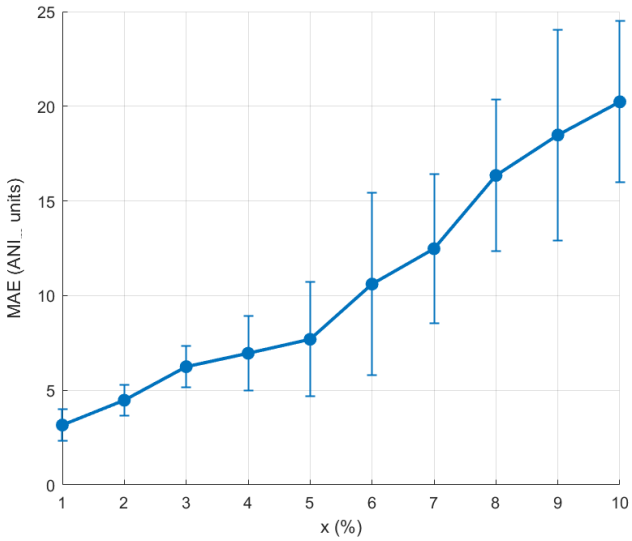

Figure 4.9: MAE calculated between the ANI_{lb} variable computed from the reference R-R tachogram and that from the artificial R-R tachograms varying the percentage of normal beats converted into ectopic beats (x)

Furthermore, to determine if it can be concluded that the difference between each of the ANI_{lb} variables from artificially generated tachograms and that from the reference tachogram is statistically significant, different comparisons for the different x were performed using the Wilcoxon Ranked-sum test since the variables were previously found not normally distributed.

x (%)	p-value
1	5.98×10^{-2}
2	1.36×10^{-18}
3	5.56×10^{-33}
4	2.52×10^{-28}
5	6.16×10^{-65}
6	9.09×10^{-117}
7	6.46×10^{-125}
8	2.08×10^{-144}
9	8.26×10^{-174}
10	9.29×10^{-196}

Table 4.6: P-values for different comparisons testing for significant differences between ANI_{lb} values from the reference R-peaks vs ANI_{lb} values from the R-peaks varying x

From the observation of Table 4.6, significant statistical differences were found when converting more than 1% of normal beats into PVCs. These results confirm what has been observed qualitatively: ectopic beats lead to hardly interpretable and comparable outputs, causing noticeable changes in the measured ANI variables.

The artificially generated ectopic beats consisted of abnormal beats occurring considerably earlier than expected and followed by a compensatory pause. Thus, the estimation of HF components of the HRV was significantly increased by the shortened R-R intervals. Since the ANI computation through the described implementation is based on the analysis of HF changes, it may be distorted by the occurrence of PVC.

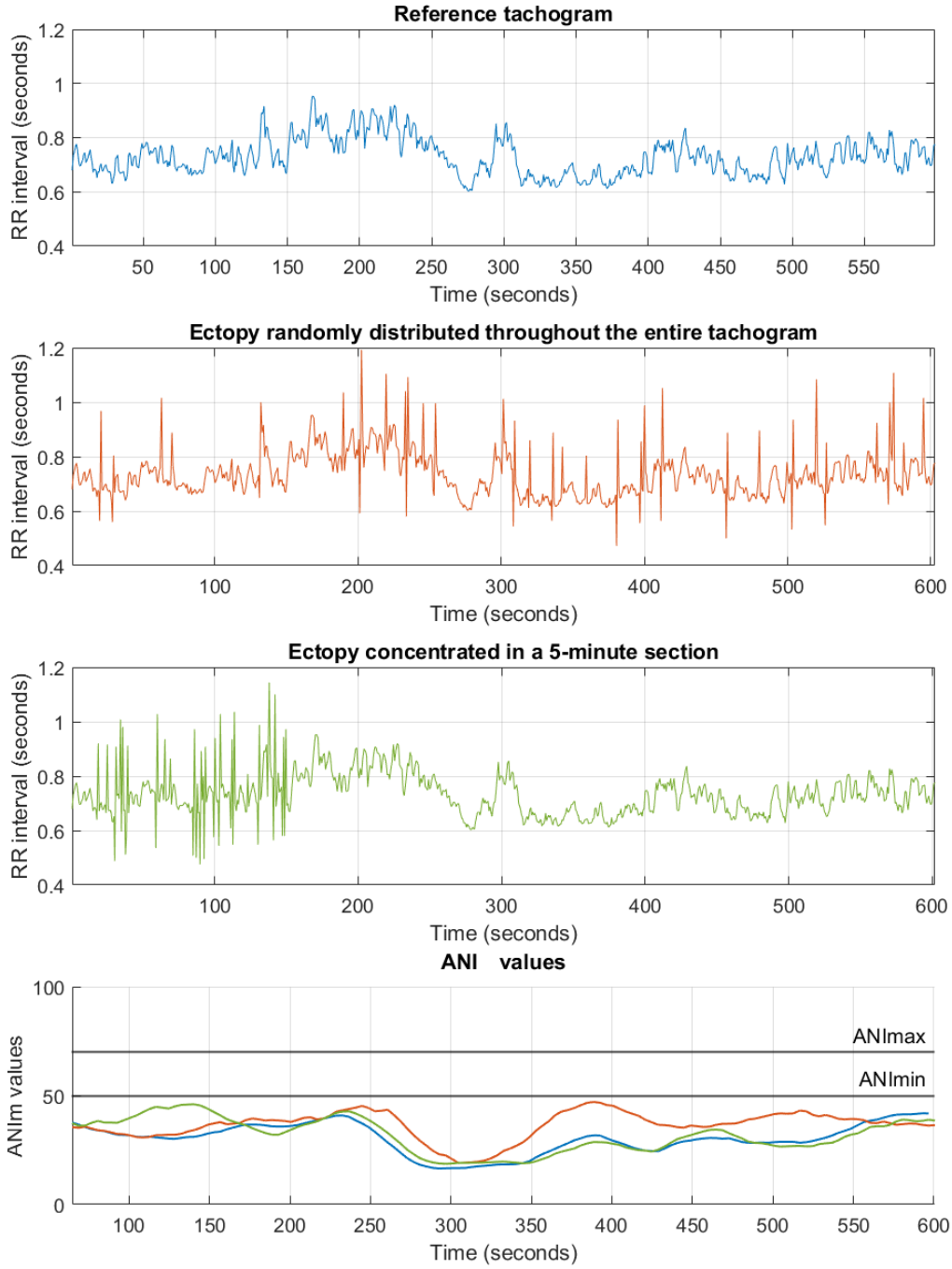

Figure 4.10: Reference tachogram extracted from the ECG of case 5 of subset A (in blue); Tachogram converting 5% of the normal R peaks from the reference tachogram to ectopic beats (in orange); Tachogram converting 5% of the normal R peaks positioned in the first quarter of the length of the reference tachogram to ectopic beats (in green); Respective ANI_{lb} variables.

One additional remark is that, beyond the number of ectopic beats, the distribution of ectopic beats across the tachogram plays an important role in the impact that non-sinus beats cause on ANI values. For suspicion that the density of ectopic beats impacts the ANI values, the ANI variables were made available for the following R-R time series:

- reference, the tachogram extracted from the ECG of case 5 of subset A;
- conversion of 5% of the normal R peaks from the reference tachogram to ectopic beats;
- conversion of 5% of the normal R peaks positioned in the first quarter of the length of the reference tachogram to ectopic beats;

The modified tachograms were obtained making use of the extension to the ECGSYNmod tool. From Figure 4.10, the ANI_{lb} variables calculated for the three tachograms corroborate the assumption previously made. The prolonged observed discrepancy between the blue and green lines of the lower plot in Figure 4.10 is probably due to the fact that the implemented algorithm uses moving average.

Overall, the results evidenced that ectopic beats should be identified and corrected previous to the computation of the ANI. In the next chapter, the performance of different methods for ectopic correction is further compared using data acquired intraoperatively to ascertain if the changes introduced by ectopic beats are large enough to obscure the analysis of the output from this implementation of the ANI algorithm.

4.3 CONCLUSIONS

The implementation of the ANI algorithm has been shown to rely heavily on precise peak timing being impacted by the performance of the peak detector and the occurrence of ectopic beats. Therefore, signal processing and R-peak detection are of utmost importance before attempting to interpret ANI or any HRV-based index.

5 PERFORMANCE ASSESSMENT OF ECTOPIC BEATS CORRECTION METHODS

With no data being shared with employees of Philips Research, this section was developed for research purposes at CISUC.

As reviewed in the previous chapters, HRV analysis may add value to the study of the underlying autonomic response to nociceptive stimuli by attempting to tease out the timing variations in the sinus rhythm caused by alterations in the SNS and PNS [25]. However, the HRV analysis may be hindered by the fact that this parameter is interdependent on regulatory systems corresponding to the adaption of the cardiac rhythm to any environmental and psychological stimulus [25]. Moreover, the implementation of the ANI algorithm described in Chapter 4 is a HRV measure and has been demonstrated to be highly sensitive to ectopic beats, enhancing the need for correction of ectopic beats before analysing this metric.

Accordingly, estimating the correct sinus R-R intervals is an essential technique for ectopy correction. In this chapter, several methods were applied to improve the estimation of R-R intervals and further ectopic correction, investigating to which extent the presence of ectopic beats would be quantitatively acceptable and contributing to a more robust solution for partial automatization of intraoperative analgesia in the future.

5.1 METHODOLOGY

A search for publicly available databases was performed so that any findings would be sufficiently reliable in an intraoperative context and passible of clinical utility. This search was carried out using keywords «Pain», «Intraoperative vital signs», «Intraoperative physiological», «perioperative physiological» and «Intensive Care Unit» conjugated either with «Database» or «Records».

Amongst several results ([121]–[131]), VitalDB was the one that seemed to fulfil best the purposes of this thesis. Being the only intraoperative monitoring database is a plus, since conscious perception would not be a bias factor. Notwithstanding, it is important to note that none of these databases fulfils all the requirements, since they were not acquired for the same purpose of this study. This would, therefore, constitute an observational study.

Following a brief overview of the selected dataset, the methodology presented below is organized into two main sections: signal processing and signal analysis. Figure 5.1 summarizes the strategy implemented in this chapter.

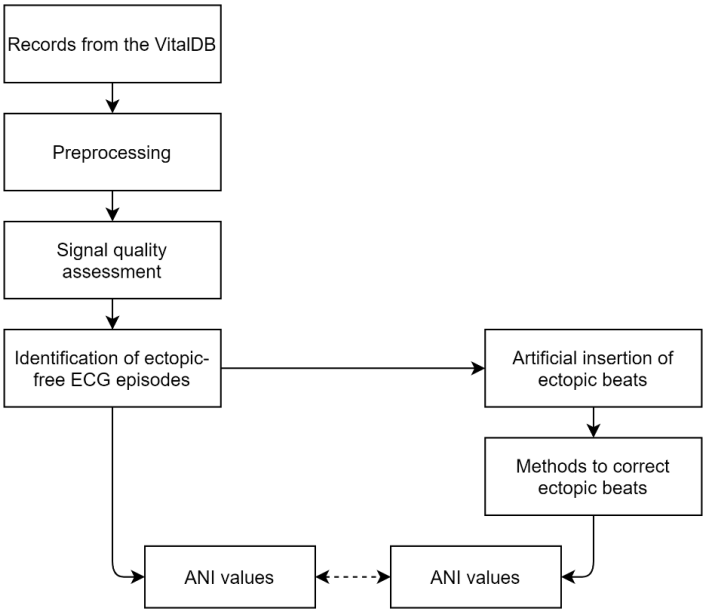

Figure 5.1: Flowchart describing the methodology adopted perform a comparative analysis of different methods for ectopic correction

5.1.1 Dataset overview

The VitalDB dataset is comprised of patients who underwent non-cardiac surgical procedures between June 2016 and August 2017 at Seoul National University Hospital, Seoul, South Korea. It contains information about the patients namely demographics, vital sign measurements and laboratory data. A more detailed description is available in [132].

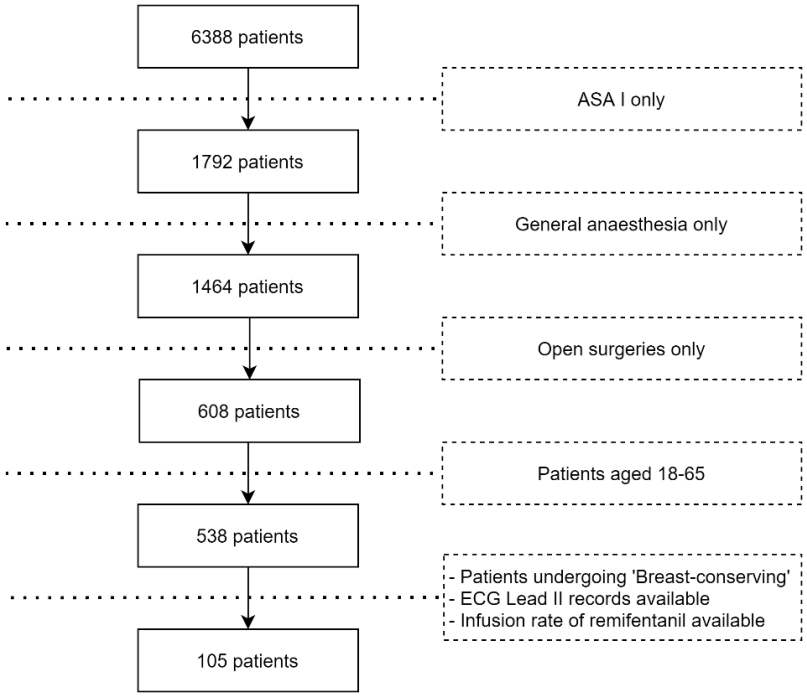

Figure 5.2: Criteria for patient selection from VitalDB.

Although the dataset is composed of data from 6,388 patients, some criteria (including patient demographics, comorbidities, type of anaesthesia, and type of surgery) were employed for patient selection and further exploration (see Figure 5.2). These criteria were applied in an attempt of reducing as much as possible the confounding factors that could impact the HRV analysis. Thus, only normal healthy adult patients (ASA I) under GA with the administration of the same type of analgesics (remifentanil) were included in this study. Furthermore, among the surgical procedures, only patients undergoing 'Breast-conserving surgeries' were selected to be explored in this work.

5.1.2 Signal processing

As previously stated, before interpreting any HRV-based index, it is of utmost importance to include a signal processing step to avoid erroneous analysis [37], [133]. Therefore, several methods were employed to prepare data for further analysis.

The ECG data was sampled rated at 500 Hz and the down sampling for 250 Hz (the admitted by the ANI algorithm) was only performed in the last step of signal processing for classification purposes according to ANI values.

5.1.2.1 Goal phase identification

If existing, no protocol was publicly available, and no annotations of painful standard events could be assessed. Therefore, the ANI variables were made available and were analysed together with the anaesthesia start annotation, the operation start annotation, and the timing of the first remifentanil bolus. Remifentanil is an analgesic of high efficacy with a rapid onset and predictable cessation of effect [6]. The timing of the first remifentanil bolus in each case was taken from the records of the infusion rates of remifentanil 20 mcg/mL.

So, the idea was to try to infer whether the timing of the first remifentanil bolus would correspond to the start of the anaesthesia (representing the anticipation of surgical stimuli warned by the surgeon) and whether the operation start annotation would correspond to the timing of the first incision (this would be verified if a drop in the instantaneous ANI values occurs at this time).

While in some cases these assumptions could be verified, in others it was not possible to find any potential relationship between the events mentioned. This must be because the surgeries were performed in ten ORs by different anaesthesiologists. The timing information on the start and end of the anaesthesia and surgery was taken from the OR anaesthesia report and not protocolized but recorded by the anaesthesiologists when they thought that a significant action to initiate or terminate anaesthesia and surgery was taken [134].

Having no strong evidence that the timings would be coherent across the different records, a goal phase was defined instead of considering the entire record. The goal phase was designed to ensure that the anaesthetic state was maintained throughout the surgical period being considered and to avoid the disturbance of ANI scores by any event during anaesthetic induction and emergency. Therefore, it was included for analysis the surgical period between 5 minutes after the timing of the annotation related to the start of the anaesthesia and 5 minutes before the timing of the annotation on the end of the anaesthesia (Figure 5.3).

T1: Anaesthesia start time (anestart);
T2: 5 minutes after anestart;
T3: 5 minutes before anaesthesia end time (aneend);
T4: aneend;

Figure 5.3: Timeline for the goal phase of the records in patients selected for this study. (Adapted to the context of this study from [67])

5.1.2.2 Noise removal

Despite of being a readily identifiable waveform, ECG signals are vulnerable to noise disturbances [37]. Therefore, the presence of several types of artefacts that could corrupt the ECG signals was inspected and filtering methods were explored.

The signals were contaminated with a combination of high-frequency noise, and low-frequency noise (wandering baseline). While trying to keep most of the signal clinical information and since the ST segment interpretation is not relevant in this approach, the ECG signals were bandpass filtered by a digital infinite impulse response filter (Butterworth) and the cut-off frequencies settled to 0.5 Hz and 30Hz, and order 6.

5.1.2.3 Event detection

The sequences of R-R intervals were obtained through the detection of QRS complexes. Taking into consideration the results from section 4.2.1, the Ralph detector would be the most appropriate as it was the algorithm performing best. However, as no data has been shared with employees of Philips Research, the full implementation of the Ralph detector algorithm was no longer accessible during the realization of this chapter. Therefore, the

implementation of the Pan Tompkins algorithm was applied to the filtered data since it seemed to be the more suitable and adaptive available algorithm.

5.1.2.4 Signal quality assessment

Following the beat detection and prior to assessing the beats' classification, segments of data with bad quality (artefacts or missing data) were excluded from the analysis of the ECG records. These artefacts could be created during surgery due to several factors, including either unexpected patient movement or repositioning of the patient by the surgery staff.

As the non-sinus beats are not representative of autonomic control mechanisms and may alter HRV analysis, the abnormal beats should be accurately identified [31]. The optimal solution to identify the abnormal beats would be the manual check of raw ECG. However, considering the number of recordings and their length, it is not practical to do it so. Numerous principles and strategies have been being employed to enhance the automatic classification of heartbeats [135]. Only approaches based on the HRV signal were considered in this thesis. In this sense, the SYN signals from subset B of the training dataset were considered to assess the ability of three techniques to distinguish between the different types of beats. The following methods were employed:

- Method I: Implementation of the algorithm proposed at [116].

- Method II: Using timing information to identify ectopic intervals by comparing the distance between the current beat and the previous beat with the distance between the current beat and the next beat.

- Method III: Calculation of the acceleration relatively to the previous N-N interval (equation (5.1)) and identification of the physiologically impossible beats (equation (5.2)) [46].

$$\triangle RR_n = \frac{|RR_n - RR_{n-1}|}{RR_{n-1}} > threshold \tag{5.1}$$

$$RR_n > 2\ seconds \ \vee \ RR_n < 0.2\ seconds \tag{5.2}$$

Defining the threshold to be used when applying Method III, the threshold percentage was varied from 1 to 25% to optimize the removal of non-sinus R-R intervals, whilst retaining as many sinus R-R intervals as possible. Similar results to those of [46] were obtained and, therefore, the threshold was set to 10%.

From this preliminary analysis on the ability of the different methods to identify ectopic intervals, the method I presented the worst performance in both terms of sensitivity and precision; method II was highly precise but failed in the detection of some of the abnormal

beats; method III presents high sensitivity but tends to overcorrect. Consequently, in order to create a control group of episodes with a normal sinus rhythm (without ectopic beats), a conservative methodology was followed by merging the cardiac cycles identified as abnormal by methods II and III. As method III tends to overcorrect, the ECG segments were manually inspected if cardiac cycles were classified as non-sinus only by this method. Then, it was composed the control dataset defining 10-minute ECG episodes with normal sinus rhythm.

5.1.2.5 Subgrouping the episodes according to the ANI_{lb} scores

The episodes of the group control were resampled at 250 Hz, the R-R time series was calculated, and the ANI_{lb} values were made available using the algorithm's implementation described in the previous chapter.

As mentioned in Chapter 2, according to the manufacturer, it is unlikely for hemodynamic reactivity to occur in the following 10 minutes if the ANI value falls in the range between 50 and 70 [22]. To assess the impact that ectopic beats may have on the clinical decisions based on the information provided by the ANI algorithm, the episodes of the control dataset were then subdivided into two subgroups by being included in the ANI+ subgroup if at least 70% of the ANI_{lb} values were of level 50 or more; otherwise, they were included in ANI- subgroup.

5.1.3 Signal analysis

Studying the reconstruction of the duration effects on R-R time series, edited datasets were constructed by replacing the normal samples of the control tachograms with ectopic samples. Then, it was assessed the performance of different methods for the correction the ectopic intervals by estimating the respective R-R intervals and performing the comparison of the results with the ones of the control dataset.

5.1.3.1 Artificially generation of ectopic intervals

Performing a comparative study, edited datasets were constructed for ten degrees of ectopic beats (x). The edited datasets were created using the ECGSYNmod extension described in chapter 3, i.e., randomly inserting synthesized ectopic beats by modifying the position of the R-peak for one cycle of the dynamics. The ten degrees of artificially inserted ectopic beats vary in units from 1 to 10%.

In this process it is ensured that the first fifty beats were not converted to ectopic beats. This rule was established in order to ensure the existence of a calibration period required

for the implementation of the autoregressive model (section 5.1.3.2.5) and further reliable comparison of all the techniques employed.

Whereas the control dataset serves as reliable baseline to assess the quality of the ectopic correction, the methods for ectopic correction under investigation are employed on the edited datasets composed.

5.1.3.2 Models for the correction of ectopic intervals

Looking at the HRV signal as a sequence of observations (R-R intervals) taken sequentially in time, the performance of different real-time methods was assessed for correcting ectopic observations. From the simplest to the most robust, the methods inspected for ectopic correction included the deletion or replacement of ectopic intervals estimating the ectopic observations based on past normal samples.

5.1.3.2.1 Deletion of ectopic intervals

The 'Deletion' method is a commonly used and the simplest strategy to deal with the presence of ectopic beats [135]. This strategy corresponds to the elimination of the ectopic observations from the HRV signal, reducing the number of beat-to-beat intervals. Figure 5.4 illustrates the method followed to correct the abnormal intervals applying the 'Deletion' method.

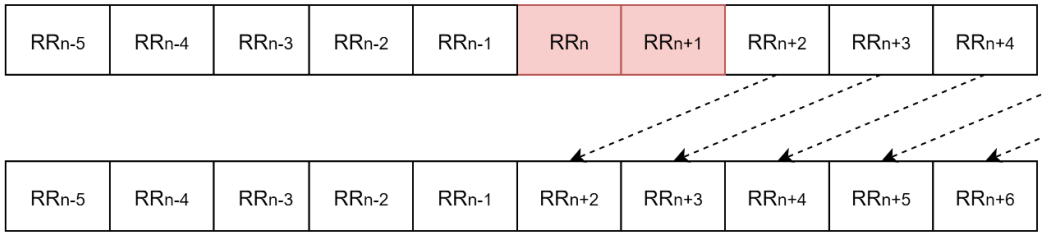

Figure 5.4: Correction of ectopic observations deleting them.

5.1.3.2.2 Interpolation

Interpolation methods were employed to replace the ectopic intervals with interpolated R-R intervals. The following interpolation methods were assessed for analysis: zero-order, first order, and spline [135]. The zero-order interpolation corresponds to the 'Nearest' interpolation and replaces the query points by the adjacent observation; the first order interpolation method connects the adjacent normal R-R intervals deriving a straight line, corresponding to the 'Linear' interpolation; and the 'Spline' interpolation is based on the approximation of a polynomial cubic curve [136].

5.1.3.2.3 Previous & Next

In comparison to the normal beat-to-beat intervals, the ectopic episodes considered in this work correspond to a shorter R-R interval followed by a longer R-R interval (the compensatory pause). The 'Previous & Next' method estimates the former observation of the ectopic episode to be equal to the previous normal sample, and the last observation of the ectopic episode to be equal to the next normal sample. Figure 5.5 illustrates the method followed to correct the ectopic intervals applying the 'Previous & Next' technique.

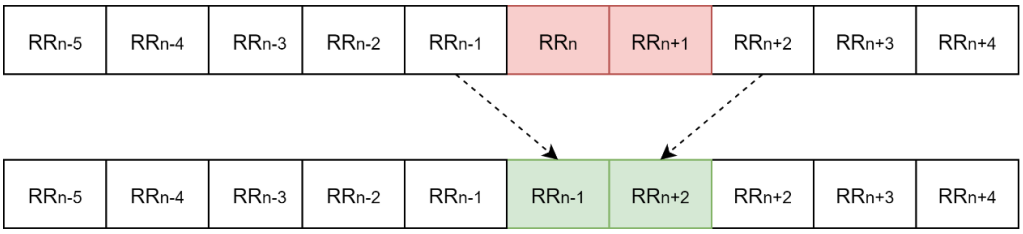

Figure 5.5: Correction of ectopic observations replacing the shortened interval by the previous normal observation and the longer interval by the next normal observation.

5.1.3.2.4 Mean

The 'Mean' method corrects the ectopic intervals by estimating the arithmetic average of the previous P normal observations (equation (5.3)). P was considered five and Figure 5.6 illustrates the method followed to correct the ectopic intervals applying the 'Mean' method.

$$\tilde{y}(n) = \frac{1}{P}\left(\sum_{i=1}^{P} x_i\right) \tag{5.3}$$

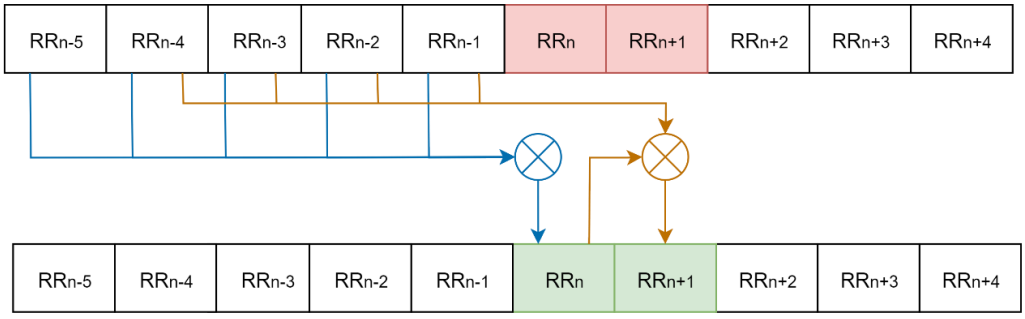

Figure 5.6: Correction of ectopic observations replacing them by the mean of the previous five normal observations.

5.1.3.2.5 Autoregressive model

The autoregressive (AR) model assumes the linear modulation of the HRV signal $\{y(n)\}$ by a time-varying system consisting of the combination of the P past values of the output and the present input. Regarding the case of biomedical signals, there is no knowledge of

the input and, so, the current sample of the output can only predict using its past values (equation (5.4)) [37], [137].

$$\tilde{y}(n) = \sum_{k=1}^{P} a_k \, y(n-k) + \epsilon(n) \tag{5.4}$$

, where P refers to the model order, n is the sample point, $\epsilon(n)$ is the white noise, and $\{\tilde{y}(n)\}$ represents the predicted value. Accordingly, the residual error can be determined by

$$e(n) = y(n) - \tilde{y}(n) \tag{5.5}$$

Over the years, several studies have been inspecting the applicability of AR models in the domain of HRV spectral analysis [137]–[139]. Figure 5.7 represents the method applied in this study to correct ectopic beats using an AR model.

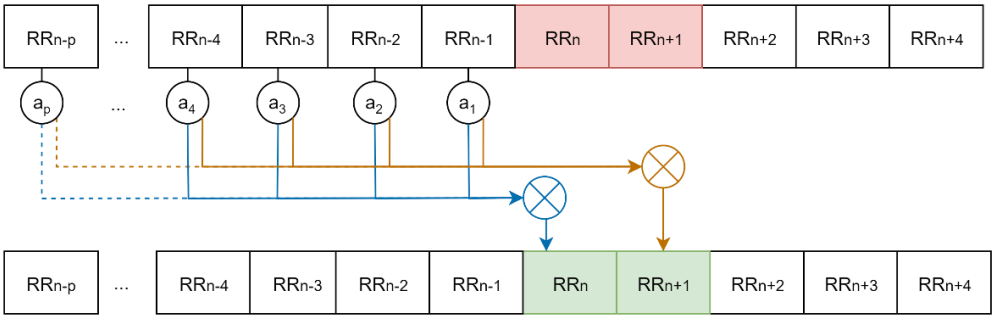

Figure 5.7: Correction of ectopic intervals using an autoregressive model

Regarding the computation of the model parameters, the least-squares method was employed to find the coefficients of the filter $(a_1, a_2, \ldots, a_P)$ by iteratively minimizing the mean-squared error. Moreover, since the best choice for the model order was not established *a priori*, the calibration process of the AR model comprised the estimation of the optimum model order. The appropriate selection of a model order is crucial to prevent from inaccurate representations of the original signal [138]. While a lower model order may provide smooth information, higher orders may increase noise dramatically [138], [139].

The Akaike Information Criterion (AIC, equation (5.6)) [140], the Rissanen's Minimum Description Length (MDL, (5.7)) [141], and the criterion proposed at [142] (referred as Kahn criterion) have been applied to the control tachograms as functions of the model order P. The Kahn criterion consists of iteratively incrementing the model order P until the error between the signal estimated through model coefficients and original signal becomes greater than the previous error calculated [142].

$$AIC_P = ln(\sigma_P^2) + \frac{2(P+1)}{N} \tag{5.6}$$

$$MDL_P = \sigma_P^2 \left(1 + \left(\frac{P+1}{N}\right) \ln(N)\right) \quad (5.7)$$

The evolution in terms of error variance (σ_P^2) of each of the four criteria were evaluated separately.

5.1.3.2.6 Neural Network

Inspired by the structure of the human brain, Neural Networks (NN) represent an experience-based learning category of Machine Learning architectures that are achieved from the model's training with a backpropagation algorithm based on fault tolerance [37], [143]. A NN can be designed using layers and activation functions and Figure 5.8 represents the NN designed in this work which is characterized as a fully connected neural network since all inputs from a layer are connected to every activation unit from the next one [143].

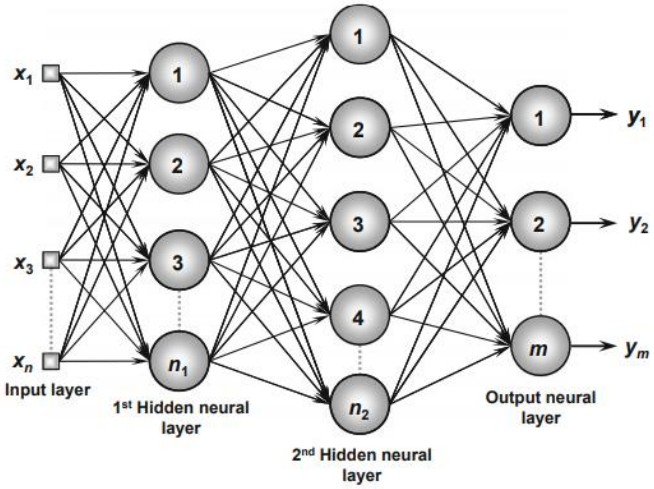

Figure 5.8: Example of a neural network with multiple layers (Source [143])

The structure of an NN is composed of an input layer (interacts with the external environment, receiving information related to the system being investigated), one or more hidden layers (responsible for patterns extraction that compose the solution), and an output layer (calculation and presentation of the final output) [143].

Figure 5.9 best summarizes the definition of a NN layer as an operation to its inputs generating an output that becomes the input of the next layer. Depending on the specific NN structure, each layer follows its own strategy. Basically, the activation potential (u) is computed with equation (5.8) which represents the sum of the multiplication of each input (x_i) by the correspondent weight (w_i), followed by the subtraction of the bias (θ); then, the output is produced using equation (5.9), limiting the activation potential by applying an activation function specified a priori $(g(u))$ [143].

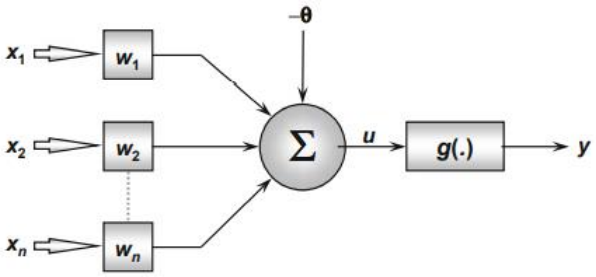

Figure 5.9: The artificial neuron (Source [143])

$$u = \sum_{i=1}^{n} w_i \cdot x_i - \theta \tag{5.8}$$

$$y = g(u) \tag{5.9}$$

The activation functions are implemented to limit the output within a reasonable range of values, adding a non-linear transformation into the layer [143]. Only fully differentiable activation functions were used to define the NN architecture, namely the sigmoid function and the linear function. The sigmoid function (equation (5.10)) is represented in Figure 5.10-A and returns a value between 0 and 1. The linear function (equation (5.11)) is represented in Figure 5.10-B and returns its input value.

$$g(u) = \frac{1}{1 + e^{-u}} \tag{5.10}$$

$$g(u) = u \tag{5.11}$$

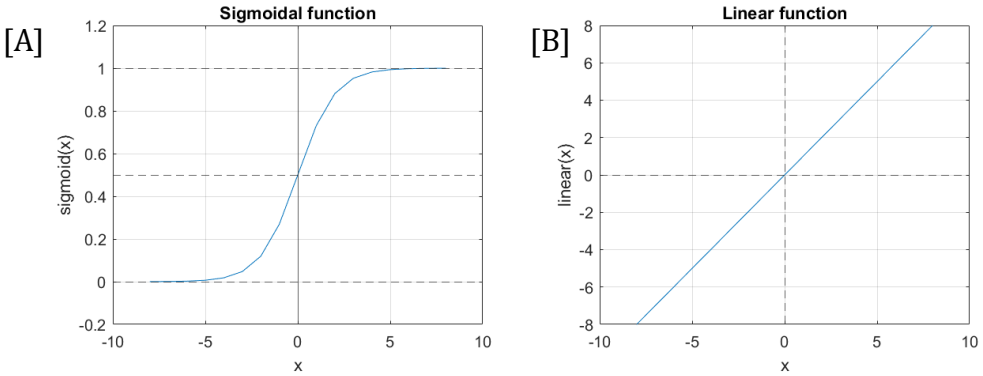

Figure 5.10: Activation functions: [A] The sigmoid function and [B] the linear function.

For the specific context of this study, Figure 5.11 represents the correction of ectopic intervals through the estimation of the respective R-R intervals with a neural network with the past P sinus intervals as input. The HRV signals are standardized by removing the mean and scaling to unit variance. Then, the dataset for the learning strategy of the NN is formed by segmenting the control R-R series into non-overlapping segments of $P + 1$ observations in which the first P observations correspond to the i^{th} example

represented as a column vector ($x^{(i)} \in \mathbb{R}^{n_x \times m}$) and the last observation of the segment is the i^{th} target output value ($y^{(i)} \in \mathbb{R}^{n_y}$).

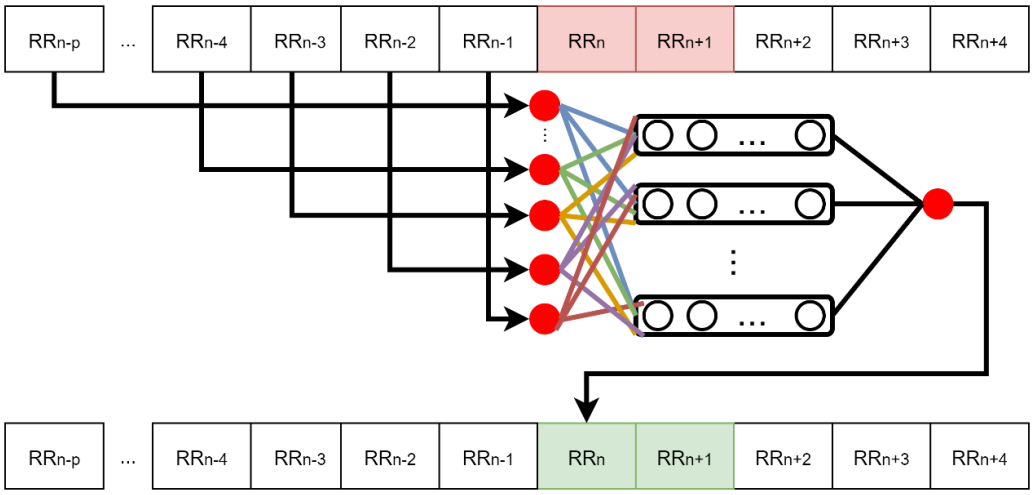

Figure 5.11: Representation of the correction of ectopic intervals using a neural network.

The NN can be seen as a modelling approach in which a mathematical model is trained to transform the input data (the past sinus observations) into a significant output (an accurate estimation of the R-R interval to replace the ectopic observation). The parameters of the NN (weights and biases) were optimized through a supervised learning strategy using the control HRV signals. The learning strategy is an iterative process of two stages: forward propagation and backward propagation [143]. The model parameters are gradually updated in a feedback mechanism through the minimization of a loss function by successively applying the forward and backward propagations. With the aim of minimizing the error between the predicted R-R interval and the target, the cost function used in this work was the Mean Squared Error (MSE – equation (5.12)) [143].

$$MSE = \frac{1}{n}\sum_{i=1}^{n}(y_i - \tilde{y}_i)^2 \qquad (5.12)$$

, where n is the number of samples, $\tilde{y}$ represents the predicted value, and y refers to the sample of the control tachogram.

Training the neural network involves a tuning process of hyperparameters (such as learning rate α, number of hidden layers, number of hidden units) [143], [144]. The random search technique was employed for hyperparameter optimization. Although the manual search and the grid search are the commonly employed strategies to optimize the hyperparameters, the random search has been demonstrated to be more efficient since the importance of tuning differs between different hyperparameters (e.g., it is more important to adjust the learning rate rather than the number of layers) [144]. Within a specified range of values, the random search sets different configurations of

hyperparameters at random and selects the best one [144]. Figure 5.12 illustrates the comparison between the grid search strategy and the random search method.

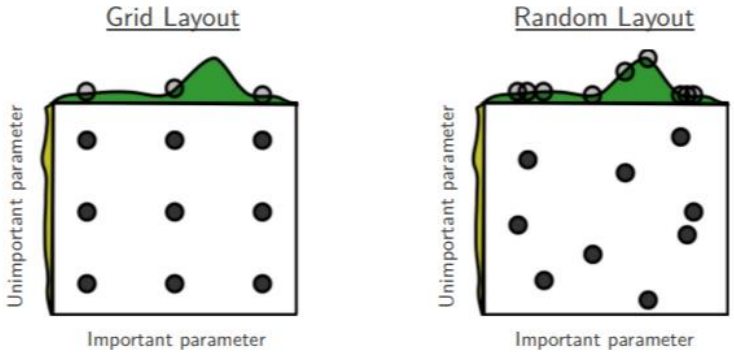

Figure 5.12: Grid and random search of nine trials for optimizing two hyperparameters. With grid search, nine trials only test three different values of the most important parameter. With random search, all nine trials explore distinct values of the most important parameter. (Source [144])

Designing the NN, the cross-validation technique was adopted to select the best NN topology, evaluating the generalization capability of the predictive models and preventing from overfitting [37], [143]. This method consists of randomly dividing the total data set into training and test set. Then, applying the k-fold cross validation, the training dataset was split in k partitions of equal size and with no overlap. Out of the k partitions, $(k-1)$ partitions are used to the learning process and the remain partition is set aside as a validation subset [143], [145]. All the partitions are used as validation subset by repeating the learning process k times [143], [145]. The k results are averaged to obtain a measure of performance for the NN architecture. The test set is used to evaluate the final retained model. Figure 5.13 represent the statistical technique described.

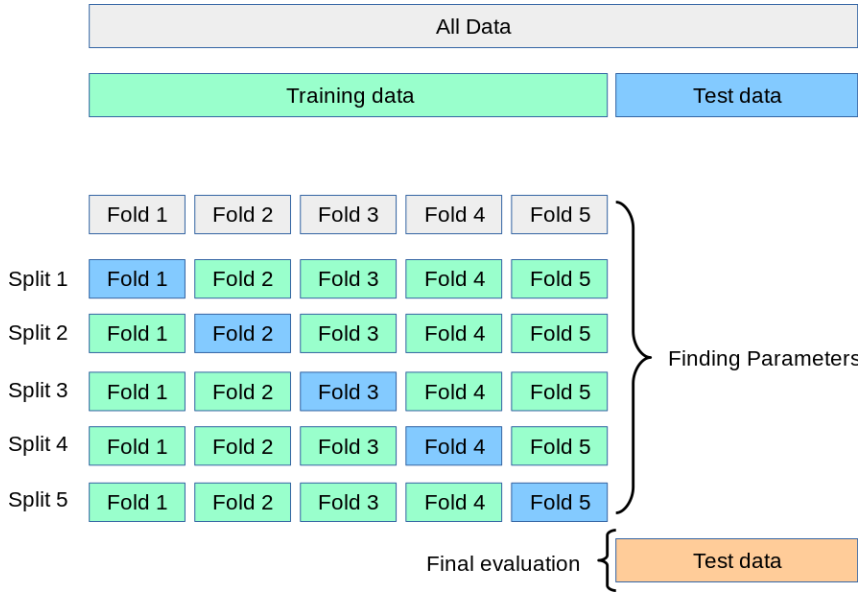

Figure 5.13: Data division for performance assessment of the neural network architecture (Source [145])

5.1.4 Assessment metrics and statistical validation

Implementing the different techniques considered for analysis, the architecture of both machine learning algorithms required training before proceeding to the assessment of which would be the best strategy to correct the ectopic intervals. So, initially, the same edited datasets (the random insertion of ectopic beats was performed only once) were used in the training and search for the best structure of the AR and NN models. These edited datasets were also used for a preliminary analysis of the results.

As shown in Chapter 4, not only does the amount of ectopy present in the HRV signal impacts ANI scores, but also its distribution along the tachogram, i.e., it is the local density of ectopic beats that most affects the ANI calculation (see Figure 4.10). Therefore, carrying out a more exhaustive analysis to determine the suitability of the different methods for correcting ectopic intervals, the process was repeated ten times considering all the data selected for inclusion in this study. That is, the performance was assessed by averaging the results obtained for ten random and dissimilar ectopic distributions per episode for the varying degree of edited datasets built.

The quantification of the performance of all the strategies was represented as mean ± standard-deviation and performed through both the MAE (equation (4.6)) and the Normalized Mutual Information (NMI) between the ANI_{lb} variables computed from the control R-R series and the respective artificially generated tachograms. The NMI between the variables X and Y is computed using equation (5.13) according to Figure 5.14 and it is a normalized value between 0 (X and Y are completely different) and 1 (perfect correlation) [146]–[148]. This is a measure that was employed to compare the mutual dependence between the ANI_{lb} variables calculated from the control R-R series and that from the R-R series corrected with each method for ectopic correction ($I(Y;X)$), taking into consideration the entropy of each variable ($H(Y)$ and $H(X)$) [146]–[148].

$$NMI\ (Y,X) = \frac{2\ \times I(Y;X)}{H(Y) + H(X)} \qquad (5.13)$$

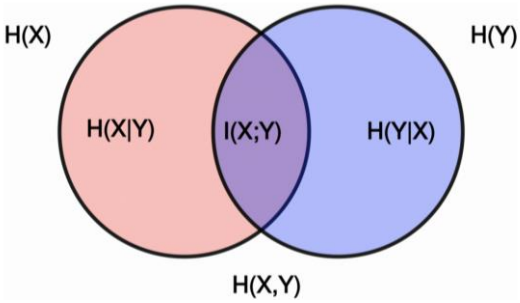

Figure 5.14: Normalized Mutual Information: Venn diagram describing the relation between the measures of entropy and Mutual Information (Source [148]).

The data was found to be non-normally distributed (applying the Kolmogorov–Smirnov test). Consequently, validating and comparing the results of all the strategies, non-parametric tests were employed [105]. The level of significance was settled at 5% throughout the analysis. The Spearman correlation coefficient (c) was employed to inspect the relationship between the ANI variables [105]. The Kruskal-Wallis test was employed to test differences between the methods applied to correct the ectopic intervals [149]. If the null hypothesis was rejected, it means that there is a difference between at least two of the methods and a post-hoc multiple comparison test with a Bonferroni correction was then employed to determine which pairs of methods were statistically different [150]. The Wilcoxon signed-rank test was used to statistically evaluate the changes in the ANI_{lb} variable calculated from the R-R series corrected with each method for ectopic correction [107].

5.2 Results and Discussion

Considering the selection criteria established, a total of 105 records of patients undergoing breast conserving surgery could be retrieved and analysed. Patient characteristics and surgery details are reported in Table 5.1.

	Patients (n = 105)
Gender (F/M)	104/1
Age (years)	48 ± 8
Weight (kg)	57 ± 8
Height (cm)	159 ± 5
BMI	22.64 ± 3.22
Duration of anaesthesia (min)	116 ± 38
Duration of operation (min)	89 ± 39

Table 5.1: Demographics of the study population a breast conserving surgery (age, weight, height, and BMI data are represented as mean ± standard-deviation).

After qualitatively isolating ECG segments and detecting the respective R-peaks as fiducial points, the classification of the R-R intervals was carefully performed trying to minimize the erroneous conclusions by including segments with non-sinus beats. Qualitative and quantitative processing of the ECGs signals verified the existence of a high number of artefacts and, although only non-cardiac surgeries were included, ectopic beats were highly incident among the signals, even leading to the complete exclusion of some cases initially considered for analysis. In total, 221 records during the goal phase of the surgery were isolated as 10-minute ECG episodes on normal sinus rhythm (Figure 5.15). These episodes were used as the control group for assessing the performance of the methods for ectopic correction.

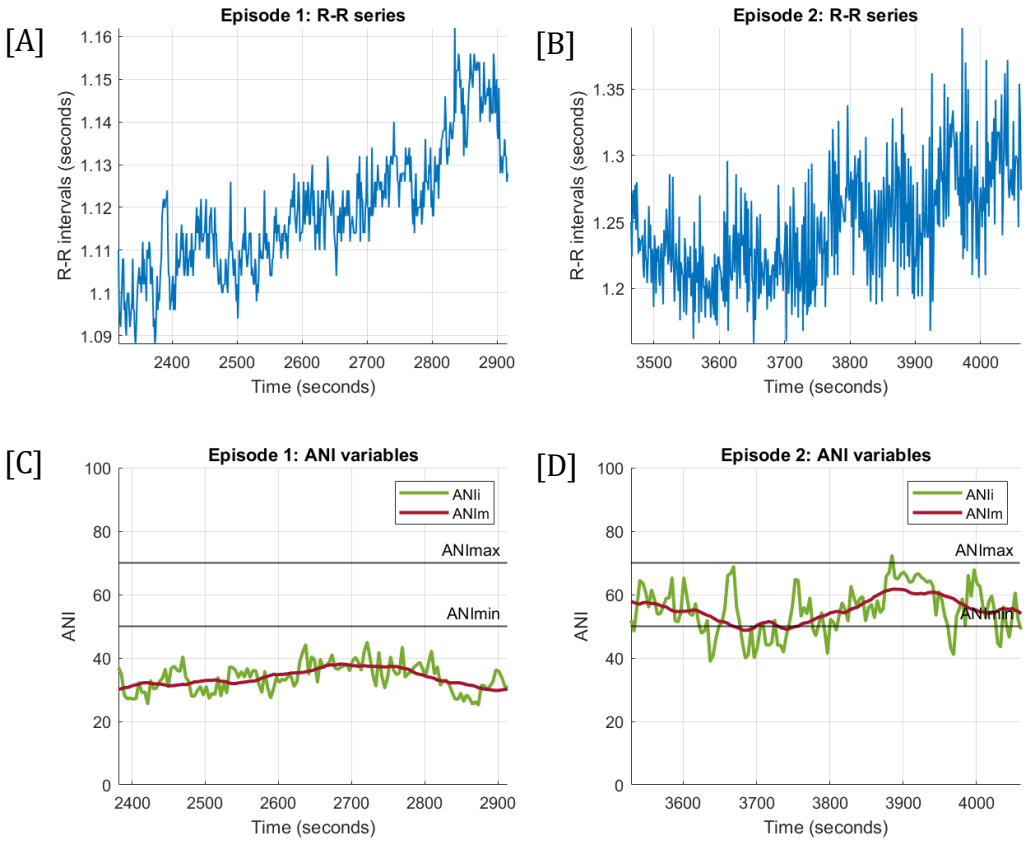

Figure 5.15: Representations of the [A] R-R series of one episode of the control group classified as type ANI- and [C] respective ANI variables; that for one episode of the control group classified as type ANI+ ([B] and [D]). The ANI variables were computed with the algorithm described in chapter 4.

The ANI variables were made available for each of the 221 episodes isolated and it was proceeded to their individual classification according to the ANI_{lb} values computed. Accordingly, 17 episodes were classified as type ANI+ and 204 were classified as type ANI- (Table 5.2).

	Number of episodes
Subgroup ANI -	204
Subgroup ANI +	17

Table 5.2: Classification of the control group ECG episodes according to the ANI_{lb} values (the episode is classified as type ANI+ if at least 70% of the ANI_{lb} values are above the level of 50, otherwise it is classified as type ANI-).

From Table 5.2, it can be noticed that the episodes considered for analysis are unbalanced in terms of classification according to the ANI_{lb} variables, with the majority being classified as type ANI-. This imbalance will be taken into consideration along the analysis, and may be due to erroneous implementation of the ANI algorithm or improper monitoring of analgesia, since no monitor was used to guide the clinician on this component of the GA. There is not enough information to support any of the pointed reasons, as further research would be required, including more detailed information on the surgeries' protocol and respective ANI variables provided by the monitor proprietary

of MDoloris. Yet, this study proceeds with the assessment of how different correction methods can reduce the impact that ectopic beats have on the ANI calculation through the implementation described in chapter 4.

Then, unitary varying from 1 to 10 the percentage of ectopic beats (x) introduced into the baseline episodes (control group, ectopy-free), ten edited datasets were constructed (one edited dataset per ectopy degree considered). The control R-R intervals and the respective edited R-R intervals are similar except for the ectopic samples randomly introduced. In a first approach, the results for the different methods considered for ectopic correction were all obtained based on the same edited data (the insertion of ectopic beats was performed only once).

Exposing the problematic being treated, the ANI scores were computed for R-R series extracted from the episodes of the edited datasets and the respective MAE relatively to the control tachograms was calculated. The results depicted in Figure 5.16 corroborate the findings on the previous chapter: the MAE between the ANI variables from the control tachograms and the edited tachograms grows with increasing percentage of normal beats converted into ectopic beats, causing noticeable changes in the measured ANI variables.

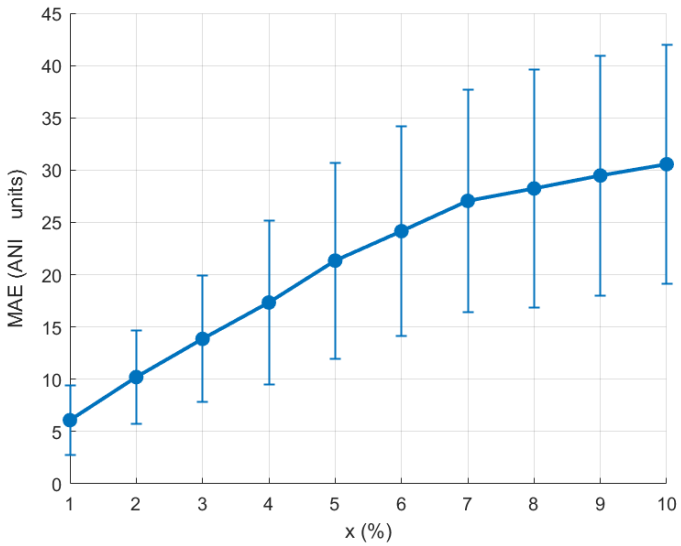

Figure 5.16: MAE calculated between the ANI_{lb} variable computed from the R-R tachogram extracted from the control group and that extracted from the edited tachograms varying the percentage of normal beats converted into ectopic beats (x).

Illustrating the extreme case considered in this work, it can be observed that there was a significant variation of ANI between the scores computed from the control group and the edited dataset converting 10% of the beats into ectopic beats. From Figure 5.17, the significant variation of ANI can be observed with the median [25th–75th percentile] at the control group (36 [30-44] ANI_{lb}) being significantly smaller than at the edited dataset with 10% of ectopy added (63 [56-69] ANI_{lb}).

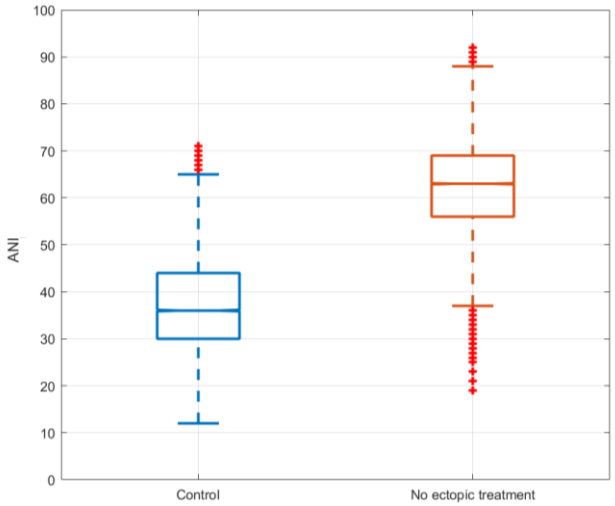

Figure 5.17: Distribution of the ANI_{lb} values calculated from the ectopy-free R-R series (in blue) and that converting 10% of the R-R intervals into ectopic beats.

In this analysis, it can be clearly noticed that ectopic beats act as confounders to the interpretation of the ANI scores since their artificial addiction to the control R-R series led to hardly comparable results. As from Table 5.3, in case of ectopy-free, the ANI scores were mostly below the level of 50 (the state of Noc/ANoc misbalance, according to the manufacturer) with 204 episodes classified as type ANI- and 17 as type ANI+; whereas, in a presence of 10% of ectopy, the episodes' classification was almost the opposite since most of the ANI scores fell within the range of adequate analgesia state (23 episodes were classified as type ANI- and 198 as type ANI+). From a clinical point of view, the mere interpretation of the ANI monitor would signify higher parasympathetic tone, representing a misinterpretation of the index for many of the episodes.

		Control group	
		ANI-	ANI+
Corrected group	ANI-	21	2
	ANI+	183	15

Table 5.3: Confusion matrix without any ectopic treatment. According to the ANI_{lb} values, classification of the control group ECG episodes and of the edited episodes converting 10% of the normal intervals into ectopic intervals.

The ANI computation through the described implementation is based on the analysis of HF changes and, therefore, the distorted results were expected because the estimation of HF components of the HRV was significantly increased by the shortened R-R intervals (Figure 5.18). Although the ANI metric may add value to the study of the underlying autonomic response to nociceptive stimuli by attempting to tease out the parasympathetic tone, the described implementation of this metric revealed to be heavily impacted by the occurrence of ectopic beats. Thus, once again, it was enhanced that

ectopic beats correction methods must be appropriately chosen before the interpretation of the ANI scores. Accordingly, several strategies were tested for correction of ectopic intervals in ECG records.

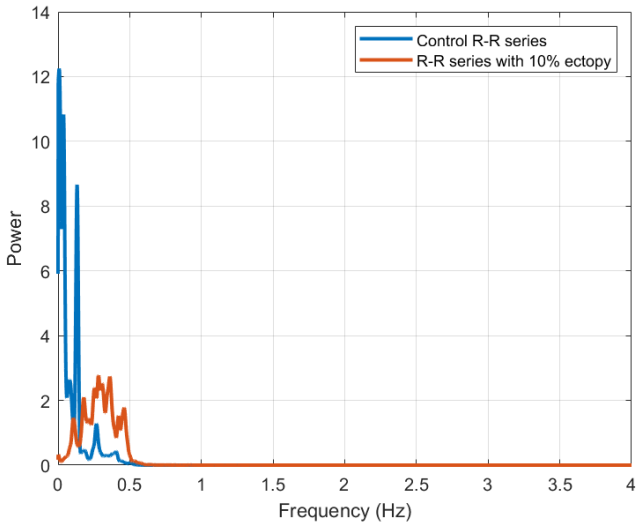

Figure 5.18: Using Welch's estimator with 300-second window and 50% of overlap, representation of the power spectrums of an R-R series extracted from one episode firstly classified as type ANI- in the control group (blue line) and that from the same episode after the introduction of 10% of ectopy then classified as type ANI+ (orange line). A significant increase can be observed between HF-HRV component of the baseline and that from the R-R series contaminated with ectopic-intervals.

5.2.1 Models' architecture

Both the AR model and NN model are considered modelling approaches that analyse the patterns of the HRV signal over time and mathematically represent the process based on the previous variations of the R-R series.

Different parametric modelling approaches were inspected in order to identify the models trying to lead to an efficient estimation of the R-R intervals. Figure 5.19 illustrates the flow chart followed to implement these two models forecasting the R-R intervals to correct ectopic intervals.

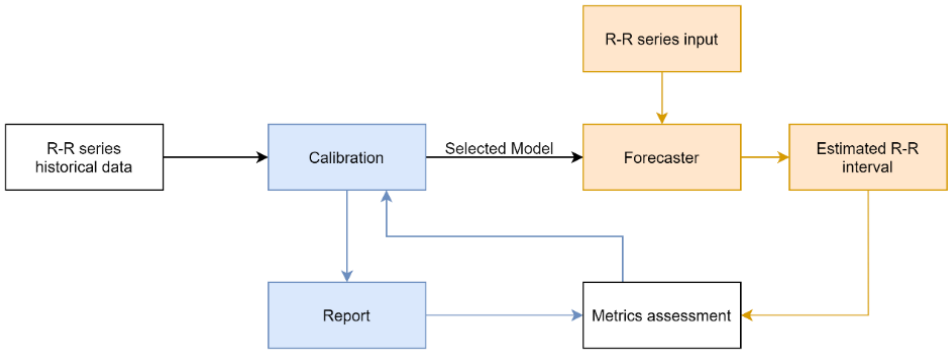

Figure 5.19: Flow chart for the implementation of both the autoregressive model and the neural network estimating R-R intervals.

5.2.1.1 Modelling the autoregressive model

Optimizing the AR modelling parameters before deploying the algorithm, the HRV signal of the control group ($y(n)$) has been assumed as the output: a discrete-time signal sampled at the unitary rate. The considered output signals were detrended and analysed individually in frames dimensioned at the respective total number of observations (N = the total number of R-R intervals).

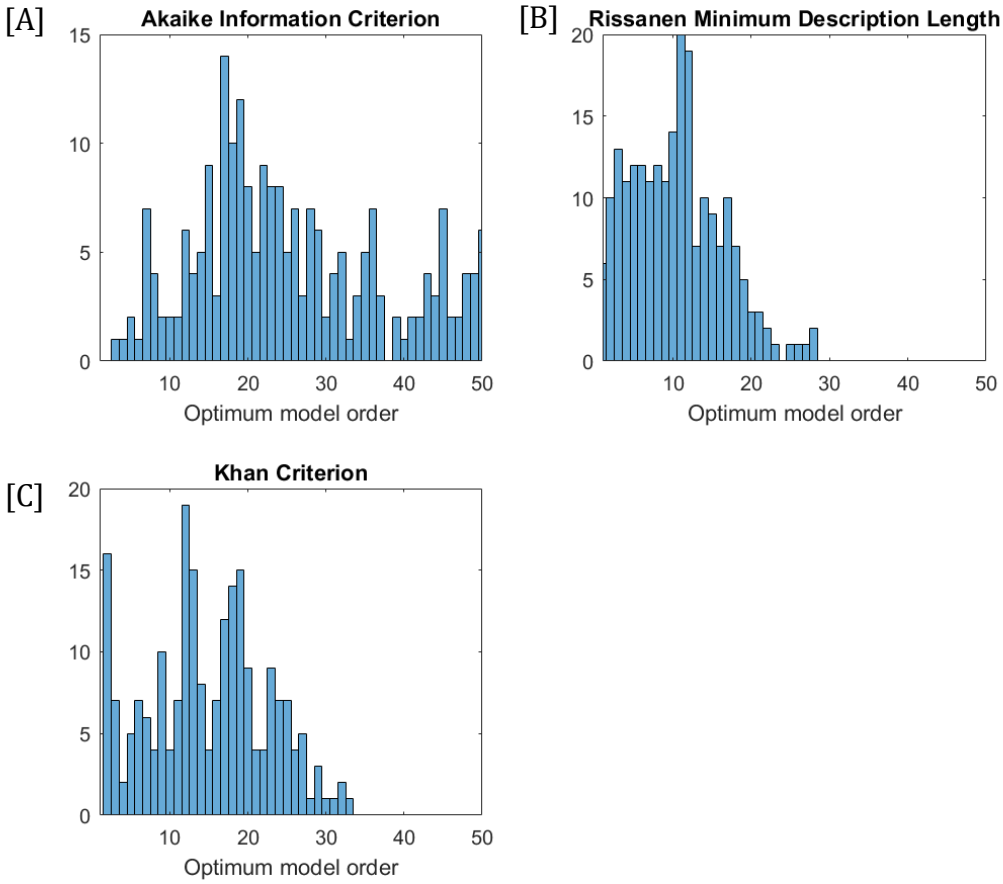

Figure 5.20: Optimum model order as found by the [A] AIC, [B] MDL, and [C] Khan criterion

Defining fifty as the maximum model order, each output signal was checked for the described criteria, and the optimum model order (P) was settled on the most frequently chosen over the set of data tested. From the histograms showed in Figure 5.20**,** the optimum model order proposed for MDL was P = 11, for the AIC criterion was P = 17, and for the Kahn criterion was P = 12. A narrower distribution of the chosen order can be observed employing the MDL criteria.

With the model orders proposed by the different criteria, the R-R intervals were estimated to correct the ectopic observations in the edited datasets. In a first approach, the R-R interval replacing an ectopic interval was predicted applying the model whose parameters were estimated using all the previous observations relative to the timing of the ectopic case (see Figure 5.21-A). Assessing the global MAE for the ANI_{lb} variables as

function of different percentages of ectopic beats present in the tachograms, it was noticeable that, regardless of the criteria chosen to optimize the model order P, the AR strategy to correct ectopic beats was not outperforming the other methods.

Revising the process of calibrating the AR model, it was concluded that the performance of this strategy to correct the ectopic intervals was being critically impacted by the fact that any previous forecasting of R-R intervals was being included in the estimation of a new following AR model. So, the error accumulation inevitably resulting from each prediction was being amplified throughout the process.

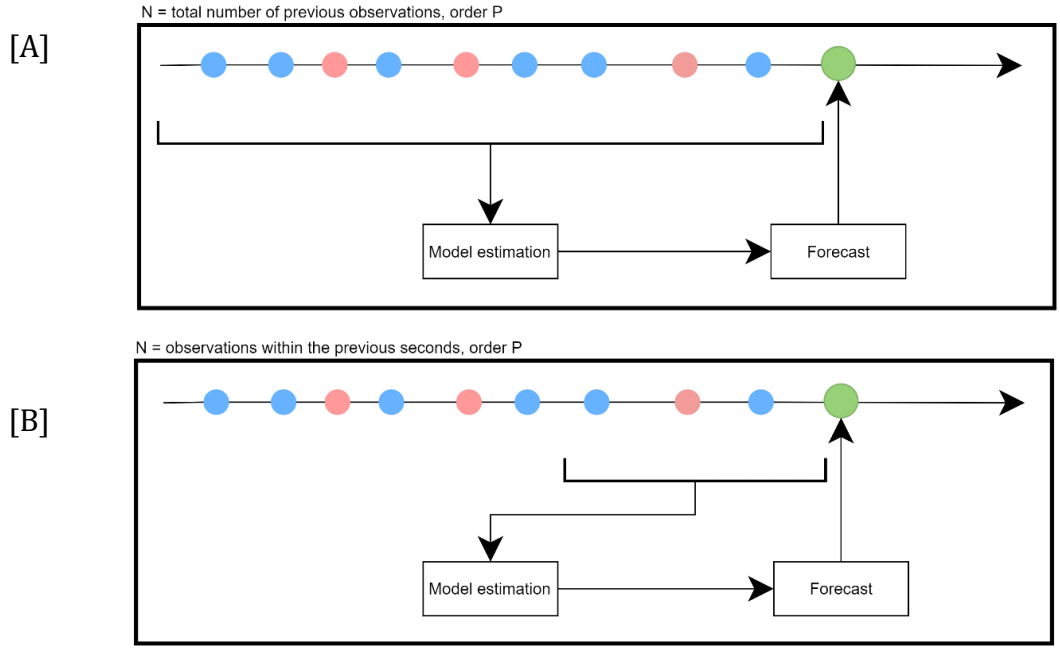

Figure 5.21: Representation of the forecasting of an R-R interval to replace an ectopic observation (in green). The estimation of the model parameters is performed using [A] all the previous observations or [B] the estimation within a specified window. The previous observations comprise sinus intervals (in blue) and R-R intervals already predicted to correct ectopic beats (in pink).

Specifying the order P and assessing the referred dependency when predicting a new sample, the parametric model estimations were performed using the control R-R series instead of the R-R series comprising the previous predictions. Hence, the resulting errors would only be influenced by residuals from AR estimation. This approach represented a considerable reduction in MAE for each degree of normal beats converted into ectopic beats. However, it is not possible to apply this methodology in a real context because no control R-R series would be available.

Trying to find a trade-off between system identification and the influence of previous predictions, a sliding window technique was employed by reducing the frame dimension used to estimate the model parameters (see Figure 5.21-B). Frames of N = 30, 60, 120, and 180 seconds before the ectopic timing were evaluated for model identification at a specified order P.

According to the results in Table 5.4, the MAE is overall diminished by reducing the frame dimension. The most considerable reduction corresponds to settling the frame dimension at 60 seconds, and this is also the setting with less significant variation of MAE between 1% of ectopic presence and 10% of ectopic presence. Therefore, the frame dimension was settled at 60 seconds as it seems to be the best trade-off between system identification and dependency to previous predictions in this dataset.

x \ N	a	30	60	120	180
1	0.49 ± 0.33	0.48 ± 0.31	0.47 ± 0.29	0.48 ± 0.20	0.47 ± 0.29
2	0.77 ± 0.47	0.78 ± 0.46	0.76 ± 0.45	0.76 ± 0.45	0.76 ± 0.47
3	0.96 ± 0.48	0.98 ± 0.49	0.93 ± 0.46	0.94 ± 0.49	0.95 ± 0.42
4	1.12 ± 0.53	1.12 ± 0.49	1.08 ± 0.50	1.09 ± 0.50	1.10 ± 0.50
5	1.25 ± 0.61	1.26 ± 0.59	1.20 ± 0.58	1.21 ± 0.59	1.21 ± 0.56
6	1.56 ± 0.75	1.42 ± 0.67	1.37 ± 0.68	1.41 ± 0.74	1.43 ± 0.60
7	1.75 ± 0.76	1.45 ± 0.73	1.43 ± 0.69	1.47 ± 0.72	1.49 ± 0.60
8	1.91 ± 0.86	1.63 ± 0.71	1.62 ± 0.71	1.65 ± 0.76	1.67 ± 0.67
9	2.17 ± 0.94	1.84 ± 0.91	1.76 ± 0.87	1.81 ± 0.89	1.82 ± 0.78
10	2.50 ± 0.91	1.88 ± 0.81	1.78 ± 0.79	1.87 ± 0.80	1.91 ± 0.75

Table 5.4: Different frame dimensions (N): MAE ± SD for the ANI_{lb} variables of control and corrected R-R series as a function of different percentages of ectopic beats (x). (a refers to the total number of previous observations being considered to estimate the AR model parameters)

Then, the R-R series of the group control were used to estimate the model parameters for the several frame dimensions, and it could be observed that the optimal model order chosen for each set of data using shorter segments was usually lower than the selected considering longer frames of data with the total number of observations. The same conclusions were found in [138] that additionally concluded that underestimating the model order would cause more dramatic effects by dampening the power spectra and not being able to fully estimate the original signal [138]. Hence, the model orders chosen by the AIC, MDL, and Kahn criterion for longer frames of data were kept in the settings for AR model identification using the 60-second window prior to the timing of the ectopic interval being corrected.

Thus, the analysis proceeded with the R-R intervals to correct the ectopic beats being predicted using the AR model estimated with a frame of 60 seconds and for each of the model orders suggested by the different criteria considered. The ANI variables were made available for the control and the corrected R-R series, and then, the MAE and respective standard deviation were calculated per each model order tested.

From Table 5.5, the estimated models using the MDL (P = 11) and Kahn criterion (P = 12) seem to be performing comparably but the Kahn criterion is computationally more expensive, having a larger running time. The MAE between the ANI_{lb} values from the control tachograms and that from the estimated tachograms is reduced when estimating

the R-R intervals to correct the ectopic intervals through AR models with order selected by these two criteria, overall outperforming the choice of the model order by the AIC criterion (P = 17). Besides the model orders, there was no difference in the processes that led to the calculation of the MAE and, therefore, these results corroborate the impact of an adequate choice for the order of the model [137]–[139], [142].

x \ P	**11**	**12**	**17**	**Adaptative**
1	0.44 ± 0.28	0.43 ± 0.28	0.46 ± 0.32	0.47 ± 0.30
2	0.76 ± 0.47	0.75 ± 0.46	0.74 ± 0.40	0.76 ± 0.47
3	0.84 ± 0.47	0.86 ± 0.42	0.87 ± 0.40	0.95 ± 0.52
4	1.03 ± 0.50	1.00 ± 0.48	1.05 ± 0.46	1.10 ± 0.54
5	1.16 ± 0.56	1.17 ± 0.59	1.17 ± 0.50	1.26 ± 0.63
6	1.30 ± 0.60	1.31 ± 0.58	1.34 ± 0.63	1.40 ± 0.69
7	1.37 ± 0.60	1.37 ± 0.60	1.40 ± 0.55	1.46 ± 0.72
8	1.59 ± 0.67	1.59 ± 0.70	1.60 ± 0.75	1.62 ± 0.76
9	1.65 ± 0.78	1.65 ± 0.76	1.71 ± 0.66	1.76 ±0.94
10	1.67 ± 0.75	1.66 ± 0.78	1.83 ± 0.84	1.80 ±0.84

Table 5.5: Different model orders (P): MAE ± SD for the ANI_{lb} variables of control and corrected R-R series as a function of different percentages of ectopic beats (x).

Nevertheless, it should be noted the disparity of selected model orders with multivariate signals (Figure 5.20). Additionally, by reducing the frame dimension used to estimate the model parameters, the model order predicted by the different criteria changes over time of the HRV signal, i.e., a progression of the model order is observed. Thus, it was investigated the use of an adaptative model order rather than specifying a fixed one. Using the MDL criterion, the optimum model order for each estimation of R-R intervals was selected from the information contained in the 60 seconds of the HRV signal before the ectopic intervals being corrected. From Table 5.5, comparing the results obtained for a fixed model order of 11 (the most frequently chosen with the MDL criterion) with the results obtained of using an adaptive model order, the global MAE between the ANI_{lb} variables from the control tachograms and that from the estimated tachograms is not reduced with the use of an adaptative AR model order. This analysis evidence what has already been stated: parametric estimation with shorter segments may produce an underestimation of the model order. Consequently, one must choose a fixed model order that still allows an accurate estimate of the R-R intervals.

Summing up, modelling an autoregressive model to estimate R-R intervals correcting ectopic intervals and subsequent ANI computation, the best architecture identified accounting the trade-offs previously mentioned was to estimate the model parameters with the 60-second frame of observations previous to the ectopic interval and settle a fixed model order of 11.

5.2.1.2 Modelling the neural network

As the choice of the AR model order is crucial, so is the choice of the neural network architecture, becoming of upmost importance [37]. The first decision to be made in the learning strategy of the NN was the number of R-R intervals considered to feed the network at the input layer. Through a trial error approach, several options were considered for the number of input values. It was even considered feeding the NN with the last eleven observations since this was identified as the optimum AR model order identified. With a maximum of 500 epochs in the learning process, the random search technique was employed to estimate the optimal learning rate parameter and number of units of the hidden layer(s).

Preventing from unbiased prediction accuracy, the cross-validation was repeated fifty times considering all the data obtained from the selection process and the performance indicator was the MSE obtained for the test sets. The test set was randomly settled on 20% of the total set and 80% of the data served as training set. The 5-fold cross validation was then applied on the training set. Table 5.6 summarizes parameters, hyperparameters, and performance of the best NN's architectures identified by feeding the network with the previous 5, 11 or 20 values of the R-R intervals.

Neural Network: best architectures				
Number of layers*1	3	3	4	4
Number of nodes	[5, 10, 1]	[20, 10, 1]	[5, 10, 7, 1]	[11, 15, 7, 1]
Activation function	[sigmoid, linear]	[sigmoid, linear]	[linear, sigmoid, linear]	[linear, sigmoid, linear]
Learning rate α	0.08	0.40	0.25	0.15
Epochs	5000	5000	5000	5000
MSE	0.28 ± 0.05	0.31 ± 0.16	0.26 ± 0.01	0.23 ± 0.06

Table 5.6: Best architectures identified for the neural networks in terms of number of input nodes and respective MSE (mean ± SD) (*1 Including the output layer of the neural networks)

Moreover, suggesting that identified models were not overfitted, the learning curves for the validation sets when a given fold was left out and those of the corresponding training sets were analysed and found to be convergent. Additionally, it appears that losses were being gradually diminished and, thus, meaningful representations may be being achieved.

Following the results in Table 5.6, the identified architecture that seems to have a more significant contribution to the prediction of the R-R intervals correcting ectopic beats can be described as a fully connected network consisting of four layers: an input layer with 11 nodes representing the last 11 observations; two hidden layer capturing the non-linearity of the problem, the first hidden layer consists of 15 nodes with linear activation function, and the second consists of 7 nodes with sigmoid activation function; an output

layer consisting of a node with a linear activation function and representing the dependent variable, the predicted R-R interval.

5.2.2 Model selection for correction of ectopic intervals

In a first approach, randomly inserting ectopic beats into the control R-R series, an edited dataset was constructed for each degree of ectopy considered in this study. The comparisons were performed between the ANI_{lb} variables calculated from the control R-R series and that from the surrogated R-R series. As expected, there are differences between the medians and interquartile ranges of the computed ANI_{lb} variables, verifying that, additionally to the need for ectopic correction, the strategy applied for correcting the ectopic intervals would influence the similarity between the ANI_{lb} variables (Figure 5.22).

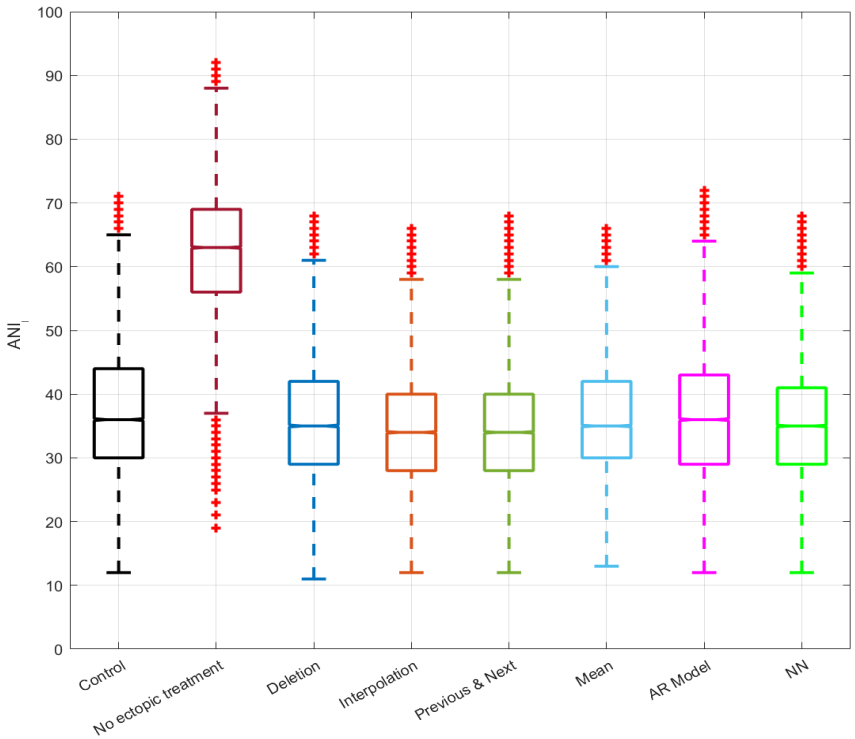

Figure 5.22: Distribution of the ANI_{lb} variables calculated from the control R-R series and that from the R-R series corrected applying the different strategies for a proportion of 10% of ectopic beats.

Table 5.7 and Table 5.8 summarize the performance in terms of NMI and MAE applying the different ectopic correction methods to the edited datasets with different degrees of ectopy. Higher performances would imply decreased MAE (as close as possible to 0) and increased NMI (as close as possible to 1). Hence, performing the comparison between the ANI_{lb} variables calculated without ectopic treatment against each of the ANI_{lb} variables calculated applying one of the ectopic correction methods, it could be verified that the performance significantly increased when ectopic treatment was applied (Mann-Whitney rank test, p-value < 0.05). Figure 5.23 depicts a graphical comparison of the performance reached by all the strategies for ectopic correction depending on the percentage of

normal beats converted to ectopic beats ($x = 1\%,\ x = 5\%,\ x = 10\ \%$). Moreover, increasing the presence of ectopy, it was observed a decrement in the NMI metric and an increment in the MAE between the ANI_{lb} variables calculated from the control R-R series and the respective estimated R-R series.

For suspicion of high variability in results since both the amount and distribution of ectopy along the tachogram were shown to affect the calculation of ANI scores, the process of inserting ectopic beats artificially was repeated ten times for each episode and each degree of ectopy. Table 5.9 and Table 5.10 list the averaged results by quantifying the performance of the different methods for correcting ectopic intervals. Figure 5.24 depicts the graphical comparison of Table 5.9 and Table 5.10 depending on the ectopy degree ($x = 1\%,\ x = 5\%,\ x = 10\ \%$). Performance evaluation for the different strategies in the same degree of ectopy and variable distributions of ectopic intervals along the HRV signal would reveal the prediction potential of each method. Regardless of the ectopic correction strategy, similar results were obtained among the iterations, which may disclose that the performance of each technique would be comparable independently of the clinical context. Nevertheless, this observation requires further clinical validation in a more heterogeneous dataset.

Despite being the simplest technique and one of the most reported for correction of ectopic intervals [135], [151], the 'Deletion' method presented the lowest performance in terms of NMI and MAE metrics. This technique implies reducing the number of R-R intervals under analysis because it removes all the ectopic intervals and, subsequently, shifts the HRV signal posterior to them. Other researches have reported similar findings since the phase shift introduced in the HRV signal by the Deletion method would have an effect on the PSD estimation, leading to changes in the frequency domain parameters [135]. The ANI values are calculated through the analysis of the HF-band of the PSD, so this should be the main source for the discrepancy in the calculation of ANI variables through the control R-R series and the R-R series in which the ectopic intervals were corrected by this method. Taking into account the previous statements, the 'Deletion' method was excluded from the procedure to select the most suitable model for correcting ectopic intervals in this work.

Furthermore, the performance of the different interpolation methods revealed that these techniques would only be suitable when the ectopic beats occur very occasionally ($x = 1\%$). Previous studies have already demonstrated that correcting ectopic applying interpolation strategies may change extremely the PSD estimation and assessment of non-linear parameters in the analysis of HRV signals having a similar effect as the 'Deletion' method [116], [135]. Thus, these three methods ('Linear', 'Spline' and 'Nearest' interpolation) were also not considered in the statistical analysis for the evaluation of which method would be performing best for the correction of ectopic intervals. Therefore, further performance analysis was restricted to the following methods: 'Previous & Next', 'Mean', 'AR Model', 'NN Model'.

x (%)	No ectopic treatment	Deletion	'Linear' interpolation	'Spline' interpolation	'Nearest' interpolation	Previous & Next	Mean	AR model	NN
1	0.15 ± 0.10	0.51 ± 0.11	0.59 ± 0.11	0.58 ± 0.11	0.57 ± 0.11	0.70 ± 0.10	0.68 ± 0.10	0.70 ± 0.11	0.71 ± 0.09
2	0.06 ± 0.03	0.46 ± 0.11	0.52 ± 0.11	0.51 ± 0.12	0.50 ± 0.11	0.61 ± 0.10	0.60 ± 0.10	0.60 ± 0.12	0.63 ± 0.10
3	0.04 ± 0.03	0.40 ± 0.11	0.49 ± 0.12	0.48 ± 0.12	0.48 ± 0.11	0.57 ± 0.11	0.55 ± 0.10	0.56 ± 0.12	0.59 ± 0.10
4	0.04 ± 0.03	0.37 ± 0.11	0.46 ± 0.12	0.45 ± 0.12	0.45 ± 0.12	0.53 ± 0.11	0.51 ± 0.11	0.52 ± 0.11	0.55 ± 0.11
5	0.04 ± 0.02	0.34 ± 0.11	0.45 ± 0.11	0.44 ± 0.11	0.44 ± 0.11	0.51 ± 0.11	0.48 ± 0.11	0.48 ± 0.12	0.54 ± 0.11
6	0.04 ± 0.02	0.32 ± 0.11	0.43 ± 0.11	0.41 ± 0.11	0.42 ± 0.12	0.48 ± 0.11	0.45 ± 0.11	0.47 ± 0.12	0.50 ± 0.11
7	0.04 ± 0.01	0.30 ± 0.12	0.44 ± 0.12	0.41 ± 0.12	0.43 ± 0.11	0.47 ± 0.11	0.44 ± 0.11	0.46 ± 0.12	0.50 ± 0.11
8	0.04 ± 0.01	0.28 ± 0.12	0.41 ± 0.12	0.38 ± 0.12	0.40 ± 0.11	0.45 ± 0.11	0.42 ± 0.11	0.42 ± 0.11	0.47 ± 0.10
9	0.05 ± 0.02	0.27 ± 0.11	0.40 ± 0.12	0.37 ± 0.12	0.38 ± 0.11	0.42 ± 0.11	0.40 ± 0.11	0.43 ± 0.12	0.46 ± 0.11
10	0.04 ± 0.01	0.26 ± 0.10	0.39 ± 0.12	0.36 ± 0.11	0.38 ± 0.11	0.41 ± 0.11	0.39 ± 0.10	0.41 ± 0.11	0.44 ± 0.11

Table 5.7: ANI_{lb} calculation performance in terms of NMI (mean ± standard deviation) for the different methods proposed for ectopic correction.

x (%)	No ectopic treatment	Deletion	'Linear' interpolation	'Spline' interpolation	'Nearest' interpolation	Previous & Next	Mean	AR model	NN
1	6.09 ± 3.55	1.21 ± 0.69	0.92 ± 0.61	0.93 ± 0.60	0.93 ± 0.65	0.54 ± 0.42	0.56 ± 0.36	0.43 ± 0.28	0.49 ± 0.36
2	10.21 ± 4.02	1.58 ± 0.67	1.33 ± 0.77	1.35 ± 0.80	1.32 ± 0.69	0.91 ± 0.63	0.88 ± 0.51	0.75 ± 0.46	0.78 ± 0.47
3	13.86 ± 5.14	1.94 ± 0.83	1.63 ± 0.95	1.63 ± 0.98	1.51 ± 0.81	1.16 ± 0.77	1.12 ± 0.58	0.86 ± 0.42	0.97 ± 0.57
4	17.34 ± 6.55	2.24 ± 0.94	1.92 ± 0.98	1.91 ± 1.05	1.77 ± 0.92	1.44 ± 0.97	1.34 ± 0.70	1.00 ± 0.48	1.18 ± 0.71
5	21.34 ± 8.05	2.55 ± 1.04	2.16 ± 1.16	2.08 ± 1.20	1.92 ± 1.00	1.67 ± 1.00	1.54 ± 0.73	1.17 ± 0.58	1.33 ± 0.76
6	24.16 ± 8.79	2.77 ± 1.10	2.45 ± 1.38	2.38 ± 1.45	2.15 ± 1.22	1.90 ± 1.34	1.78 ± 1.05	1.31 ± 0.59	1.56 ± 0.96
7	27.06 ± 9.56	2.98 ± 1.20	2.62 ± 1.40	2.52 ± 1.41	2.17 ± 1.15	2.11 ± 1.40	1.86 ± 0.96	1.37 ± 0.60	1.63 ± 0.99
8	28.24 ± 10.22	3.19 ± 1.45	3.01 ± 1.71	2.88 ± 1.77	2.55 ± 1.42	2.42 ± 1.62	2.09 ± 1.16	1.59 ± 0.70	1.88 ± 1.13
9	29.48 ± 10.24	3.47 ± 1.49	3.28 ± 1.86	3.08 ± 1.87	2.80 ± 1.69	2.67 ± 1.84	2.31 ± 1.38	1.65 ± 0.76	2.01 ± 1.34
10	30.56 ± 10.18	3.63 ± 1.62	3.63 ± 2.00	3.56 ± 2.19	3.02 ± 1.78	2.90 ± 1.98	2.46 ± 1.43	1.66 ± 0.78	2.16 ± 1.32

Table 5.8: ANI_{lb} calculation performance in terms of MAE (mean ± standard deviation) for the different methods proposed for ectopic correction.

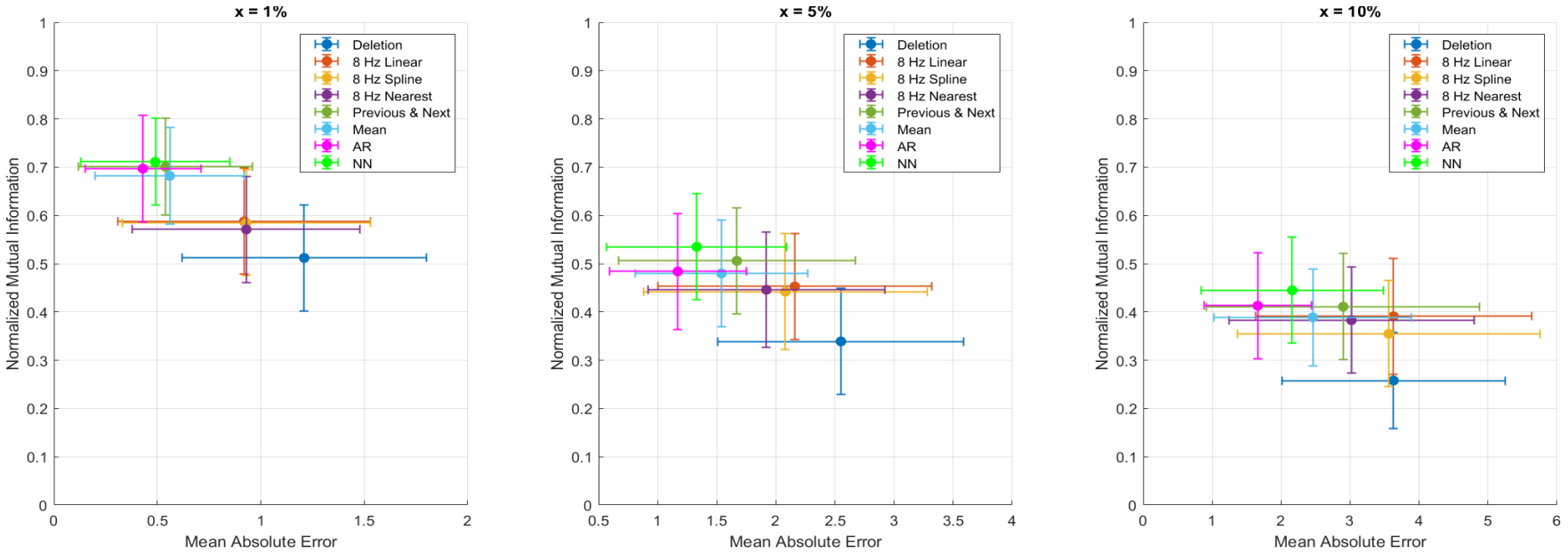

Figure 5.23: Graphical comparison of the performance metrics (represented as mean ± standard deviation) between the ANI_{lb} variables calculated from the control R-R series and that from the R-R series after correcting the ectopic intervals using each of the different methods.

x (%)	No ectopic treatment	Deletion	'Linear' interpolation	'Spline' interpolation	'Nearest' interpolation	Previous & Next	Mean	AR model	NN
1	0.14 ± 0.00	0.50 ± 0.01	0.59 ± 0.00	0.57 ± 0.01	0.56 ± 0.00	0.70 ± 0.00	0.68 ± 0.01	0.71 ± 0.01	0.71 ± 0.01
2	0.06 ± 0.00	0.45 ± 0.00	0.52 ± 0.00	0.51 ± 0.00	0.50 ± 0.01	0.62 ± 0.01	0.60 ± 0.01	0.70 ± 0.02	0.64 ± 0.00
3	0.04 ± 0.01	0.41 ± 0.00	0.50 ± 0.00	0.48 ± 0.00	0.48 ± 0.00	0.57 ± 0.00	0.55 ± 0.00	0.58 ± 0.00	0.60 ± 0.01
4	0.04 ± 0.01	0.38 ± 0.00	0.47 ± 0.01	0.45 ± 0.01	0.45 ± 0.01	0.53 ± 0.01	0.51 ± 0.01	0.54 ± 0.01	0.55 ± 0.01
5	0.04 ± 0.00	0.34 ± 0.01	0.45 ± 0.00	0.43 ± 0.00	0.44 ± 0.00	0.50 ± 0.01	0.48 ± 0.01	0.51 ± 0.01	0.53 ± 0.00
6	0.04 ± 0.00	0.32 ± 0.00	0.43 ± 0.01	0.42 ± 0.00	0.42 ± 0.01	0.48 ± 0.01	0.46 ± 0.01	0.50 ± 0.00	0.51 ± 0.01
7	0.04 ± 0.00	0.30 ± 0.00	0.42 ± 0.01	0.40 ± 0.00	0.41 ± 0.01	0.46 ± 0.01	0.44 ± 0.01	0.48 ± 0.01	0.49 ± 0.01
8	0.04 ± 0.00	0.28 ± 0.24	0.41 ± 0.00	0.38 ± 0.01	0.40 ± 0.00	0.45 ± 0.01	0.42 ± 0.00	0.47 ± 0.01	0.48 ± 0.01
9	0.04 ± 0.00	0.27 ± 0.00	0.39 ± 0.01	0.37 ± 0.00	0.39 ± 0.00	0.42 ± 0.01	0.40 ± 0.00	0.45 ± 0.00	0.46 ± 0.00
10	0.04 ± 0.00	0.26 ± 0.00	0.39 ± 0.00	0.36 ± 0.01	0.38 ± 0.00	0.41 ± 0.01	0.39 ± 0.01	0.44 ± 0.01	0.45 ± 0.01

Table 5.9: ANI_{lb} calculation performance in terms of NMI (mean ± standard deviation) for the different methods proposed for ectopic correction considering ten distributions of ectopic beats.

x (%)	No ectopic treatment	Deletion	'Linear' interpolation	'Spline' interpolation	'Nearest' interpolation	Previous & Next	Mean	AR model	NN
1	6.22 ± 0.06	1.26 ± 0.03	0.91 ± 0.02	1.01 ± 0.03	1.00 ± 0.02	0.53 ± 0.01	0.55 ± 0.02	0.45 ± 0.02	0.47 ± 0.02
2	9.94 ± 0.09	1.58 ± 0.03	1.29 ± 0.02	1.35 ± 0.02	1.31 ± 0.03	0.84 ± 0.04	0.86 ± 0.02	0.63 ± 0.00	0.74 ± 0.02
3	13.73 ± 0.12	1.86 ± 0.03	1.53 ± 0.03	1.58 ± 0.02	1.49 ± 0.04	1.11 ± 0.01	1.10 ± 0.02	0.89 ± 0.01	0.94 ± 0.04
4	17.74 ± 0.22	2.16 ± 0.03	1.86 ± 0.06	1.90 ± 0.07	1.75 ± 0.05	1.41 ± 0.03	1.33 ± 0.04	1.06 ± 0.04	1.18 ± 0.04
5	21.29 ± 0.22	2.46 ± 0.03	2.14 ± 0.03	2.16 ± 0.04	1.95 ± 0.03	1.65 ± 0.04	1.54 ± 0.04	1.19 ± 0.05	1.33 ± 0.02
6	23.96 ± 0.16	2.73 ± 0.02	2.42 ± 0.03	2.37 ± 0.04	2.15 ± 0.04	1.92 ± 0.04	1.74 ± 0.05	1.27 ± 0.03	1.50 ± 0.02
7	26.90 ± 0.13	2.94 ± 0.03	2.74 ± 0.09	2.63 ± 0.10	2.38 ± 0.08	2.15 ± 0.06	1.92 ± 0.06	1.42 ± 0.07	1.68 ± 0.05
8	28.21 ± 0.24	3.17 ± 0.03	3.02 ± 0.03	2.94 ± 0.05	2.56 ± 0.03	2.37 ± 0.02	2.08 ± 0.04	1.52 ± 0.02	1.79 ± 0.03
9	30.12 ± 0.24	3.39 ± 0.04	3.40 ± 0.04	3.25 ± 0.06	2.81 ± 0.06	2.68 ± 0.09	2.30 ± 0.04	1.63 ± 0.03	2.01 ± 0.05
10	30.78 ± 0.14	3.60 ± 0.04	3.69 ± 0.07	3.54 ± 0.06	3.03 ± 0.05	2.88 ± 0.05	2.40 ± 0.07	1.71 ± 0.04	2.11 ± 0.05

Table 5.10: ANI_{lb} calculation performance in terms of MAE (mean ± standard deviation) for the different methods proposed for ectopic correction considering ten distributions of ectopic beats.

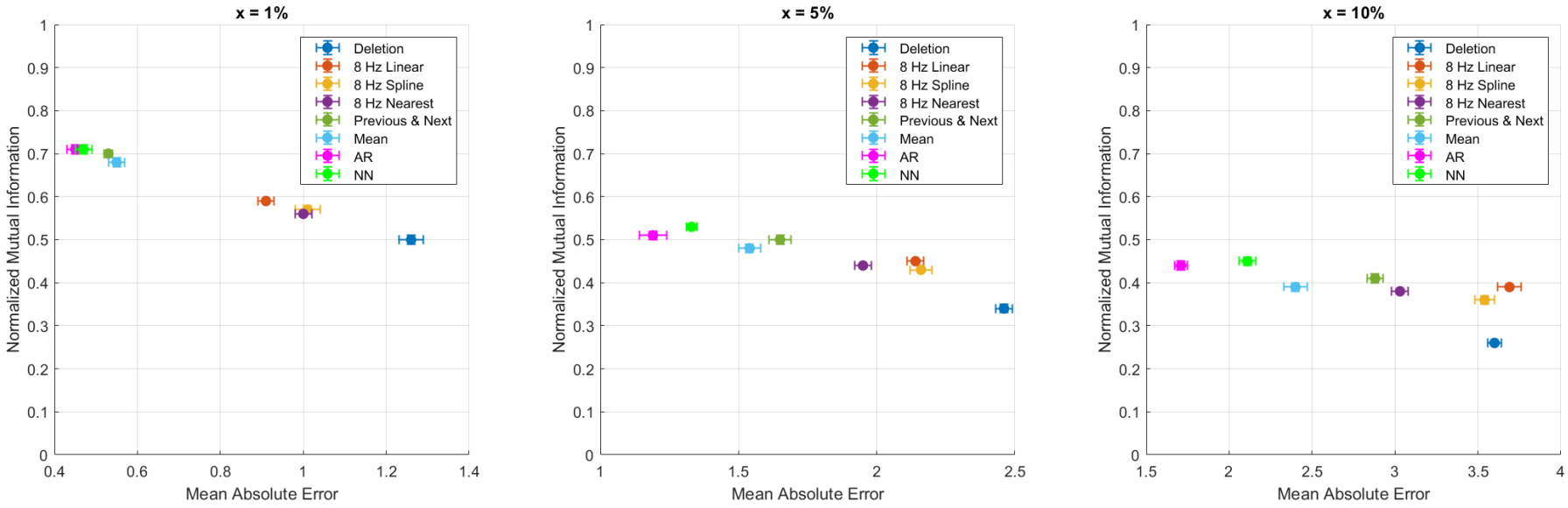

Figure 5.24: Considering ten distributions of ectopic beats, graphical comparison of the performance metrics (represented as mean ± standard deviation) between the ANI_{lb} variables calculated from the control R-R series and that from the R-R series after correcting the ectopic intervals using each of the different methods.

The performance of the four methods to correct ectopic intervals was evaluated for three different degrees of ectopy ($x = 1\%,\ x = 5\%,\ x = 10\ \%$) (Figure 5.25). Regardless of the proportion of ectopic intervals to correct, the best performance in terms of MAE was obtained by replacing the ectopic intervals with R-R intervals estimated using the AR model. In terms of NMI, when a percentage of 1% of ectopy is present, the AR model seems to be the best performing technique but at 5% or 10% of ectopic presence applying the NN model to estimate R-R intervals seems to perform best. Hence, it becomes more difficult to select the method with the best performance, and statistical validation was implemented to compare the performance of the different methods considered for ectopic correction.

For the NMI and the MAE and for each of the three different degrees of ectopy, the Kruskal Wallis H test was employed to determine if the differences between the performance of the methods to correct the ectopic intervals would be statistically significant. The given p-values were all < 0.05 when compared with a χ^2 distribution with 3 degrees of freedom which indicates that, at each degree of ectopy, there is a significant difference in the ANI_{lb} variables between at least two of the strategies applied for ectopic correction.

Since the null hypothesis of no difference between the methods to correct ectopic intervals were rejected, the post-hoc multiple comparison test with a Bonferroni correction was employed to determine which groups would be statistically different. However, in the three different degrees of ectopy, all NMI and MAE differences between the ectopic interval correction methods were found to be statistically significant (p-value < 0.05). According to each performance metric, one of the methods used to correct the ectopic intervals would be outperforming the others. However, there is no guarantee that the same method was considered the best by both the NMI and the MAE metrics. These results indicate that the ideal method employed to correct the ectopic intervals would depend on the proportion of ectopic intervals present in the HRV signal and the operating region, taking into account the dynamics of the HRV signal and the position of the ectopic intervals to be corrected.

Accordingly, at $x = 1\%$, $x = 5\%$, and $x = 10\ \%$, the Mann–Whitney rank test was employed to test whether the ANI_{lb} variables calculated from the R-R series corrected with each method were statistically different from the ANI_{lb} variables calculated from the control R-R series (Table 5.11).

x (%)	**Previous & Next**	**Mean**	**AR Model**	**NN model**
1	0.0045	0.2030	0.8526	0.0845
5	3.28×10^{-45}	9.31×10^{-7}	0.1304	6.62×10^{-17}
10	3.41×10^{-90}	7.77×10^{-8}	0.0433	1.32×10^{-30}

Table 5.11: P-values for $x = 1\%$, $x = 5\%$, and $x = 10\ \%$ performing the comparison of the ANI_{lb} variables calculated from the control R-R series and that from the R-R series after correcting the ectopic intervals using the 'Previous & Next', 'Mean', 'AR Model', and 'NN Model' methods.

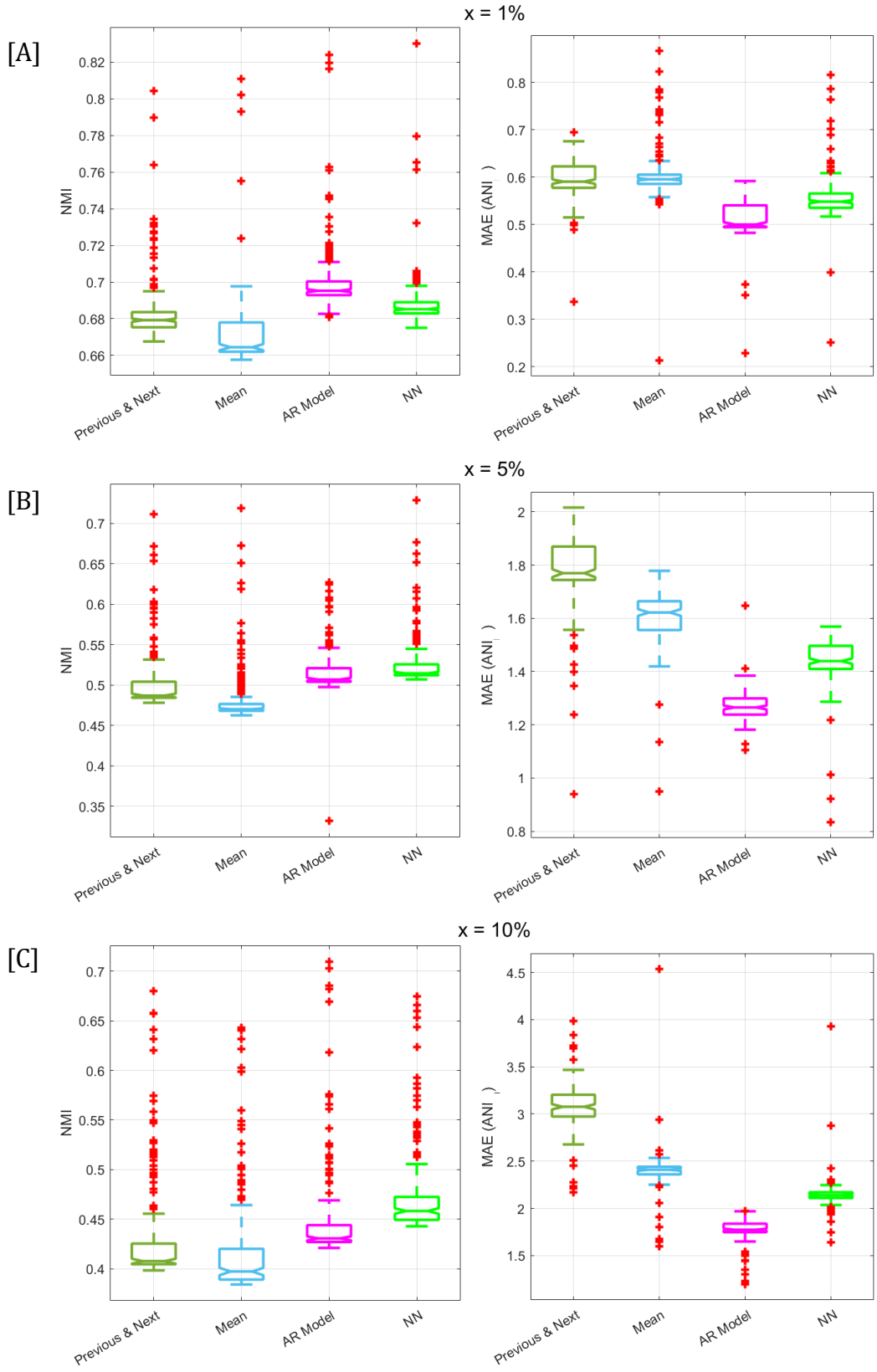

Figure 5.25: Distribution of the MAE and NMI metrics at $x = 1\%$, $x = 5\%$, and $x = 10\ \%$ correcting the ectopic intervals using the 'Previous & Next', 'Mean', 'AR Model', and 'NN Model' methods.

The evaluation was performed by assessing the similarity between the ANI scores calculated from control R-R series (ectopic-free) and that from R-R series contaminated with ectopic intervals and posteriorly corrected making use of different strategies. Analysing the results in Table 5.11, at $x = 1\%$, a statistically significant difference was only found performing the comparison between the ANI_{lb} variable calculated from the control R-R series and that calculated from the R-R series after the correction of ectopic intervals with the 'Previous & Next' method. Except when applying the 'AR Model', at a proportion of 5% of ectopy presence, the ANI_{lb} variable calculated from the control R-R series was proved to be significantly different from that calculated from the R-R series after the correction of ectopic intervals with any of the considered methods. At $x = 10\%$, statistically significant differences were found performing the comparisons between the ANI_{lb} variable calculated from the control R-R series and that from the R-R series after the correction of ectopic intervals with any of the considered methods.

The techniques assessed to correct ectopic intervals are of real-time implementation and easily derived from HRV signals obtained from the physiological parameters available in the OR. Although results have shown that performance is strengthened by using any of the ectopic correction methods, they also showed that performance is influenced by the strategy used to do it.

Regarding the 'Previous and Next' method, despite showing comparable performance to the AR model at $x = 1\%$, its performance rapidly deteriorates increasing the percentage of ectopic intervals in the HRV signal and, in a proportion of 10% of ectopy, this method has identical effect and performance to the 'Nearest interpolation' method (Figure 5.23). With a high density of ectopic intervals, this method is not able to translate the oscillation in consecutive cardiac cycles as it does not have adaptive modulation capacity and, therefore, it becomes ineffective in describing the autonomic dynamics. In fact, being influenced by the distribution of ectopic intervals across the HRV signal, this is one of the methods with the highest standard deviation in calculating the MAE (Table 5.8).

The 'Mean' method outperformed the 'Previous and Next' in terms of MAE (Table 5.8), which may be explained by the fact that this method, replacing the ectopic intervals with the arithmetic mean of the last five samples, is capable of translating more appropriately the oscillation of the consecutive cardiac cycles. However, any event may lead to a sudden variation in the HRV signal and then, in case of a high presence of ectopic intervals, the performance of the "Mean" method would also be worsened because, apart from the last five samples, the system is memoryless and not enough information exists to describe the activity of the HRV signal.

Concerning the 'AR Model' approach, as described in section 5.1, a straightforward method was applied by assuming that the HRV signal would exhibit serial autocorrelation and then, using the past eleven observations to predict the R-R interval and correct the ectopic samples in the HRV signal. Despite being the most effective among the strategies

implemented to correct ectopic intervals, the approach of using the AR model to estimate R-R intervals is mathematically limited as it only considers the linear modulation of the HRV signal and non-linear phenomena are indicated as responsible for the dynamics of this signal [25]. Furthermore, the performance of this method may depend on the ability of the estimated model parameters to describe the system's behaviour and recognize patterns in data. The influence of the parametric modelling approach was observed to differ between the HRV signals and may be related to the fact that each HRV dynamics is defined by distinct physical or physiological aspects, including the complex interactions of neurocardiac regulations [25], [138]. Therefore, the loss of HRV information predicting R-R intervals using this linear approach and the influence of previous predictions on the parametric model estimations (fully explained in section 5.2.1.1) may account for the error accumulation throughout the process.

Using the architecture defined in section 5.2.1.2, the 'NN model' predicts the R-R intervals to replace the ectopic intervals by feeding a multi-layer artificial neural network with the last eleven observations. Although this strategy is usually employed for automatic feature extraction and classification problems [37], [143], the NN was applied for a task of system identification. Results have shown that using NNs to correct ectopic intervals can improve the similarity of ANI scores computed from the R-R series contaminated with ectopic intervals compared to that from the ectopic-free R-R series (Figure 5.24). Compared to the other strategies, the NN model could be expected to be a more effective predictor for time-varying signals due to their non-linear properties. However, from the presented results, the use of the AR model outperformed the NN strategy. Training a NN with a high capability to predict future samples in HRV signals requires a large number of examples [143], [152]. Accordingly, as only those ECG records of a single type of surgery would be analysed and a high proportion of data was qualitatively discarded, the relatively small size of the dataset could constraint the learning strategy and, consequently, the drawing of meaningful conclusions through the employment of this method to estimate R-R intervals and correct the ectopic intervals. Additionally, the complexity of the learning algorithm is rather dependent on the complexity of the inputted data than by the network structure [152]. Notwithstanding its simplicity, the input vector considered seemed to be adequate for the context, as results showed that valuable information for the prediction of HRV signal was retrieved. Even so, it is expectable that the performance of the 'NN Model' method would be improved by incorporating additional information investigating the extraction of features in the time, frequency, and non-linear domains of the HRV signal.

In line with the presented and discussed results, it is proposed to correct ectopic intervals by replacing them with R-R intervals predicted with an AR model with parametric estimation based on the 60-second frame previous to the timing of the ectopic observation and model order 11.

5.2.3 Clinical implications from the use of the selected model

The method of correcting ectopic intervals estimating R-R intervals with the AR model compares well with the reference ANI score at a proportion of $x = 1\%$ and $x = 5\%$ of ectopic beats (Table 5.11). Despite not being highly significant (p-value > 0.01), a statistically significant difference was found when 10% of the normal intervals were converted into ectopic intervals (p-value < 0.05) (Table 5.11).

The implementation of this strategy for correction of ectopic intervals may not appear to be sufficiently significant for clinical implementation in a level of 10% of ectopy presence. However, it is noteworthy the significant performance improvement compared to when no ectopic treatment is applied (Figure 5.26) or even compared to the most currently employed techniques, the deletion and interpolation methods (Figure 5.23). The improved performance is perceived by a substantial reduction in the MAE and a considerable increase in the NMI.

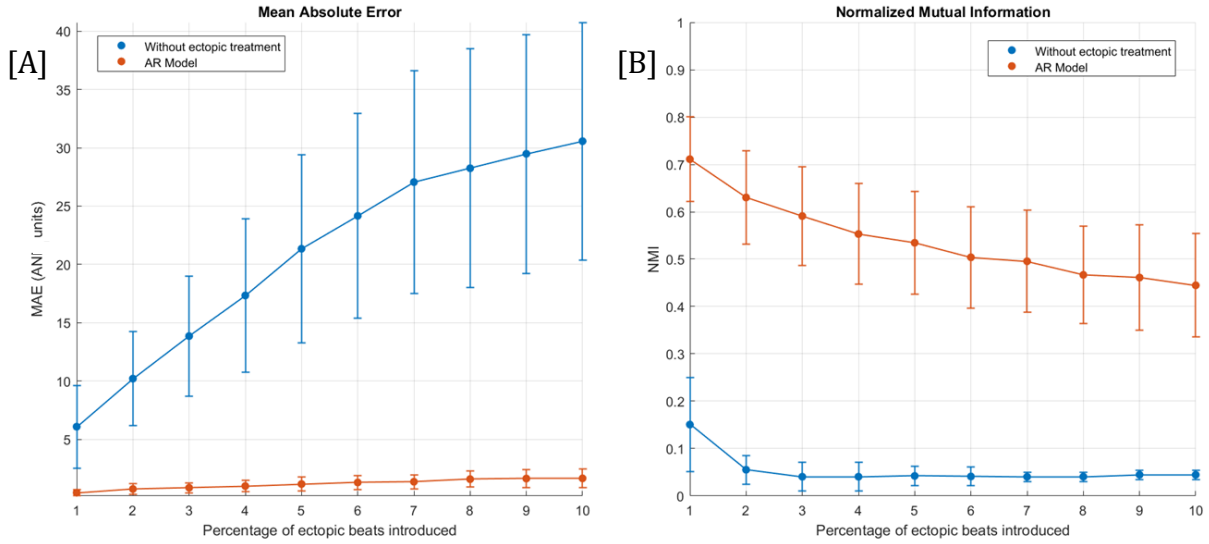

Figure 5.26: [A] MAE and [B] NMI calculated between the ANI_{lb} variable computed from the R-R tachogram extracted from the control group and that extracted from the edited tachograms (with no ectopic treatment or applying the proposed AR model to correct ectopic intervals) and varying the percentage of normal beats converted into ectopic beats.

Even though no statistical difference was found, the impact that the use of the AR model strategy to correct ectopic intervals could have in the decision-making process according to the ANI interpretation was assessed for $x = 1\%$ and $x = 5\%$. Results are summarized in the confusion matrices shown in Table 5.12 and Table 5.13, respectively. Since no episode was misclassified, it is thus corroborated that this technique is a promising tool for correction of ectopic intervals to an extent of up to 5%.

		Control group	
		ANI-	ANI+
Corrected group	ANI-	204	0
	ANI+	0	17

Table 5.12: At a proportion of 1% of ectopy, confusion matrix for the classification of the episodes according to the ANI_{lb} values and using the 'AR model' to correct ectopic intervals.

		Control group	
		ANI-	ANI+
Corrected group	ANI-	204	0
	ANI+	0	17

Table 5.13: At a proportion of 5% of ectopy, confusion matrix for the classification of the episodes according to the ANI_{lb} values and using the 'AR model' to correct ectopic intervals.

Illustrating the extreme case studied in this thesis, it has already been assessed the impact on the ANI_{lb} values converting 10% of the normal beats into ectopic beats and without applying any ectopic treatment (Figure 5.17). A significant variation of ANI was found between the scores computed from the control group and the edited dataset with a proportion of 10% of ectopic beats. However, as from the detailed distributions of the ANI_{lb} variables in Figure 5.22, correcting the ectopic intervals with the 'AR Model' method lead to much more comparable results, since the median [25th–75th percentile] at the control group is (36 [30-44] ANI_{lb}) and that at the edited dataset with 10% of ectopy added and posteriorly corrected is (35 [29-43] ANI_{lb}).

Additionally, at $x = 10\%$, the ANI_{lb} variable calculated from the control R-R series proved to be uncorrelated with the ANI_{lb} variable calculated from the R-R series in a proportion of 10% of ectopy and with no ectopic treatment; whereas the ANI_{lb} variable calculated from the control R-R series and that from the R-R series in a proportion of 10% of ectopy and posteriorly corrected using the 'AR Model' method were found to be highly correlated ($c > 0.98$).

In case of no ectopic treatment being applied, the ectopic intervals artificially introduced were found to act as confounders to the interpretation of the ANI scores since they would lead to the misclassification of many of the episodes (Table 5.3). The analysis proceeded to the interpretation of whether the ANI_{lb} scores derived in the presence of 10% of ectopy and posteriorly corrected using the 'AR Model' would be able to replicate the classification made using the control group. Thus, the suitability of the 'AR Model' to correct ectopic intervals was analysed in terms of its impact on the prediction of the different clinical situations defined according to the specifications of the ANI manufacturer. Results are summarized in the confusion matrix shown in Table 5.14.

		Control group	
		ANI-	ANI+
Corrected group	ANI-	203	5
	ANI+	1	12

Table 5.14: At a proportion of 10% of ectopy, confusion matrix for the classification of the episodes according to the ANI_{lb} values and using the 'AR model' to correct ectopic intervals.

Comparing to the performance when no ectopic treatment was employed (Table 5.3), the results showed in Table 5.14 evidence that the identified 'AR Model' may contribute to the drawing of meaningful conclusions while interpreting ANI values in the presence of non-sinus intervals at a degree of 10%. The accuracy of 97.29% was reached. However, the analysis must be carefully driven due to the existing unbalance between the original classification of the episodes, which can lead to unfounded optimistic conclusions. In fact, representing a considerable proportion, approximately 29% of episodes originally classified as type ANI+ were misclassified when a proportion of 10% of ectopic beats was added to the control R-R series and posteriorly corrected applying the 'AR Model'. This may indicate that correcting ectopic intervals with the 'AR Model' is leading to an underestimation of the parasympathetic tone according to the interpretation of the ANI values, and thus, rise false alarms of inappropriate levels of analgesia. Verifying the previous findings, it may be hindered the clinical implementation of this strategy to correct ectopic intervals to an extent of 10% of ectopy presence. To overcome this limitation, it would be interesting to attach a confidence measure to the calculated ANI values.

To understand whether this strategy for correcting ectopic intervals would be appropriate to be clinically implemented, it is important to understand the intrinsic medical connotation of the proportions $x = 1\%$, $x = 5\%$, and $x = 10\ \%$ of ectopic beats introduced in the ECG records. From a clinical point of view, the proportion $x = 1\%$ of ectopic beats may represent the single premature ventricular contraction (PVC) in which, sporadically, one ectopic beat is superimposed with the normal sequence of heart beats [28], [104]. This is the most recurrent situation in healthy individuals and often benign in nature without clinical significance [27], [28]. At the proportion $x = 5\%$ of ectopic beats, more complex medical cases of single PVCs were simulated to occur. Specifically, the simulated medical conditions associated with PVC comprise the occurrence of bigeminy (every other beat is a PVC), trigeminy (every third beat is a PVC), and couplet (two consecutive PVCs) [104], [153]. At the proportion $x = 10\%$ of ectopic beats, most of the simulated clinical situations correspond to non-sustained ventricular tachycardias (NSVT) characterized by sequences of three or more consecutive PVCs [154]. NSVT is linked to a wide range of prognostics, as it may be a marker of increased risk of subsequent sustained ventricular tachycardias and sudden cardiac death, or it may have no significant clinical importance [154], [155]. As previously stated, the results have evidenced the proposed AR model to be capable of accurately limiting the impact that the

occurrence of ectopic beats in a proportion of up to 5% has on the analysis of HRV signs in different clinical situations and, at $x = 10\%$, it was verified a reduction of the sensibility of the ANI to the presence of ectopic beats, making it sturdier and leading to a substantial improvement in its clinical interpretation.

Nonetheless, the clinical implementation of the proposed technique still requires further validation in real contexts since this study was performed with controlled simulated constraints. This analysis covered a wide range of clinical conditions to various degrees, but, in addition to PVCs, it should also be studied other phenomena recognized to be associated with the occurrence of ectopic beats, namely modifications of HRV by other pathologies or specific interventions [25]. Accordingly, the application of the proposed method to correct ectopic intervals in HRV signals should be independently assessed in the several clinical pathologies, as they may have different statistical characteristics. Feedback from physicians would be of uttermost importance to obtain accurate descriptions of the possible clinical situations, including more realistic assumptions about the prevalence, proportion, and distribution of ectopic intervals on ECG recording during surgery.

6 CONCLUSION AND FURTHER WORK

This dissertation outlined that the correction of ectopic intervals by predicting samples of the HRV signal would be one of the main targets of information processing in the monitoring of analgesia through the assessment of the parasympathetic tonus in anaesthetized patients.

The ECGSYNmod tool was developed as a basis for this research with the aim of generating ECG signals with realistic features and R-R series dynamic known a priori. Notwithstanding the recognized limitations, the results revealed that the software is capable of simulating ECG signals (encompassing both normal and abnormal beats) statistically similar to real signals. The ECGSYNmod tool was extended, allowing to modify the original tachograms by selectively or randomly converting normal intervals to ectopic intervals. Beyond the scope of this thesis, a more sophisticated approach to replace the post-processing step can be further considered so that the performance of the ECGSYNmod tool is improved.

The described implementation of the ANI algorithm could be assumed as an HRV metric throughout this thesis. The limits of this metric were assessed, and it could be verified that this implementation of the ANI algorithm heavily relies on precise peak timing being impacted by the performance of the peak detector and the occurrence of ectopic beats. This was an expected finding because the ANI computation is based on the analysis of HF changes, and the estimation of HRV-HF components was significantly distorted by the shortened R-R intervals characteristic of the ectopic episodes. Therefore, it was evidenced the importance of signal processing and accurate R-peak detection before attempting to interpret the ANI values.

The presence of ectopic beats proved to be a significant hindrance for a meaningful interpretation of the ANI values and the assessment of autonomic reactivity, consequently constraining the accurate monitoring of the parasympathetic tone. This thesis found that predicting R-R intervals based on the previous samples of the HRV signals might represent an important step towards the accurate correction of ectopic beats. Although results have shown that performance is strengthened using any of the ectopic correction methods, they also showed that it depends on the applied strategy.

The proposed technique to correct the ectopic intervals consists of replacing them with R-R intervals predicted with an autoregressive model with a parametric estimation based on the 60-second frame prior to the timing of the ectopic observation and a model order of 11. Throughout this study, the technique based on the autoregressive model proved its potential towards a proper assessment of HRV dynamics in the presence of non-sinus beats. Accordingly, it is plausible to assume that the strategy proposed to correct ectopic intervals would make the ANI algorithm sturdier to the presence of ectopic beats to an

extent of 10%, leading to a substantial improvement in the interpretation of the parasympathetic tone assessment through this technology.

Despite being verified a significant performance improvement compared to the techniques most currently employed, correct ectopic intervals using a strategy based on an autoregressive model has some inherent limitations. Some HRV information can be lost by not including the non-linear phenomena responsible for the HRV dynamics in the signal modelling approach. Furthermore, regardless of being shown that the parametric modelling approach often led to efficient representations of the HRV signals, its performance is dependent on the capability of the estimated parameters to model the specific HRV dynamics resulting from inter- and intra-patient variability. Further performance improvements can be obtained by incorporating complementary information, such as different physiological parameters. Additionally, the potential of other strategies to correct ectopic intervals can be assessed by either introducing more advanced non-linear models (including random forest or support vector regression) to better deal with the characteristic neurocardiac complexity of the HRV signal or by attempting to characterize and quantify the HRV dynamics integrating a mathematical combination of linear and non-linear methods.

From a clinical point of view, further research should be carried out with a larger number of records covering other types of surgery with more heterogeneous and balanced data, as not all possible situations observed in clinical practice were included in this analysis. Specifically, patients with frequent comorbidities or any systemic condition in their medical history were automatically excluded by only including for analysis patients of ASA I. Moreover, the application of the proposed method to correct ectopic intervals in HRV signals should be independently assessed in several clinical pathologies, as they may have different statistical characteristics.

Furthermore, for the clinical implementation of the proposed technique, the encouraging results still require further validation in real contexts since this study was mainly performed with controlled simulated constraints. It would also be interesting to add a confidence measure on the clinical information provided by the ANI metric when ectopic beats are present in the HRV signal. This confidence measure would require validation from clinicians involved throughout the perioperative period in order to enable realistic assumptions on the different clinical contexts and understand the clinical value intrinsic to the proposed strategy.

As the proposal of this study can be integrated into the development of oncoming HRV-based algorithms, further work comprises the submission of one paper covering the main findings of this thesis.

REFERENCES

[1] T. G. Weiser *et al.*, "Size and distribution of the global volume of surgery in 2012," *Bull. World Health Organ.*, vol. 94, no. 3, pp. 201-209F, Mar. 2016, doi: 10.2471/BLT.15.159293.

[2] L. A. Fleisher, N. H. Cohen, J. P. Wiener-Kronish, W. L. Young, and R. D. Miller, *Miller's Anesthesia*, 8th ed. Elsevier saunders, 2014.

[3] J. G. Meara *et al.*, "Global Surgery 2030: evidence and solutions for achieving health, welfare, and economic development," *Lancet*, vol. 386, no. 9993, pp. 569–624, Aug. 2015, doi: 10.1016/S0140-6736(15)60160-X.

[4] T. D. Egan and C. H. Svensen, "Multimodal general anesthesia: A principled approach to producing the drug-induced, reversible coma of anesthesia," *Anesth. Analg.*, vol. 127, no. 5, pp. 1104–1106, 2018, doi: 10.1213/ANE.0000000000003743.

[5] A. Cividjian, F. Petitjeans, N. Liu, M. Ghignone, M. de Kock, and L. Quintin, "Do we feel pain during anesthesia? A critical review on surgery-evoked circulatory changes and pain perception," *Best Pract. Res. Clin. Anaesthesiol.*, vol. 31, no. 4, pp. 445–467, 2017, doi: 10.1016/j.bpa.2017.05.001.

[6] B. Katzung, S. Masters, and A. Trevor, *Basic and Clinical Pharmacology*, 11th ed. McGraw-Hill Medical, 2009.

[7] A. I. R. Castro, "Nociception level during anaesthesia: Analysis and control," Universidade do Porto (Portugal), 2011.

[8] T. J. Gan *et al.*, "Bispectral Index Monitoring Allows Faster Emergence and Improved Recovery from Propofol, Alfentanil, and Nitrous Oxide Anesthesia," *Anesthesiology*, vol. 87, no. 4, pp. 808–815, Oct. 1997, doi: 10.1097/00000542-199710000-00014.

[9] A. Vakkuri *et al.*, "Spectral entropy monitoring is associated with reduced propofol use and faster emergence in propofol-nitrous oxide-alfentanil anesthesia," *Anesthesiology*, vol. 103, no. 2, pp. 274–279, 2005, doi: 10.1097/00000542-200508000-00010.

[10] M. Duțu *et al.*, "Neuromuscular monitoring: An update," *Rom. J. Anaesth. Intensive Care*, vol. 25, no. 1, pp. 55–60, 2018, doi: 10.21454/rjaic.7518.251.nrm.

[11] T. Ledowski, "Objective monitoring of nociception: a review of current commercial solutions," *Br. J. Anaesth.*, vol. 123, no. 2, pp. e312–e321, 2019, doi: 10.1016/j.bja.2019.03.024.

[12] E. N. Brown, K. J. Pavone, and M. Naranjo, "Multimodal general anesthesia: Theory and practice," *Anesth. Analg.*, vol. 127, no. 5, pp. 1246–1258, 2018, doi: 10.1213/ANE.0000000000003668.

[13] M. Glarcher, F. S. Kundt, W. Meissner, and J. Osterbrink, "Quality Indicators (QI) of Acute Pain after Surgery in European Countries," *Pain Manag. Nurs.*, no. xxxx, pp. 1–10, 2021, doi: 10.1016/j.pmn.2021.01.012.

[14] A. A. Rabinstein, *Neurologic Disorders and Anesthesia*. Elsevier Inc., 2014.

[15] P. S. Sebel *et al.*, "The incidence of awareness during anesthesia: A multicenter United States study," *Anesth. Analg.*, vol. 99, no. 3, pp. 833–839, 2004, doi: 10.1213/01.ANE.0000130261.90896.6C.

[16] D. Reddi and N. Curran, "Chronic pain after surgery: Pathophysiology, risk factors and prevention," *Postgrad. Med. J.*, vol. 90, no. 1062, pp. 222–227, 2014, doi: 10.1136/postgradmedj-2013-132215.

[17] R. D. Searle and K. H. Simpson, "Chronic post-surgical pain," *Contin. Educ. Anaesthesia, Crit. Care Pain*, vol. 10, no. 1, pp. 12–14, 2009, doi: 10.1093/bjaceaccp/mkp041.

[18] M. Gruenewald and C. Ilies, "Monitoring the nociception-anti-nociception balance," *Best Pract. Res. Clin. Anaesthesiol.*, vol. 27, no. 2, pp. 235–247, 2013, doi: 10.1016/j.bpa.2013.06.007.

[19] M. Esler, "The autonomic nervous system and cardiac," *Clin. Auton. Res.*, vol. 2, pp. 133–135, 1992.

[20] R. B. Fillingim, "Sex, Gender, and Pain: Women and Men Really Are Different," *Curr. Rev. Pain*, vol. 4, no. 1, pp. 24–30, 2000, doi: 10.1039/J19680001293.

[21] M. Huiku, L. Kamppari, and H. Viertio-oja, "Surgical Plethysmographic Index (SPI) in Anesthesia Practice," 2012.

[22] MDoloris Medical Systems, "ANI - Analgesia Nociception Index," *MDoloris*, 2021. https://mdoloris.com/technologies/adults-and-pediatrics/.

[23] J. Höcker *et al.*, "Surgical stress index in response to pacemaker stimulation or atropine," *Br. J. Anaesth.*, vol. 105, no. 2, pp. 150–154, Aug. 2010, doi: 10.1093/bja/aeq114.

[24] S. D. Kristensen *et al.*, "2014 ESC/ESA Guidelines on non-cardiac surgery: Cardiovascular assessment and management: The Joint Task Force on non-cardiac surgery: Cardiovascular assessment and management of the European Society of Cardiology (ESC) and the European Society of Anaesth," *Eur. Heart J.*, vol. 35, no. 35, pp. 2383–2431, 2014, doi: 10.1093/eurheartj/ehu282.

[25] T. F. of the E. S. of C. the N. A. Electrophysiology, "Heart Rate Variability," *Circulation*, vol. 93, no. 5, pp. 1043–1065, Mar. 1996, doi: 10.1161/01.CIR.93.5.1043.

[26] A. Saurav, A. Smer, A. Abuzaid, O. Bansal, and H. Abuissa, "Premature ventricular contraction-induced cardiomyopathy," *Clin. Cardiol.*, vol. 38, no. 4, pp. 251–258, 2015, doi: 10.1002/clc.22371.

[27] P. Harris and D. Lysitsas, "Ventricular arrhythmias and sudden cardiac death," *BJA Educ.*, vol. 16, no. 7, pp. 221–229, Jul. 2016, doi: 10.1093/bjaed/mkv056.

[28] G. A. Ng, "Treating patients with ventricular ectopic beats," *Heart*, vol. 92, no. 11, pp. 1707–1712, Nov. 2006, doi: 10.1136/hrt.2005.067843.

[29] G. M. Marcus, "Evaluation and Management of Premature Ventricular Complexes," *Circulation*, vol. 141, no. 17, pp. 1404–1418, Apr. 2020, doi: 10.1161/CIRCULATIONAHA.119.042434.

[30] M. Gruenewald *et al.*, "Influence of nociceptive stimulation on analgesia nociception index (ANI) during propofol-remifentanil anaesthesia," *Br. J. Anaesth.*, vol. 110, no.

6, pp. 1024–1030, 2013, doi: 10.1093/bja/aet019.

[31] T. F. of the E. S. of C. the N. A. Electrophysiology, "Heart Rate Variability," *Circulation*, vol. 93, no. 5, pp. 1043–1065, Mar. 1996, doi: 10.1161/01.CIR.93.5.1043.

[32] International Association for the Study of Pain, "International Association for the Study of Pain," 2021. https://www.iasp-pain.org/ (accessed Jul. 10, 2021).

[33] M. J. Hudspith, "Anatomy, physiology and pharmacology of pain," *Anaesth. Intensive Care Med.*, vol. 17, no. 9, pp. 425–430, Sep. 2016, doi: 10.1016/j.mpaic.2016.06.003.

[34] J. Brooks and I. Tracey, "From nociception to pain perception: Imaging the spinal and supraspinal pathways," *J. Anat.*, vol. 207, no. 1, pp. 19–33, 2005, doi: 10.1111/j.1469-7580.2005.00428.x.

[35] E. E. Benarroch, "Pain-autonomic interactions: A selective review," *Clin. Auton. Res.*, vol. 11, no. 6, pp. 343–349, 2001, doi: 10.1007/BF02292765.

[36] D. Morton, A. Jones, and J. Sandhu, "Brain imaging of pain: state of the art," *J. Pain Res.*, vol. Volume 9, pp. 613–624, Sep. 2016, doi: 10.2147/JPR.S60433.

[37] R. M. Rangayyan, *Biomedical Signal Analysis*, 2nd ed. Wiley-IEEE Press, 2015.

[38] M. Jeanne, R. Logier, J. De Jonckheere, and B. Tavernier, "Validation of a graphic measurement of heart rate variability to assess analgesia/nociception balance during general anesthesia," in *2009 Annual International Conference of the IEEE Engineering in Medicine and Biology Society*, Sep. 2009, pp. 1840–1843, doi: 10.1109/IEMBS.2009.5332598.

[39] A. Mouraux, G. D. Iannetti, E. Colon, S. Nozaradan, V. Legrain, and L. Plaghki, "Nociceptive steady-state evoked potentials elicited by rapid periodic thermal stimulation of cutaneous nociceptors," *J. Neurosci.*, vol. 31, no. 16, pp. 6079–6087, 2011, doi: 10.1523/JNEUROSCI.3977-10.2011.

[40] A. Mouraux and G. D. Iannetti, "Nociceptive laser-evoked brain potentials do not reflect nociceptive-specific neural activity," *J. Neurophysiol.*, vol. 101, no. 6, pp. 3258–3269, 2009, doi: 10.1152/jn.91181.2008.

[41] I. Korhonen and A. Yli-Hankala, "Photoplethysmography and nociception: Review Article," *Acta Anaesthesiol. Scand.*, vol. 53, no. 8, pp. 975–985, 2009, doi: 10.1111/j.1399-6576.2009.02026.x.

[42] J. Allen, "Photoplethysmography and its application in clinical physiological measurement," *Physiol. Meas.*, vol. 28, no. 3, 2007, doi: 10.1088/0967-3334/28/3/R01.

[43] H. Storm, "Changes in skin conductance as a tool to monitor nociceptive stimulation and pain," *Curr. Opin. Anaesthesiol.*, vol. 21, no. 6, pp. 796–804, 2008, doi: 10.1097/ACO.0b013e3283183fe4.

[44] R. K. Ellerkmann, A. Grass, A. Hoeft, and M. Soehle, "The response of the Composite Variability Index to a standardized noxious stimulus during propofol-remifentanil anesthesia," *Anesth. Analg.*, vol. 116, no. 3, pp. 580–588, 2013, doi: 10.1213/ANE.0b013e31827ced18.

[45] N. Ben-Israel, M. Kliger, G. Zuckerman, Y. Katz, and R. Edry, "Monitoring the nociception level: A multi-parameter approach," *J. Clin. Monit. Comput.*, vol. 27, no.

6, pp. 659–668, Dec. 2013, doi: 10.1007/s10877-013-9487-9.

[46] G. D. Clifford, “Signal processing methods for heart rate variability,” 2002.

[47] R. Couceiro, “Cardiovascular Performance Assessment for p-Health Applications,” *Undefined*, no. September, 2015.

[48] J. de Jong, “ECGpedia,” 2017. .

[49] F. Shaffer and J. P. Ginsberg, “An Overview of Heart Rate Variability Metrics and Norms,” *Front. Public Heal.*, vol. 5, no. September, pp. 1–17, 2017, doi: 10.3389/fpubh.2017.00258.

[50] D. E. Vaillancourt and K. M. Newell, “Changing complexity in human behavior and physiology through aging and disease,” *Neurobiol. Aging*, vol. 23, no. 1, pp. 1–11, Jan. 2002, doi: 10.1016/S0197-4580(01)00247-0.

[51] F. Beckers, B. Verheyden, and A. E. Aubert, “Aging and nonlinear heart rate control in a healthy population,” *Am. J. Physiol. Circ. Physiol.*, vol. 290, no. 6, pp. H2560–H2570, Jun. 2006, doi: 10.1152/ajpheart.00903.2005.

[52] S. Lautenbacher, J. H. Peters, M. Heesen, J. Scheel, and M. Kunz, “Age changes in pain perception: A systematic-review and meta-analysis of age effects on pain and tolerance thresholds,” *Neurosci. Biobehav. Rev.*, vol. 75, pp. 104–113, 2017, doi: 10.1016/j.neubiorev.2017.01.039.

[53] G. M. Marcus, “Evaluation and Management of Premature Ventricular Complexes,” *Circulation*, pp. 1404–1418, 2020, doi: 10.1161/CIRCULATIONAHA.119.042434.

[54] J.-E. Ban *et al.*, “Electrocardiographic and electrophysiological characteristics of premature ventricular complexes associated with left ventricular dysfunction in patients without structural heart disease,” *EP Eur.*, vol. 15, no. 5, pp. 735–741, May 2013, doi: 10.1093/europace/eus371.

[55] H. E. Goldberger, A., Amaral, L., Glass, L., Hausdorff, J., Ivanov, P. C., Mark, R., ... & Stanley, “PhysioBank, PhysioToolkit, and PhysioNet: Components of a new research resource for complex physiologic signals.,” *Circulation [Online]*, 2000. https://www.physionet.org/content/nsrdb/1.0.0/.

[56] G. A. Hawker, S. Mian, T. Kendzerska, and M. French, “Measures of adult pain: Visual Analog Scale for Pain (VAS Pain), Numeric Rating Scale for Pain (NRS Pain), McGill Pain Questionnaire (MPQ), Short-Form McGill Pain Questionnaire (SF-MPQ), Chronic Pain Grade Scale (CPGS), Short Form-36 Bodily Pain Scale (SF,” *Arthritis Care Res.*, vol. 63, no. SUPPL. 11, pp. 240–252, 2011, doi: 10.1002/acr.20543.

[57] M. Luginbühl *et al.*, “Noxious Stimulation Response Index,” *Anesthesiology*, vol. 112, no. 4, pp. 872–880, 2010, doi: 10.1097/aln.0b013e3181d40368.

[58] D. Wildemeersch, N. Peeters, V. Saldien, M. Vercauteren, and G. Hans, “Pain assessment by pupil dilation reflex in response to noxious stimulation in anaesthetized adults,” *Acta Anaesthesiol. Scand.*, vol. 62, no. 8, pp. 1050–1056, 2018, doi: 10.1111/aas.13129.

[59] F. Von Dincklage, C. Correll, M. H. N. Schneider, B. Rehberg, and J. H. Baars, “Utility of Nociceptive Flexion Reflex Threshold, Bispectral Index, Composite Variability Index and Noxious Stimulation Response Index as measures for nociception during general anaesthesia,” *Anaesthesia*, vol. 67, no. 8, pp. 899–905, 2012, doi:

10.1111/j.1365-2044.2012.07187.x.

[60] J. De Jonckheere *et al.*, "Physiological Signal Processing for Individualized Anti-nociception Management During General Anesthesia: a Review," *Yearb. Med. Inform.*, vol. 10, no. 1, pp. 95–101, 2015, doi: 10.15265/IY-2015-004.

[61] J. Y. Martinez *et al.*, "A beat-by-beat cardiovascular index, CARDEAN: A prospective randomized assessment of its utility for the reduction of movement during colonoscopy," *Anesth. Analg.*, vol. 110, no. 3, pp. 765–772, 2010, doi: 10.1213/ANE.0b013e3181cc9ebe.

[62] M. Rossi *et al.*, "A beat-by-beat, on-line, cardiovascular index, CARDEAN, to assess circulatory responses to surgery: A randomized clinical trial during spine surgery," *J. Clin. Monit. Comput.*, vol. 26, no. 6, pp. 441–449, 2012, doi: 10.1007/s10877-012-9372-y.

[63] D. M. Mathews, L. Clark, J. Johansen, E. Matute, and C. V. Seshagiri, "Increases in electroencephalogram and electromyogram variability are associated with an increased incidence of intraoperative somatic response," *Anesth. Analg.*, vol. 114, no. 4, pp. 759–770, 2012, doi: 10.1213/ANE.0b013e3182455ac2.

[64] N. Ben-Israel, M. Kliger, G. Zuckerman, Y. Katz, and R. Edry, "Monitoring the nociception level: A multi-parameter approach," *J. Clin. Monit. Comput.*, vol. 27, no. 6, pp. 659–668, 2013, doi: 10.1007/s10877-013-9487-9.

[65] A. C. Gjerstad, H. Storm, R. Hagen, M. Huiku, E. Qvigstad, and J. Ræder, "Comparison of skin conductance with entropy during intubation, tetanic stimulation and emergence from general anaesthesia," *Acta Anaesthesiol. Scand.*, vol. 51, no. 1, pp. 8–15, 2007, doi: 10.1111/j.1399-6576.2006.01189.x.

[66] C. J. Brouse *et al.*, "Monitoring nociception during general anesthesia with cardiorespiratory coherence," *J. Clin. Monit. Comput.*, vol. 27, no. 5, pp. 551–560, 2013, doi: 10.1007/s10877-013-9463-4.

[67] J. M. Gonzalez-Cava *et al.*, "Machine learning based method for the evaluation of the Analgesia Nociception Index in the assessment of general anesthesia," *Comput. Biol. Med.*, vol. 118, no. October 2019, 2020, doi: 10.1016/j.compbiomed.2020.103645.

[68] M. J. Susano, S. Vide, A. D. Ferreira, and P. Amorim, "Effects of varying remifentanil concentrations on Analgesia Nociception Index® under propofol: an observational study," *J. Clin. Monit. Comput.*, vol. 35, no. 1, pp. 199–205, Feb. 2021, doi: 10.1007/s10877-020-00457-3.

[69] S. Tribuddharat, T. Sathitkarnmanee, P. Sukhong, M. Thananun, P. Promkhote, and D. Nonlhaopol, "Comparative study of analgesia nociception index (ANI) vs. standard pharmacokinetic pattern for guiding intraoperative fentanyl administration among mastectomy patients," *BMC Anesthesiol.*, vol. 21, no. 1, Dec. 2021, doi: 10.1186/s12871-021-01272-2.

[70] K. Sriganesh, K. A. Theerth, M. Reddy, C. Dhritiman, and G. Rao, "Analgesia nociception index and systemic haemodynamics during anaesthetic induction and tracheal intubation: A secondary analysis of a randomised controlled trial," *Indian J. Anaesth.*, vol. 49, no. 4, pp. 257–262, 2019, doi: 10.4103/ija.IJA_656_18.

[71] T. LEDOWSKI, L. AVERHOFF, W. S. TIONG, and C. LEE, "Analgesia Nociception Index (ANI) to predict intraoperative haemodynamic changes: results of a pilot

investigation," *Acta Anaesthesiol. Scand.*, vol. 58, no. 1, pp. 74–79, Jan. 2014, doi: 10.1111/aas.12216.

[72] E. Jozefowicz *et al.*, "Prediction of reactivity during tracheal intubation by pre-laryngoscopy tetanus-induced ANI variation," *J. Clin. Monit. Comput.*, 2021, doi: 10.1007/s10877-020-00624-6.

[73] G. Jess, E. M. Pogatzki-Zahn, P. K. Zahn, and C. H. Meyer-Frieem, "Monitoring heart rate variability to assess experimentally induced pain using the analgesia nociception index," *Eur. J. Anaesthesiol.*, vol. 33, no. 2, pp. 118–125, Feb. 2016, doi: 10.1097/EJA.0000000000000304.

[74] E. Boselli, L. Bouvet, G. Bégou, S. Torkmani, and B. Allaouchiche, "Prediction of hemodynamic reactivity during total intravenous anesthesia for suspension laryngoscopy using Analgesia/Nociception Index (ANI): a prospective observational study.," *Minerva Anestesiol.*, vol. 81, no. 3, pp. 288–97, Mar. 2015, [Online]. Available: http://www.ncbi.nlm.nih.gov/pubmed/25014481.

[75] M. Jeanne, R. Logier, J. De Jonckheere, and B. Tavernier, "Heart rate variability during total intravenous anesthesia: Effects of nociception and analgesia," *Auton. Neurosci.*, vol. 147, no. 1–2, pp. 91–96, May 2009, doi: 10.1016/j.autneu.2009.01.005.

[76] A. Ş. Köprülü, A. Haspolat, Y. G. Gül, and N. Tanrikulu, "Can postoperative pain be predicted? New parameter: Analgesia nociception index," *Turkish J. Med. Sci.*, vol. 50, no. 1, pp. 49–58, 2020, doi: 10.3906/sag-1811-194.

[77] E. Boselli, A. Fatah, S. Ledochowski, and B. Allaouchiche, "ANI and BIS variations in supine and prone position during closed-tracheal suction in sedated and myorelaxed ICU patients with severe COVID-19: A retrospective study," *J. Clin. Monit. Comput.*, Nov. 2020, doi: 10.1007/s10877-020-00612-w.

[78] M. Soral, G. T. Altun, P. Ç. Dinçer, M. K. Arslantaş, and Z. Aykaç, "Effectiveness of the analgesia nociception index monitoring in patients who undergo colonoscopy with sedo-analgesia," *Turkish J. Anaesthesiol. Reanim.*, vol. 48, no. 1, pp. 50–57, 2020, doi: 10.5152/TJAR.2019.45077.

[79] L. Le Gall *et al.*, "Benefits of intraoperative analgesia guided by the Analgesia Nociception Index (ANI) in bariatric surgery: An unmatched case-control study," *Anaesth. Crit. Care Pain Med.*, vol. 38, no. 1, pp. 35–39, 2019, doi: 10.1016/j.accpm.2017.09.004.

[80] V. Dostalova, J. Schreiberova, M. Bartos, L. Kukralova, and P. Dostal, "Surgical pleth index and analgesia nociception index for intraoperative analgesia in patients undergoing neurosurgical spinal procedures: A comparative randomized study," *Minerva Anestesiol.*, vol. 85, no. 12, pp. 1265–1272, Dec. 2019, doi: 10.23736/S0375-9393.19.13765-0.

[81] K. A. Theerth, K. Sriganesh, K. M. Reddy, D. Chakrabarti, and G. S. Umamaheswara Rao, "Analgesia Nociception Index-guided intraoperative fentanyl consumption and postoperative analgesia in patients receiving scalp block versus incision-site infiltration for craniotomy," *Minerva Anestesiol.*, vol. 84, no. 12, pp. 1361–1368, Dec. 2018, doi: 10.23736/S0375-9393.18.12837-9.

[82] E. Boselli *et al.*, "Prospective observational study of the non-invasive assessment of

immediate postoperative pain using the analgesia/nociception index (ANI)," *Br. J. Anaesth.*, vol. 111, no. 3, pp. 453–459, 2013, doi: 10.1093/bja/aet110.

[83] E. Boselli *et al.*, "Prediction of immediate postoperative pain using the analgesia/nociception index: A prospective observational study," *Br. J. Anaesth.*, vol. 112, no. 4, pp. 715–721, 2014, doi: 10.1093/bja/aet407.

[84] A. Ramos-Luengo, A. Gardeta Pallarés, and F. Asensio Merino, "Usefulness of ANI (analgesia nociception index) monitoring for outpatient saphenectomy surgery outcomes: an observational study," *J. Clin. Monit. Comput.*, vol. 35, no. 3, pp. 491–497, 2021, doi: 10.1007/s10877-020-00491-1.

[85] D. Charier *et al.*, "Assessing pain in the postoperative period: Analgesia Nociception IndexTM versus pupillometry," *Br. J. Anaesth.*, vol. 123, no. 2, pp. e322–e327, 2019, doi: 10.1016/j.bja.2018.09.031.

[86] A. Jendoubi, A. Khalloufi, O. Nasri, A. Abbes, S. Ghedira, and M. Houissa, "Analgesia nociception index as a tool to predict hypotension after spinal anaesthesia for elective caesarean section," *J. Obstet. Gynaecol. (Lahore).*, vol. 41, no. 2, pp. 193–199, 2021, doi: 10.1080/01443615.2020.1718624.

[87] N. Dundar, A. Kus, Y. Gurkan, · Kamil Toker, and · Mine Solak, "Analgesia nociception index (ani) monitoring in patients with thoracic paravertebral block: a randomized controlled study," *J Clin Monit Comput*, vol. 32, pp. 481–486, 2018, doi: 10.1007/s10877-017-0036-9.

[88] M. Gazi, S. Abitağaoğlu, G. Turan, C. Köksal, F. N. Akgün, and D. E. Arı, "Evaluation of the effects of dexmedetomidine and remifentanil on pain with the analgesia nociception index in the perioperative period in hysteroscopies under general anesthesia: A randomized prospective study," *Saudi Med. J.*, vol. 39, no. 10, pp. 1017–1022, Oct. 2018, doi: 10.15537/smj.2018.10.23098.

[89] E. Boselli *et al.*, "Effects of hypnosis on the relative parasympathetic tone assessed by ANI (Analgesia/Nociception Index) in healthy volunteers: a prospective observational study," *J. Clin. Monit. Comput.*, vol. 32, no. 3, pp. 487–492, Jun. 2018, doi: 10.1007/s10877-017-0056-5.

[90] R. Abdullayev, E. Yildirim, B. Celik, and L. Topcu Sarica, "Analgesia Nociception Index: Heart Rate Variability Analysis of Emotional Status," *Cureus*, vol. 11, no. 4, 2019, doi: 10.7759/cureus.4365.

[91] J. De Jonckheere, D. Rommel, J. Nandrino, M. Jeanne, and R. Logier, "Heart rate variability analysis as an index of emotion regulation processes: Interest of the Analgesia Nociception Index (ANI).," *Proc. Annu. Int. Conf. IEEE Eng. Med. Biol. Soc. EMBS*, no. August 2012, pp. 3432–3435, 2012, doi: 10.1109/EMBC.2012.6346703.

[92] J. De Jonckheere, R. Logier, R. Jounwaz, R. Vidal, and M. Jeanne, "From pain to stress evaluation using Heart Rate Variability analysis: Development of an evaluation platform," *2010 Annu. Int. Conf. IEEE Eng. Med. Biol. Soc. EMBC'10*, pp. 3852–3855, 2010, doi: 10.1109/IEMBS.2010.5627661.

[93] C. Aragón-Benedí *et al.*, "Is the heart rate variability monitoring using the analgesia nociception index a predictor of illness severity and mortality in critically ill patients with COVID-19? A pilot study," *PLoS One*, vol. 16, no. 3, p. e0249128, Mar. 2021, doi: 10.1371/journal.pone.0249128.

[94] B.-M. Choi, H. Shin, J.-H. Lee, J.-Y. Bang, E.-K. Lee, and G.-J. Noh, "Performance of the Surgical Pleth Index and Analgesia Nociception Index in Healthy Volunteers and Parturients.," *Front. Physiol.*, vol. 12, p. 554026, Mar. 2021, doi: 10.3389/fphys.2021.554026.

[95] T. Ledowski, W. S. Tiong, C. Lee, B. Wong, T. Fiori, and N. Parker, "Analgesia nociception index: evaluation as a new parameter for acute postoperative pain," *Br. J. Anaesth.*, vol. 111, no. 4, pp. 627–629, Oct. 2013, doi: 10.1093/bja/aet111.

[96] J.-H. Lee, B.-M. Choi, Y.-R. Jung, Y.-H. Lee, J.-Y. Bang, and G.-J. Noh, "Evaluation of Surgical Pleth Index and Analgesia Nociception Index as surrogate pain measures in conscious postoperative patients: an observational study," *J. Clin. Monit. Comput.*, vol. 34, no. 5, pp. 1087–1093, Oct. 2020, doi: 10.1007/s10877-019-00399-5.

[97] J. Behar, F. Andreotti, S. Zaunseder, Q. Li, J. Oster, and G. D. Clifford, "An ECG simulator for generating maternal-foetal activity mixtures on abdominal ECG recordings," *Physiol. Meas.*, vol. 35, no. 8, pp. 1537–1550, Aug. 2014, doi: 10.1088/0967-3334/35/8/1537.

[98] E. K. Roonizi and R. Sameni, "Morphological modeling of cardiac signals based on signal decomposition," *Comput. Biol. Med.*, vol. 43, no. 10, pp. 1453–1461, Oct. 2013, doi: 10.1016/j.compbiomed.2013.06.017.

[99] P. E. McSharry, G. D. Clifford, L. Tarassenko, and L. A. Smith, "A dynamical model for generating synthetic electrocardiogram signals," *IEEE Trans. Biomed. Eng.*, vol. 50, no. 3, pp. 289–294, 2003, doi: 10.1109/TBME.2003.808805.

[100] G. D. Clifford and P. E. McSharry, "A realistic coupled nonlinear artificial ECG, BP, and respiratory signal generator for assessing noise performance of biomedical signal processing algorithms," *Fluctuations Noise Biol. Biophys. Biomed. Syst. II*, vol. 5467, p. 290, 2004, doi: 10.1117/12.544525.

[101] J. Healeyl, G. D. Clifford, L. Kontothanassisl, P. E. Mcsharrysl, H. Laboratories, and C. Ma, "An Open-Source Method for Simulating Atrial Fibrillation Using ECGSYN," pp. 425–427, 2004.

[102] P. E. McSharry and G. D. Clifford, "Open-source software for generating electrocardiogram signals," *Proc. 3rd IASTED Int. Conf. Biomed. Eng. 2005*, pp. 410–414, 2005.

[103] R. D. Anderson *et al.*, "Differentiating Right-and Left-Sided Outflow Tract Ventricular Arrhythmias: Classical ECG Signatures and Prediction Algorithms," *Circ. Arrhythmia Electrophysiol.*, vol. 12, no. 6, pp. 1–15, 2019, doi: 10.1161/CIRCEP.119.007392.

[104] M. Bachler, M. Hörtenhuber, M. Frank, S. Wassertheurer, and C. Mayer, "Simulation of physiologic ectopic beats in heartbeat intervals to validate algorithms," *IFAC-PapersOnLine*, vol. 28, no. 1, pp. 123–128, 2015, doi: 10.1016/j.ifacol.2015.05.105.

[105] J.-B. du Prel, B. Röhrig, G. Hommel, and M. Blettner, "Choosing Statistical Tests," *Dtsch. Aerzteblatt Online*, vol. 107, no. 19, pp. 343–348, May 2010, doi: 10.3238/arztebl.2010.0343.

[106] F. J. Massey, "The Kolmogorov-Smirnov Test for Goodness of Fit," *J. Am. Stat. Assoc.*, vol. 46, no. 253, pp. 68–78, 1951.

[107] H. B. Mann and D. R. Whitney, "On a Test of Whether one of Two Random Variables

is Stochastically Larger than the Other," *Ann. Math. Stat.*, vol. 18, no. 1, pp. 50–60, Mar. 1947, doi: 10.1214/aoms/1177730491.

[108] M. Jeanne, C. Clément, J. De Jonckheere, R. Logier, and B. Tavernier, "Variations of the analgesia nociception index during general anaesthesia for laparoscopic abdominal surgery," *J. Clin. Monit. Comput.*, vol. 26, no. 4, pp. 289–294, 2012, doi: 10.1007/s10877-012-9354-0.

[109] C. Garabedian *et al.*, "A new analysis of heart rate variability in the assessment of fetal parasympathetic activity: An experimental study in a fetal sheep model," *PLoS One*, vol. 12, no. 7, pp. 1–10, 2017, doi: 10.1371/journal.pone.0180653.

[110] J. De Jonckheere, M. Delecroix, M. Jeanne, A. Keribedj, N. Couturier, and R. Logier, "Automated analgesic drugs delivery guided by vagal tone evaluation: Interest of the Analgesia Nociception Index (ANI).," *Proc. Annu. Int. Conf. IEEE Eng. Med. Biol. Soc. EMBS*, pp. 1952–1955, 2013, doi: 10.1109/EMBC.2013.6609910.

[111] J. De Jonckheere, D. Rommel, J. Nandrino, M. Jeanne, and R. Logier, "Heart rate variability analysis as an index of emotion regulation processes: Interest of the Analgesia Nociception Index (ANI).," *Proc. Annu. Int. Conf. IEEE Eng. Med. Biol. Soc. EMBS*, pp. 3432–3435, 2012, doi: 10.1109/EMBC.2012.6346703.

[112] J. De Jonckheere, T. Rakza, R. Logier, M. Jeanne, R. Jounwaz, and L. Storme, "Heart rate variability analysis for newborn infants prolonged pain assessment," *Proc. Annu. Int. Conf. IEEE Eng. Med. Biol. Soc. EMBS*, pp. 7747–7750, 2011, doi: 10.1109/IEMBS.2011.6091909.

[113] J. De Jonckheere, M. Jeanne, A. Keribedj, M. Delecroix, and R. Logier, "Closed-loop administration of analgesic drugs based on heart rate variability analysis∗," *Proc. Annu. Int. Conf. IEEE Eng. Med. Biol. Soc. EMBS*, vol. 2018-July, pp. 506–509, 2018, doi: 10.1109/EMBC.2018.8512330.

[114] R. Logier, M. Jeanne, B. Tavernier, and J. De Jonckheere, "Pain / analgesia evaluation using heart rate variability analysis," *Annu. Int. Conf. IEEE Eng. Med. Biol. - Proc.*, pp. 4303–4306, 2006, doi: 10.1109/IEMBS.2006.260494.

[115] R. Logier, M. Jeanne, J. De Jonckheere, A. Dassonneville, M. Delecroix, and B. Tavernier, "PhysioDoloris: A monitoring device for Analgesia / Nociception balance evaluation using Heart Rate Variability analysis," *2010 Annu. Int. Conf. IEEE Eng. Med. Biol. Soc. EMBC'10*, pp. 1194–1197, 2010, doi: 10.1109/IEMBS.2010.5625971.

[116] R. Logier, J. De Jonckheere, and A. Dassonneville, "An efficient algorithm for R-R intervals series filtering," *Annu. Int. Conf. IEEE Eng. Med. Biol. - Proc.*, vol. 26 VI, pp. 3937–3940, 2004, doi: 10.1109/iembs.2004.1404100.

[117] "R Wave Detection in the ECG - MATLAB & Simulink." https://www.mathworks.com/help/wavelet/ug/r-wave-detection-in-the-ecg.html (accessed Jul. 10, 2021).

[118] H. Sedghamiz, "Matlab Implementation of Pan Tompkins ECG QRS detector," 2014, doi: 10.13140/RG.2.2.14202.59841.

[119] J. Pan and W. J. Tompkins, "A Real-Time QRS Detection Algorithm," *IEEE Trans. Biomed. Eng.*, vol. BME-32, no. 3, pp. 230–236, Mar. 1985, doi: 10.1109/TBME.1985.325532.

[120] R. W. C. G. R. Wijshoff, M. Mischi, and R. M. Aarts, "Reduction of periodic motion artifacts in photoplethysmography," *IEEE Trans. Biomed. Eng.*, vol. 64, no. 1, pp. 196–207, 2017, doi: 10.1109/TBME.2016.2553060.

[121] S. Walter *et al.*, "The BioVid Heat Pain Database," *IEEE Int. Conf. Cybern.*, pp. 128–131, 2013.

[122] X. Zhang *et al.*, "BP4D-Spontaneous: A high-resolution spontaneous 3D dynamic facial expression database," *Image Vis. Comput.*, vol. 32, no. 10, pp. 692–706, 2014, doi: 10.1016/j.imavis.2014.06.002.

[123] P. Lucey, J. F. Cohn, K. M. Prkachin, P. E. Solomon, and I. Matthews, "Painful data: The UNBC-McMaster shoulder pain expression archive database," *2011 IEEE Int. Conf. Autom. Face Gesture Recognit. Work. FG 2011*, pp. 57–64, 2011, doi: 10.1109/FG.2011.5771462.

[124] V. K. Mittal, "Discriminating the Infant Cry Sounds Due to Pain vs. Discomfort Towards Assisted Clinical Diagnosis," no. September, pp. 37–42, 2017, doi: 10.21437/slpat.2016-7.

[125] D. Harrison *et al.*, "Too many crying babies: A systematic review of pain management practices during immunizations on YouTube," *BMC Pediatr.*, vol. 14, no. 1, pp. 1–8, 2014, doi: 10.1186/1471-2431-14-134.

[126] G. Zamzmi, P. Chih-Yun, D. Goldgof, R. Kasturi, T. Ashmeade, and Y. Sun, "A Comprehensive and Context-Sensitive Neonatal Pain Assessment Using Computer Vision," *IEEE Trans. Affect. Comput.*, vol. 3045, no. c, pp. 1–19, 2019, doi: 10.1109/TAFFC.2019.2926710.

[127] M. A. Haque *et al.*, "Deep multimodal pain recognition: A database and comparison of spatio-temporal visual modalities," *Proc. - 13th IEEE Int. Conf. Autom. Face Gesture Recognition, FG 2018*, pp. 250–257, 2018, doi: 10.1109/FG.2018.00044.

[128] J. O. Egede *et al.*, "EMOPAIN Challenge 2020: Multimodal Pain Evaluation from Facial and Bodily Expressions," *Proc. - 2020 15th IEEE Int. Conf. Autom. Face Gesture Recognition, FG 2020*, no. March, pp. 849–856, 2020, doi: 10.1109/FG47880.2020.00078.

[129] S. Brahnam, C. F. Chuang, F. Y. Shih, and M. R. Slack, "SVM classification of neonatal facial images of pain," *Lect. Notes Comput. Sci. (including Subser. Lect. Notes Artif. Intell. Lect. Notes Bioinformatics)*, vol. 3849 LNAI, pp. 121–128, 2006, doi: 10.1007/11676935_15.

[130] S. Gruss *et al.*, "Multi-modal signals for analyzing pain responses to thermal and electrical stimuli," *J. Vis. Exp.*, vol. 2019, no. 146, 2019, doi: 10.3791/59057.

[131] M. S. H. Aung *et al.*, "The Automatic Detection of Chronic Pain-Related Expression: Requirements, Challenges and the Multimodal EmoPain Dataset," *IEEE Trans. Affect. Comput.*, vol. 7, no. 4, pp. 435–451, Oct. 2016, doi: 10.1109/TAFFC.2015.2462830.

[132] H. C. Lee and C. W. Jung, "Vital Recorder- A free research tool for automatic recording of high-resolution time-synchronised physiological data from multiple anaesthesia devices," *Sci. Rep.*, vol. 8, no. 1, pp. 1–8, 2018, doi: 10.1038/s41598-018-20062-4.

[133] Vest A *et al.*, "An Open Source Benchmarked Toolbox for Cardiovascular Waveform

and Interval Analysis," *Physiol. Meas. (In Press.*, 2018, doi: https://doi.org/10.5281/zenodo.1243112.

[134] S. T. Vistisen, T. J. Pollard, J. Enevoldsen, and T. W. L. Scheeren, "VitalDB: fostering collaboration in anaesthesia research," *Br. J. Anaesth.*, vol. 127, no. 2, pp. 184–187, 2021, doi: 10.1016/j.bja.2021.03.011.

[135] D. Nabil and F. Bereksi Reguig, "Ectopic beats detection and correction methods: A review," *Biomed. Signal Process. Control*, vol. 18, pp. 228–244, Apr. 2015, doi: 10.1016/j.bspc.2015.01.008.

[136] MathWorks, "1-D data interpolation - MATLAB interp1." https://www.mathworks.com/help/matlab/ref/interp1.html (accessed Oct. 10, 2021).

[137] K. Takata, Y. Watanabe, and K. Yokoyama, "Quantification of the heartbeat rhythm using characteristic equation of autoregressive model of R-R intervals in ECG," *Syst. Comput. Japan*, vol. 20, no. 4, pp. 89–97, 1989, doi: 10.1002/scj.4690200409.

[138] A. Boardman, F. S. Schlindwein, A. P. Rocha, and A. Leite, "A study on the optimum order of autoregressive models for heart rate variability," *Physiol. Meas.*, vol. 23, no. 2, pp. 325–336, May 2002, doi: 10.1088/0967-3334/23/2/308.

[139] E. Miranda Dantas *et al.*, "Spectral analysis of heart rate variability with the autoregressive method: What model order to choose?," *Comput. Biol. Med.*, vol. 42, no. 2, pp. 164–170, Feb. 2012, doi: 10.1016/j.compbiomed.2011.11.004.

[140] H. Akaike, "A new look at the statistical model identification," *IEEE Trans. Automat. Contr.*, vol. 19, no. 6, pp. 716–723, Dec. 1974, doi: 10.1109/TAC.1974.1100705.

[141] J. Rissanen, "Universal coding, information, prediction, and estimation," *IEEE Trans. Inf. Theory*, vol. 30, no. 4, pp. 629–636, Jul. 1984, doi: 10.1109/TIT.1984.1056936.

[142] D. M. Khan, N. Yahya, and N. Kamel, "Optimum Order Selection Criterion for Autoregressive Models of Bandlimited EEG Signals," *Proc. - 2020 IEEE EMBS Conf. Biomed. Eng. Sci. IECBES 2020*, pp. 389–394, 2021, doi: 10.1109/IECBES48179.2021.9398836.

[143] I. N. da Silva, D. Hernane Spatti, R. Andrade Flauzino, L. H. B. Liboni, and S. F. dos Reis Alves, *Artificial Neural Networks*. Cham: Springer International Publishing, 2017.

[144] B. James and B. Yoshua, "Random Search for Hyper-Parameter Optimization," *J. Mach. Learn. Res.*, vol. 13, no. 1, pp. 281–305, 2012.

[145] F. Pedregosa *et al.*, "Cross-validation: evaluating estimator performance," *Journal of Machine Learning Research*, 2011. https://scikit-learn.org/stable/modules/cross_validation.html.

[146] T. Kvålseth, "On Normalized Mutual Information: Measure Derivations and Properties," *Entropy*, vol. 19, no. 11, p. 631, Nov. 2017, doi: 10.3390/e19110631.

[147] A. Amelio and C. Pizzuti, "Is Normalized Mutual Information a Fair Measure for Comparing Community Detection Methods?," in *Proceedings of the 2015 IEEE/ACM International Conference on Advances in Social Networks Analysis and Mining 2015*, Aug. 2015, pp. 1584–1585, doi: 10.1145/2808797.2809344.

[148] L. Rita, "Normalized Mutual Information," *Medium*, 2020.

https://luisdrita.com/normalized-mutual-information-a10785ba4898 (accessed Sep. 19, 2021).

[149] W. H. Kruskal and W. A. Wallis, “Use of Ranks in One-Criterion Variance Analysis,” *J. Am. Stat. Assoc.*, vol. 47, no. 260, p. 583, Dec. 1952, doi: 10.2307/2280779.

[150] V. Bewick, L. Cheek, and J. Ball, “Statistics review 10: Further nonparametric methods,” *Crit. Care*, vol. 8, no. 3, pp. 196–199, 2004, doi: 10.1186/cc2857.

[151] A. Choi and H. Shin, “Quantitative analysis of the effect of an ectopic beat on the heart rate variability in the resting condition,” *Front. Physiol.*, vol. 9, no. JUL, 2018, doi: 10.3389/fphys.2018.00922.

[152] DeepLearning.AI, “DeepLearning.AI,” *2021*. https://www.deeplearning.ai/ (accessed Sep. 30, 2021).

[153] E. Burns, “Premature Ventricular Complex (PVC),” *Life in the Fast Lane (LITFL)*, 2021. https://litfl.com/premature-ventricular-complex-pvc-ecg-library/ (accessed Oct. 28, 2021).

[154] D. KATRITSIS, “Nonsustained ventricular tachycardia: where do we stand?,” *Eur. Heart J.*, vol. 25, no. 13, pp. 1093–1099, Jul. 2004, doi: 10.1016/j.ehj.2004.03.022.

[155] D. G. Katritsis, W. Zareba, and A. J. Camm, “Nonsustained Ventricular Tachycardia,” *J. Am. Coll. Cardiol.*, vol. 60, no. 20, pp. 1993–2004, Nov. 2012, doi: 10.1016/j.jacc.2011.12.063.

[156] K. Theerth, K. Sriganesh, D. Chakrabarti, K. Reddy, and G. Rao, “Analgesia nociception index and hemodynamic changes during skull pin application for supratentorial craniotomies in patients receiving scalp block versus pin-site infiltration: A randomized controlled trial,” *Saudi J. Anaesth.*, vol. 13, no. 4, pp. 306–311, 2019, doi: 10.4103/sja.SJA_812_18.

[157] G. B. Moody and R. G. Mark, “The impact of the MIT-BIH arrhythmia database.,” *IEEE Eng. Med. Biol. Mag.*, vol. 20, no. 3, pp. 45–50, doi: 10.1109/51.932724.

APPENDICES

APPENDIX A: ANI STUDIES

REF.	YEAR	N (M/F)	DESCRIPTION OF THE CONTEXT		MAIN FINDINGS/CONCLUSIONS
[68]	2020	16 (5/11)	**Procedure** **Stimulation** **Anaesthesia** **Analgesics**	Craniotomy Tetanic General Remifentanil	- ANI may perform better than traditional hemodynamic parameters at reflecting noxious stimulation. - Following a noxious stimulation, the results showed that it takes around 1 min for the ANI to change which may be considered too long for clinical purposes.
[87]	2018	44 (-/44)	**Procedure** **Stimulation** **Anaesthesia** **Analgesics**	Breast None General Remifentanil	- ANI monitoring may optimize opioid consumption in patients - It was not precisely concluded that ANI monitoring help hemodynamic stabilization neither reflects Noc/ANoc balance
[67]	2020	17 (4/13)	**Procedure** **Stimulation** **Anaesthesia** **Analgesics**	Cholecystectomy None General Remifentanil	- ANI monitoring outperforms decisions only based on hemodynamic parameters - ANI may be suitable for anticipate the need of a change of dose before the occurrence of a hemodynamic event
[85]	2019	345 (170/175)	**Procedure** **Stimulation** **Anaesthesia** **Analgesics**	All types of surgery conducted in the institution (except for heart, intracerebral, and ophthalmologic) None General Not protocolized	- VCPD correlated more strongly with pain (VAS measurement) than ANI, HR, and SBP - ANI discrepancies between patients with pain and those without pain revealed to be clinically irrelevant.
[84]	2020	129 (45/86)	**Procedure** **Stimulation** **Anaesthesia** **Analgesics**	Varicose vein (saphenectomy) None General Metamizole	- Hospital discharge might be reduced by an adequate nociception level measured by ANI.
[72]	2020	35 (18/17)	**Procedure** **Stimulation** **Anaesthesia** **Analgesics**	Inner or middle ear Tetanic stimulation of the ulnar nerve General Remifentanil	- ANI varied after a short moderate tetanic stimulation before laryngoscopy - The variation of the ANI pre-laryngoscopy was not predictive of any hemodynamic or somatic reaction during intubation
[89]	2018	40 (9/31)	**Procedure** **Stimulation** **Anaesthesia** **Analgesics**	Hypnotic trance None None None	- ANI monitoring may provide an objective tool for the measurement of the intensity of the hypnotic process;
[96]	2019	192 (84/108)	**Procedure** **Stimulation** **Anaesthesia** **Analgesics**	Thyroid, breast or abdominal None General Remifentanil	- ANI values significantly different between conscious patients with and without pain. - The cut-off values for detecting pain in postoperative conscious state were calculated different from the suggested by the manufacturer.

Table A - 1: ANI studies elected for systematic review between 2018 and 2021

REF.	YEAR	N (M/F)	DESCRIPTION OF THE CONTEXT		MAIN FINDINGS/CONCLUSIONS
[80]	2019	32 (76/76)	**Procedure** **Stimulation** **Anaesthesia** **Analgesics**	Neurosurgical spinal None General Sufentanil	- ANI monitoring significantly impacted the intraoperative opioid use, but no effect was observed on the postoperative cortisol levels and postoperative pain.
[88]	2018	30 (-/30)	**Procedure** **Stimulation** **Anaesthesia** **Analgesics**	Hysteroscopy None General Remifentanil or dexmedetomidine	- Maintaining the ANI measurements within the target range (50-70), the ANI was statistically higher in the group with administration of remifentanil. - No difference was found between the postoperative VAS scores of the group with remifentanil administration and the group with dexmedetomidine administration.
[79]	2019	60 (7/53)	**Procedure** **Stimulation** **Anaesthesia** **Analgesics**	Bariatric None General Sufentanil	- The intraoperative consumption of sufentanil was reduced using ANI monitoring, but it does not appear to be associated with by a reduction in the side-effects of sufentanil.
[76]	2021	36 (15/21)	**Procedure** **Stimulation** **Anaesthesia** **Analgesics**	Laparoscopic cholecystectomy None General Remifentanil	- ANI monitoring seemed ineffective predicting potential postoperative pain.
[70]	2019	57 (29/28)	**Procedure** **Stimulation** **Anaesthesia** **Analgesics**	Craniotomy for supra-tentorial brain tumours None General Fentanyl	- Unlike systemic hemodynamic parameters, ANI provides an objective assessment of the balance between pain and analgesia during intubation.
[69]	2021	60 (-/60)	**Procedure** **Stimulation** **Anaesthesia** **Analgesics**	Mastectomy None General Fentanyl	- ANI may be a reliable monitor for analgesia intraoperatively since the ANI values of the control group and of the ANI-guided group were almost parallel. - The intraoperative consumption of fentanyl in patients undergoing mastectomy was not reduced using ANI monitoring. - The clinical outcomes were not impacted by ANI-guided intraoperative administration of fentanyl.
[94]	2021	20 (7/13)	**Procedure** **Stimulation** **Anaesthesia** **Analgesics**	Parturients (natural childbirth) vs healthy volunteers Healthy volunteers: pressure area over the anterior tibial bone; Parturients: regional anaesthesia (epidural**)** Healthy volunteers: Remifentanil	- ANI and SPI were found to effectively distinguish between intensity of pain in healthy volunteers and parturients. - Under administration of remifentanil, SPI may be more appropriate for reflecting the degree of pain because, although ANI may have good responsiveness to opioids, it may be likely to overestimate pain in case of remifentanil infusion.

Table A – 1 (continuation): ANI studies elected for systematic review between 2018 and 2021

REF.	YEAR	N (M/F)	DESCRIPTION OF THE CONTEXT		MAIN FINDINGS/CONCLUSIONS
[81]	2018	57 (29/28)	**Procedure** **Stimulation** **Anaesthesia** **Analgesics**	Craniotomy for supra-tentorial brain tumours None Regional Fentanyl	- The intraoperative consumption of fentanyl was reduced using ANI monitoring, but it does not appear to be associated with by a reduction of postoperative pain.
[156]	2019	57 (29/28)	**Procedure** **Stimulation** **Anaesthesia** **Analgesics**	Craniotomy for supra-tentorial brain tumours None Regional Fentanyl	- Both the ANI monitoring and hemodynamic parameters reported a reduction of the autonomic response to noxious stimulus using the scalp block technique rather than the pin-site infiltration. - A strong negative linear correlation was reported between ANI and HR, and ANI and mean BP following skull pin application.
[78]	2020	102 (34/68)	**Procedure** **Stimulation** **Anaesthesia** **Analgesics**	Colonoscopy None Sedo-analgesia Remifentanil	- The intraoperative consumption of opioids was reduced using ANI monitoring. - No differences were found in terms of side effects, complications or duration of recovery using ANI monitoring.
[93]	2021	14 (11/3)	**Procedure** **Stimulation** **Anaesthesia** **Analgesics**	Patients diagnosed with COVID-19 and on mechanical ventilation (orotracheal intubation or tracheostomy) None Sedo-analgesia Remifentanil and/or dexmedetomidine	- The spectral analysis of HRV may allow to infer the state of the ANS and the immune system of critically ill patients. - High ANIm values were associated with worse prognosis, higher mortality, and higher IL-6 levels.
[86]	2021	100 (-/100)	**Procedure** **Stimulation** **Anaesthesia** **Analgesics**	Caesarean delivery None Spinal Not specified	- ANI may predict the risk of spinal anaesthesia-related hypotension.
[90]	2019	20 (10/10)	**Procedure** **Stimulation** **Anaesthesia** **Analgesics**	Awake healthy volunteers Emotional stimulus None None	- ANI may be employed for assessment of parasympathetic changes related to the emotional state of conscious patients.
[77]	2020	15 (11/4)	**Procedure** **Stimulation** **Anaesthesia** **Analgesics**	Patients in ICU for severe COVID-19 pneumonia None Sedation Remifentanil or sufentanil	- ANI monitoring significantly impacted the intraoperative opioid use, but no effect was observed on the postoperative cortisol levels and postoperative pain.

Table A – 1 (continuation): ANI studies elected for systematic review between 2018 and 2021

APPENDIX B: TRAINING DATASET

The training dataset is based on physiological data acquired from Phisionet.org, a free online archive of physiological signals. Two subsets (subset A and subset B) have been composed using different databases. The ECG records of these databases were annotated using Physionet tools, and these annotations were used as a reference for further categorization in segments.

Subset A was taken from the MIT-BIH Normal Sinus Rhythm Database.[55] This database comprises 18 records of mixed-gender adult individuals aged 20 to 50 who did not present significant arrhythmias. Accordingly, subset A is composed of six ECG segments with a Normal Sinus Rhythm, duration of 10 minutes, and sampled at a frequency of 250 Hz. The segments composing the subset A were acquired from the parts of the MIT records whose annotations other than normal beats were not found. Table B - 1 details the ECG segments that were selected.

MIT	SYN	N	A	V	F	S	J	~	|	+
19140m	Norm1	959	0	0	0	0	0	0	0	0
19140m	Norm2	829	0	0	0	0	0	0	0	0
18184m	Norm3	911	0	0	0	0	0	0	0	0
18184m	Norm4	780	0	0	0	0	0	0	0	0
16795m	Norm5	787	0	0	0	0	0	0	0	0
16483m	Norm6	821	0	0	0	0	0	0	0	0

Table B - 1: Description of the ECG signals composing the subset A of the training dataset.[1]

Subset B was taken from the MIT-BIH Arrhythmia Database.[157] This database comprises ECG records of 47 subjects of mixed gender aged 23 to 89 who presented clinically significant arrhythmias. Although only PVC beats were considered throughout the study presented in this thesis, the construction of this subset also considered signals with premature auricular contractions (PAC) because the only differences in terms of ECG analysis are that PAC does not have a full compensatory pause and the morphology. Table B - 2 details the ECG segments sampled at 360 Hz that were selected.

[1] N - Normal beat; A - Atrial premature beat; V - Premature ventricular contraction; F - Fusion of ventricular and normal beat; S - Supraventricular premature or ectopic beat (atrial or nodal); J - Nodal (junctional) premature beat; ~ - Change in signal quality; | - Isolated QRS-like artifact; + - Rhythm change.

MIT	SYN	N	A	V	F	S	J	~	|	+
106m	PVC1	959	0	0	0	0	0	0	0	0
116m	PVC2	2302	1	10	0	0	0	8	0	1
119m	PVC3	1543	0	444	0	0	0	4	0	103
209m	PVC4	2621	383	1	0	0	0	19	7	21
228m	PVC5	1688	3	362	0	0	0	20	24	41

Table B - 2: Description of the ECG signals composing the subset B of the training dataset[2].

[2] N - Normal beat; A - Atrial premature beat; V - Premature ventricular contraction; F - Fusion of ventricular and normal beat; S - Supraventricular premature or ectopic beat (atrial or nodal); J - Nodal (junctional) premature beat; ~ - Change in signal quality; | - Isolated QRS-like artifact; + - Rhythm change.

APPENDIX C: IMPLEMENTATION OF THE ANI ALGORITHM

The implementation of the ANI algorithm described in chapter 4 (ANI_{lb}) was compared against another literature-based implementation that has been shown in previous works to be congruent with the ANI monitor (ANI_{lb2}). Proper statistical validation of the ANI_{lb} would require comparison to data provided by an ANI monitor commercialized by MDoloris. As no ANI monitor was available for set-up, statistical tests were employed to evaluate whether there is a statistically significant difference between the performances of ANI_{lb} and ANI_{lb2}. The two implementations of the ANI algorithm may differ because the details publicly available at the moment of their implementation could be different.

Regarding the validation of ANI_{lb} implementation against the ANI_{lb2} implementation, the ANI variables from the two implementations were tested for correlation and were found to be highly correlated. As data was found not to be normally distributed, employing the Wilcoxon rank-sum test, the null hypothesis stating that the two ANI variables would follow the same distribution could be accepted (p-value = 0.8412) which is corroborated by the detailed distribution of the variables depicted in Figure C - 1.

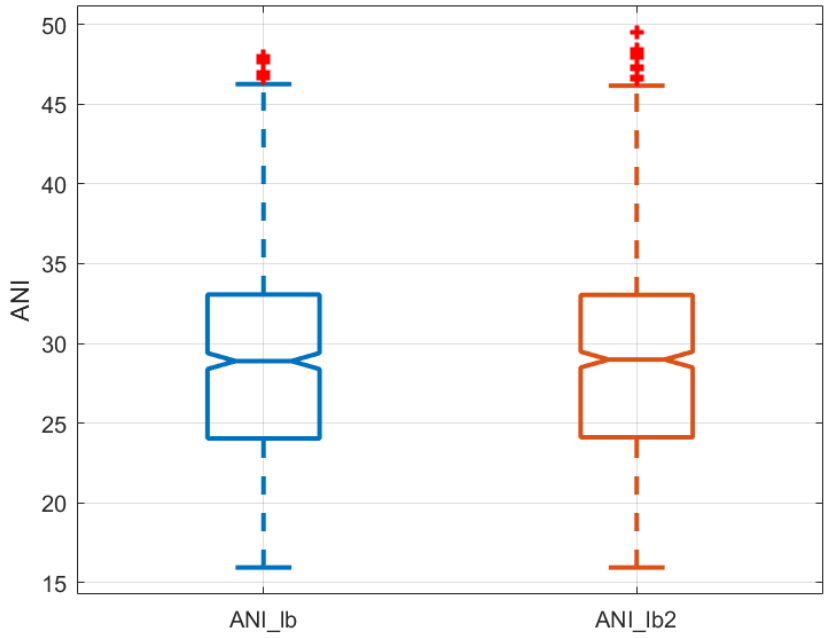

Figure C - 1: Boxplots showing the distributions of the ANI variables corresponding to R-R times series extracted from the ECGs of subset A computed applying the two implementations of the ANI algorithm.

To note that the same R-R time series and strategies to remove ectopic or incorrectly detected beats were employed to compute the ANI values from the two implementations so that this would not be a source of the discrepancies between the two curves in this

analysis. Nevertheless, no information was found in the publicly available literature regarding the techniques employed by algorithm proprietary of MDoloris.

From Figure C - 2, slight differences can be observed between the ANI variables corresponding to R-R times series extracted from the ECGs of subset A (described at Appendix B) and computed applying the two considered implementations of the ANI algorithm. These differences are probably because the publicly available information on the details of ANI calculation is ambiguous and scarce and, so, at certain points some assumptions had to be made. Figure C - 3 illustrates the step-by-step output of the ANI_{lb}.

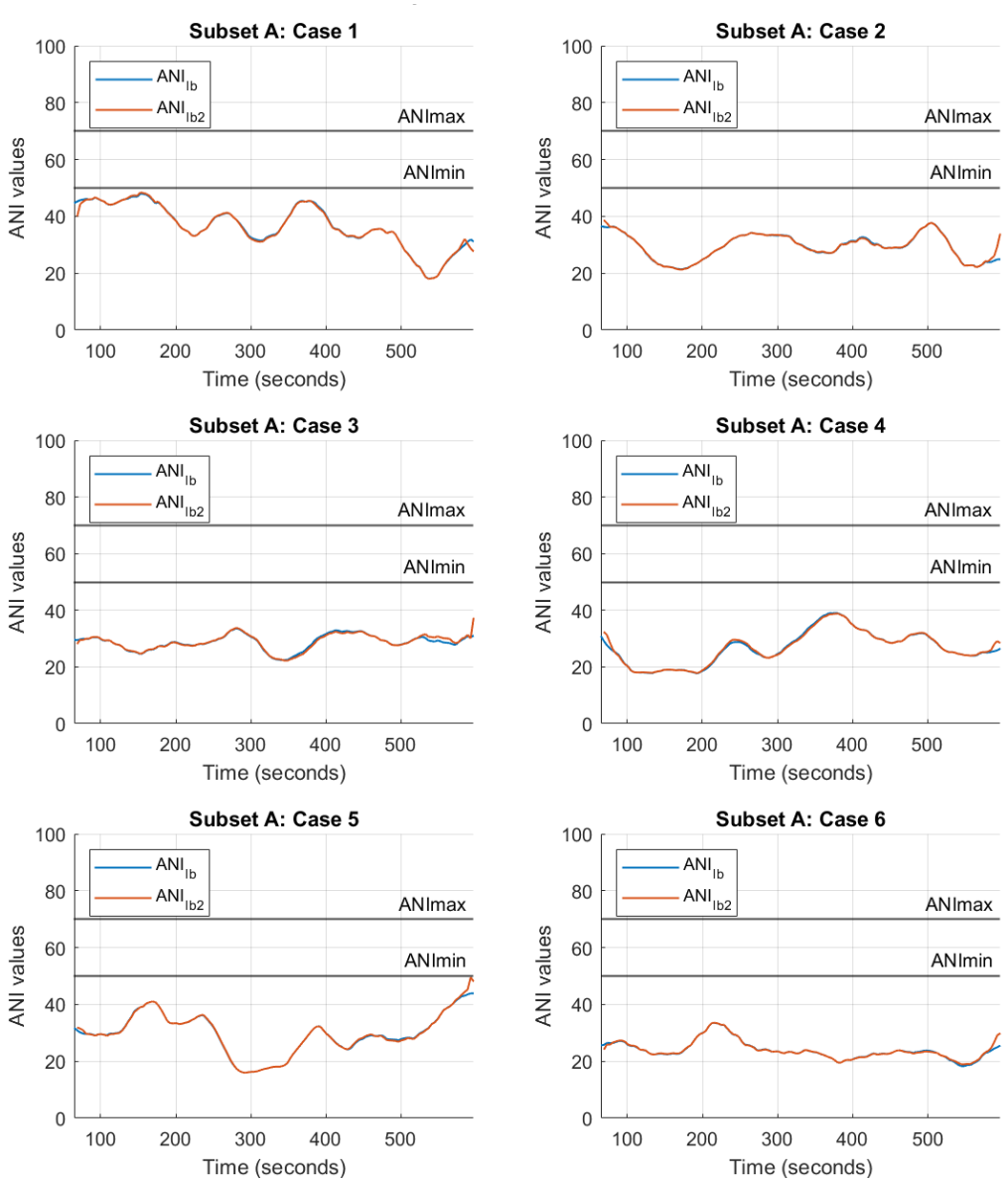

Figure C - 2: ANI variables computed for each case of subset A. The ANI variables were computed with a moving window of 44 seconds and using the implementation ANI_{lit1} (in blue) and ANI_{lit2} (in orange).

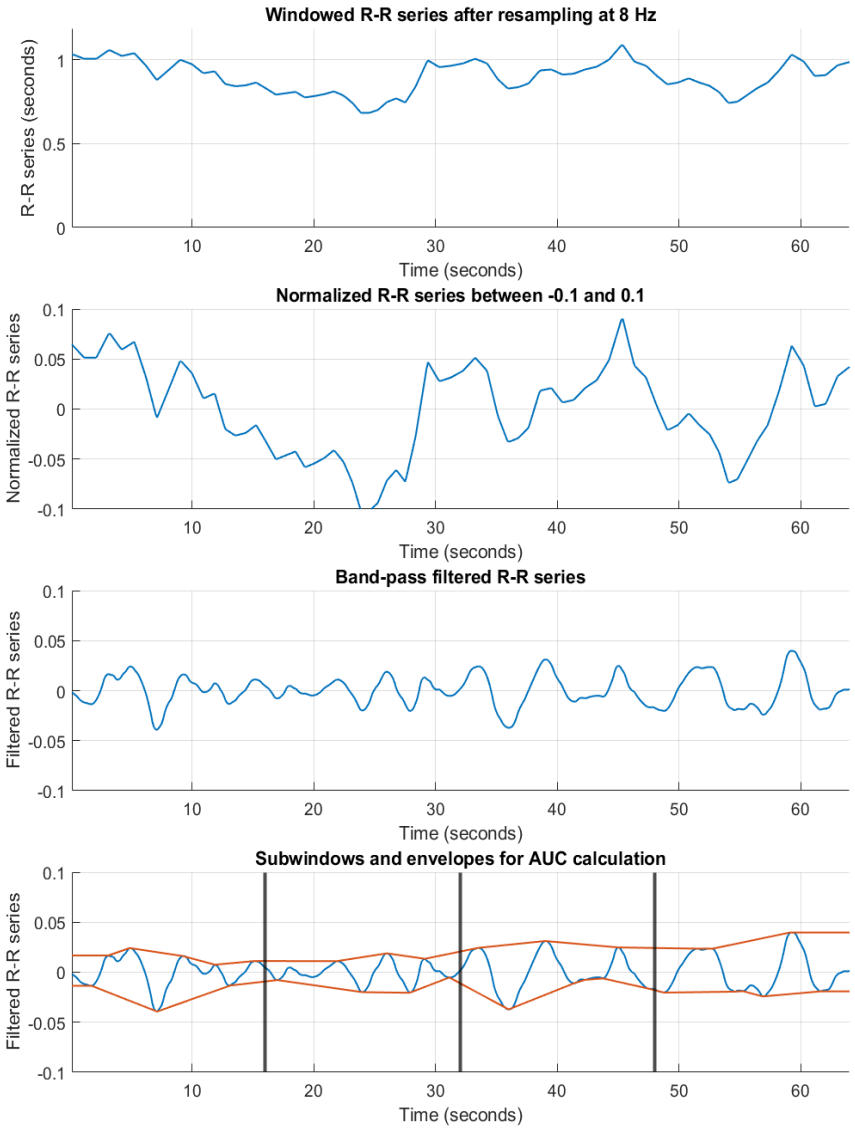

Figure C - 3: First window output for each step of the described implementation of the ANI algorithm applied to the R-R time series extracted from the Case 1 of subset A of the training dataset.

Wavelet component	Scale	Frequency band (Hz)
Detail level 1, d_1	2	2 – 4
Detail level 2, d_2	4	1 – 2
Detail level 3, d_3	8	0.5 – 1
Detail level 4, d_4	16	0.25 – 0.5
Detail level 5, d_5	32	0.125 – 0.25
Approximation level 6, a_6	32	0 – 0.125

Table C - 1: Frequency bands as function of wavelet decomposition levels, $f_s = 8\ Hz$

As the ANI calculation is based on the analysis of high frequency changes, the R-R series is bandpass filtered between 0.15 and 0.5 Hz using a Daubechies wavelet filter which allows isolating the frequency domains of the signal without any phase shift [92], [108], [110]–[112], [115]. When designing the filter, contradictory information was found in the literature: [92] states that wavelet levels 3 to 5 must be maintained, while [38] claims that only wavelet levels 4 and 5 must be kept to apply the reverse wavelet transform and retrieve the signal in the time-domain without the frequencies outside the range of [0.1667; 0.6667] Hz. As the highest frequency in the resampled RR-series signal is not specified, it was assumed to be 4 Hz and, considering the frequency bands in Table C - 1, wavelet levels 4 and 5 were kept for the design of the bandpass filter and the extraction of the frequency components between 0.125 and 0.5 Hz.

Furthermore, the method used by MDoloris [22] to detect local minima and maxima and construct the envelopes was not specified in the publicly available literature. Based on the observation of ANI monitors from previous publications, it was hypothesized that only the local maxima above half the mean of the maxima points detected and the local minima below half the average of the minima points detected would be considered. Then, the trapezoidal numerical integration method was employed to determine the area delimited by the envelopes.

Additionally, it was noticed that the border conditions on the construction of the envelopes are defined differently in the two considered implementations of the ANI algorithm. Attempting to disclose this difference, another version of ANI_{lb} was developed in which the first sample of envelopes is defined based on the last sample of the respective envelope from the previous window; and the last sample of envelopes is defined based on the first sample of the respective envelope from the next window. Inspecting the results, this second version was discarded as the discrepancies between the curves increased slightly, altering only the first and last samples of the envelopes. Although the discrepancies between the curves were not disclosed, this observation envisioned that this implementation of the ANI algorithm would not be robust to timing interferences.

The referred assumptions are probably the sources of discrepancy between the output values of ANI_{lb} and ANI_{lb2}. Overall, the ANI_{lb} implementation could be validated against the ANI_{lb2}. Yet it should be noted that, because the methods employed in the algorithm proprietary of MDoloris are not publicly referenced and could be others than the ones mentioned here, it is expected to obtain even more noticeable differences performing a comparison against ANI values output by the monitor commercialized by MDoloris [22].